TECHNISCHE UNIVERSITÄT MÜNCHEN

Department Chemie
Lehrstuhl für Biotechnologie

# Identification and Characterization of Oxidative Stress Related Proteins

**Yan Le**

Vollständiger Abdruck der von der Fakultät für Chemie der Technischen Universität München zur Erlangung des akademischen Grades eines Doktors der Naturwissenschaften genehmigten Dissertation.

Vorsitzender: Univ. - Prof. Dr. Johannes Buchner

Prüfer der Dissertation:

1. TUM Junior Fellow Dr. Jeannette Winter
2. Univ. - Prof. Dr. Michael Sattler

Die Dissertation wurde am 28.02.2013 bei der Technischen Universität München eingereicht und durch die Fakultät für Chemie am 24.04.2013 angenommen.

Hiermit erkläre ich, dass die vorliegende Arbeit selbständig verfasst und keine anderen als die angegebenen Quellen und Hilfsmittel benutzt wurden. Die Arbeit wurde bisher noch keiner Prüfungsbehörde vorgelegt und nicht veröffentlicht.

München, den 3. Juni 2013

Yan Le

# Table of Contents

# 1 Summary

Reactive oxygen species (ROS) including superoxide ($O^{2-}$), hydrogen peroxide ($H_2O_2$) and hydroxyl radicals (·OH), can be generated as byproducts in the respiration chain in aerobic organisms (*1*). Additionally, they can be generated by the host immune system to kill invading bacteria (e.g., the hypochlorite, HOCl) (*2*). ROS can oxidize different kinds of biological molecules, and consequently destroy their function (*3*). Thus, once ROS largely accumulate in cells, cells suffer greatly under this condition, termed oxidative stress (*4*). Confronted with this unfavorable condition, cells activate ROS-specific transcription factors to modulate the expression of genes involved in detoxifying the oxidants and repairing damaged macromolecules (*5*).

Compared to $O^{2-}$ and $H_2O_2$, HOCl is extremely reactive and severely insults cells by non-selectively modifying most of cellular macromolecules (*6*). Very recently, the HOCl-responsive transcription factor **YjiE** in *E.coli* was identified in our lab (*7*). YjiE confers bacterial resistance to HOCl and forms unusual dodecamic ring-like structure (*7*). Nevertheless, how YjiE is activated upon HOCl stress was unknown. As LysR type transcription factor (LTTR), YjiE is potentially activated by either binding of a small molecule (co-inducer) or direct covalent modification of conserved amino acids. To unravel the activation mechanism of YjiE, both possibilities were tested in this work. However, no co-inducer bound to YjiE isolated from HOCl stressed cells was identified. On the other hand, mass spectrometry suggested that oxidation of the conserved methionines at position 206 and 230 in YjiE could potentially regulate YjiE activity. Analysis of the activity of mutants mimicking oxidized or reduced methionine did not provide clear and consistent information about their activity. Furthermore, it was difficult to identify further potentially inactive mutants of YjiE, since cells expressing wild type *yjiE* did not show strong and reproducible HOCl-resistance and other assays were not applicable. Thus, it is still not clear how YjiE is activated by HOCl.

In addition, to identify new proteins contributing to the bacterial resistance to $H_2O_2$, an *E.coli* genomic library was screened in this work. A novel conserved *E.coli* protein, **YifE**, with

unknown function and unknown structure was discovered to confer significant resistance to $H_2O_2$. To assess the cellular function of YifE, sequence alignments and structure predictions were performed. They suggested that YifE could be a ribosome related protein or a sigma factor. Several ribosomal proteins were identified as interaction partners of YifE, indicating that YifE is likely to be a ribosome related protein. YifE could associate with 70S ribosomes as well as 50S and 30S ribosomal subunits, and bind to 23S and 16S ribosomal RNA. Furthermore, YifE exerted a positive influence on translation, whereas the ribosome biogenesis and assembly were not affected at all. Deletion of *yifE* rendered cells hypersensitive to treatment with tetracycline, chloramphenicol and spectinomycin, all of which target the ribosome function. This suggests that YifE is a ribosome related protein, which protects cells from $H_2O_2$-killing by potentially promoting stress-impaired translation.

# 2 Introduction

Cells display their optimal growth and function in specific environment. Once this environment changes even a little, cells suffer from this unfavorable condition, referred to as stress. As response, cells employ diverse strategies to adapt to stress.

In the last three decades, cellular stress responses have been intensively studied. Cells have evolved folding helper proteins (i.e., chaperones) to assist the folding of nascent polypeptide chains or to rescue the heat-induced misfolded proteins (*8*). Under acid stress (pH2.5), the acid resistance systems, such as the glutamate-dependent system in *E.coli*, are activated to withstand this challenge (*9*). Meeting osmotic shock, cells modulate, for example, the expression of *omp* genes to regulate the intracellular osmotic balance (*10*, *11*). Oxidative stress occurs upon increasing accumulation of ROS (*4*). Many diseases including neurodegenerative diseases and cancer are accompanied by oxidative stress (*12*, *13*).

## 2.1 ROS and Oxidative Damage

### 2.1.1 ROS

In aerobic organisms, ROS are continuously generated as byproducts during respiration (*1*) [Fig. 2-1]. In addition, ROS can also be produced by the host immune system upon bacterial infection. Myeloperoxidase, which is secreted by activated neutrophils, catalyzes the formation of the bactericidal HOCl (*2*). HOCl is also produced by intestinal mucosal barrier cells to regulate bacterial colonization (*14*). Exogenously, visible or UV light can generated ROS as well. Thus, oxidative stress is an inevitable biological challenge for all organisms.

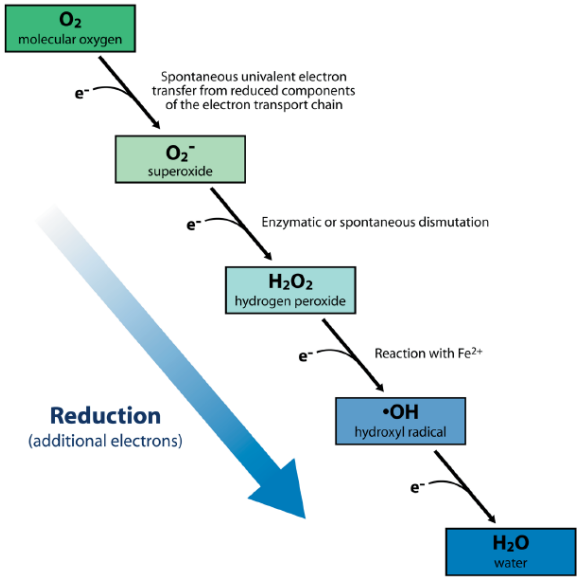


Figure 2-1: Reduction of $O_2$ to $H_2O$. $O_2$ receives one electron to form superoxide. Superoxide can be dismutated to hydrogen peroxide. Hydrogen peroxide reacts further with $Fe^{2+}$ to generate hydroxyl radicals. Finally, this radical is then reduced to water. (Figure from *15*).

### 2.1.2 Oxidative Damage

Since ROS insult cells by modifying various cellular vital components, leading to the loss of their fundamental functions (*4*), an increased cellular level of ROS is threatening to cells.

Being highly reactive, ROS can modify a wide scale of biological molecules such as DNA, RNA, lipids, carbohydrates and proteins (*3*). Owing to their high cellular abundance, proteins are the major target of ROS. Damage or modifications can occur at both the backbone and amino acid side chains (*3*). Especially the sulfur-containing amino acids in protein or iron-sulfur clusters are mainly targeted by ROS (*16*). For example, $O_2^-$ attacks the iron-sulfur cluster in dehydratases by oxidizing the cluster to an unstable state, in which the enzyme loses its catalytic iron atom and becomes inactive (*4*). $H_2O_2$ oxidizes the thiol group in cysteine to sulfenic acid that can either form a disulfide bond with other cysteines/glutathione or be further oxidized to the stable sulfinic and sulfonic acid (*15*) [Fig. 2-2]. Oxidation can also cause irreversible protein carbonylation, which targets proteins for degradation or aggregation (*17*). ·OH is the only ROS that can directly damage most biomolecules at a diffusion-limited rate (*4*). It is formed through the Fenton-reaction, in which ferrous iron

transfers an electron to $H_2O_2$ [Formula 2-1]. ·OH is particularly harmful to DNA because it can introduce lesions in DNA and thereby injuring cells (*18*, *19*).

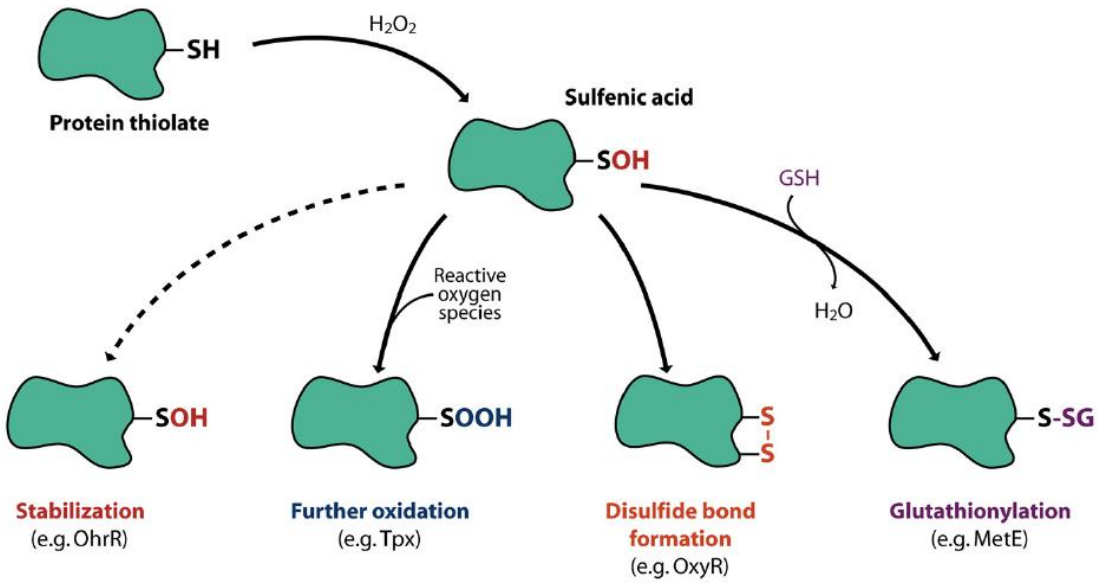


Figure 2-2: Thiol modification of proteins. Hydrogen peroxide can oxidize thiol groups in proteins to a sulfenic acid. This intermediate may be stabilized or further oxidized to sulfinic and sulfonic acid derivatives. Additionally, from sulfenic acid intermediate, an intramoelcular disulfide bridge or a mixed disulfide bond with glutathione can be formed. (Figure from *15*).

Among ROS, HOCl is extremely reactive und it non-selectively modifies all biomolecules especially proteins, leading to largely inactivation of proteins and consequently severe damages to cells (*6*). It is known that HOCl inactivates GroEL, an *E. coli* chaperone essential for the folding of proteins, by oxidizing methionine to methionine sulfoxide and cysteine to cysteic acid (*20*). Besides, HOCl attacks or damages the energy-transducing and transport proteins located in the bacterial plasma membrane giving rise to inactivation of ATPase (*21*) and, as a consequence, decline of the intracellular ATP level (*22*). Furthermore, HOCl is also known to induce protein unfolding. In HOCl challenged *E. coli* cells, a large number of proteins including some essential proteins, aggregate (*23*). HOCl reacts with DNA to form short-lived chloramine (*24*). Disrupting the hydrogen bonds in DNA, this species can cause the dissociation of double-stranded DNA (*24*). Unsaturated fatty acids and cholesterol can be oxidized by HOCl, generating chlorohydrins (*25*). These products can cause destabilization of

membrane structure and exert cytotoxicity to cells (*25*).

$$Fe^{2+} + H_2O_2 \rightarrow Fe^{3+} + \cdot OH + OH^-$$

Formula 2-1: Fenton reaction. $H_2O_2$ oxidizes ferrous iron to ferric iron generating hydroxyl radical and hydroxyl ion.

## 2.2 Cellular Response to Oxidative Stress

The cytoplasm is a highly reducing environment, in which thiol groups in proteins are kept in the reduced state and disulfide bonds are barely formed. Encountering ROS, cells increasingly produce detoxifying enzymes or proteins to maintain the cellular redox homeostasis. Thioredoxin and glutaredoxin systems are two highly conserved pathways, evolved in all organisms to sustain the reducing environment using NADPH as the electron source (*26*). On the other hand, superoxide dismutases (SOD), which catalyze the dismutation of superoxide into oxygen and hydrogen peroxide (*27*), and catalases, which degrade hydrogen peroxide to water and oxygen in the presence of iron, directly devastate ROS (*4, 27*).

However, once the elevated level of ROS exceeds the antioxidant capacity, cells suffer greatly. Under this condition, ROS-specific transcription factors are activated to induce or regulate genes involved in the cellular defense against oxidative stress (*5*).

### 2.2.1 $O^{2-}$-Responsive Transcription Factor SoxR

Upon superoxide stress, the bacterial transcriptional activator SoxR is activated (*28*). SoxR belongs to the MerR family of transcription factors, containing an N-terminal helix-turn-helix DNA binding domain and C-terminal effector binding regions that are specifically recognized by certain effectors (*29*).

Harboring one $[2Fe\text{-}2S]^{2+}$ cluster per monomer, SoxR takes advantage of this iron-sulfur

cluster to sense superoxide and accordingly regulate its activity (*30*). Once exposed to superoxide, the iron-sulfur cluster of SoxR becomes oxidized to $[2Fe\text{-}2S]^{3+}$, being the transcription active form (*5*, *30*) [Fig. 2-3].

The activated SoxR regulates several genes encoding reductases (Fdr, Fpr), manganese superoxide dismutase (SodA), endonuclase IV (Nfo), an efflux pump (AcrAB), an untranslated small RNA (MicF) that down regulates the expression of the porin OmpF and protein (YggX*)*, which is potentially involved in the protection of iron-sulfur cluster containing proteins from oxidative damage (*5*). The products of the induced SoxR regulon contribute together to avoiding or repairing oxidative damages using different mechanisms, which includes scavenging of oxidants (SodA), DNA repair (Nfo), re-reduction of oxidized metals in prosthetic groups (Fdr, Fpr), reconstitution of the NADPH pool, reduced permeability (MicF) and excretion of toxicants (efflux pumps) (*5*). Recently, the structure of DNA bound SoxR has been solved (*31*) [Fig. 2-4].

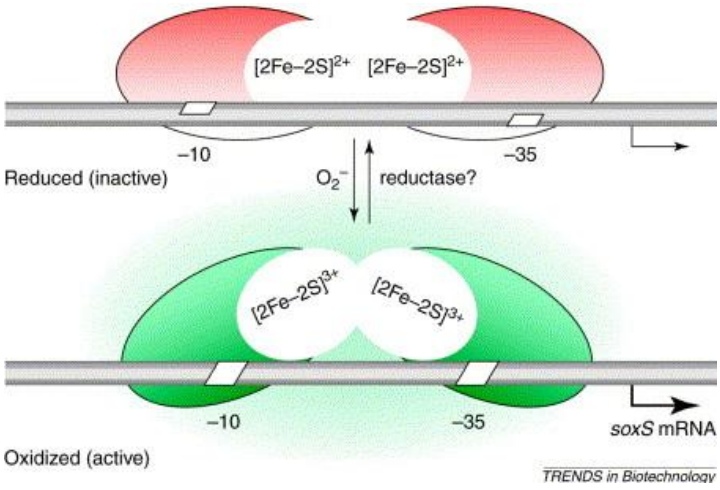


Figure 2-3: Oxidative activation of SoxR by $O^{2-}$. $O^{2-}$ oxidizes the iron-sulfur clusters in SoxR, leading to a conformational change of this protein. This active SoxR modulates the transcription of *soxS*. (Figure from *5*).

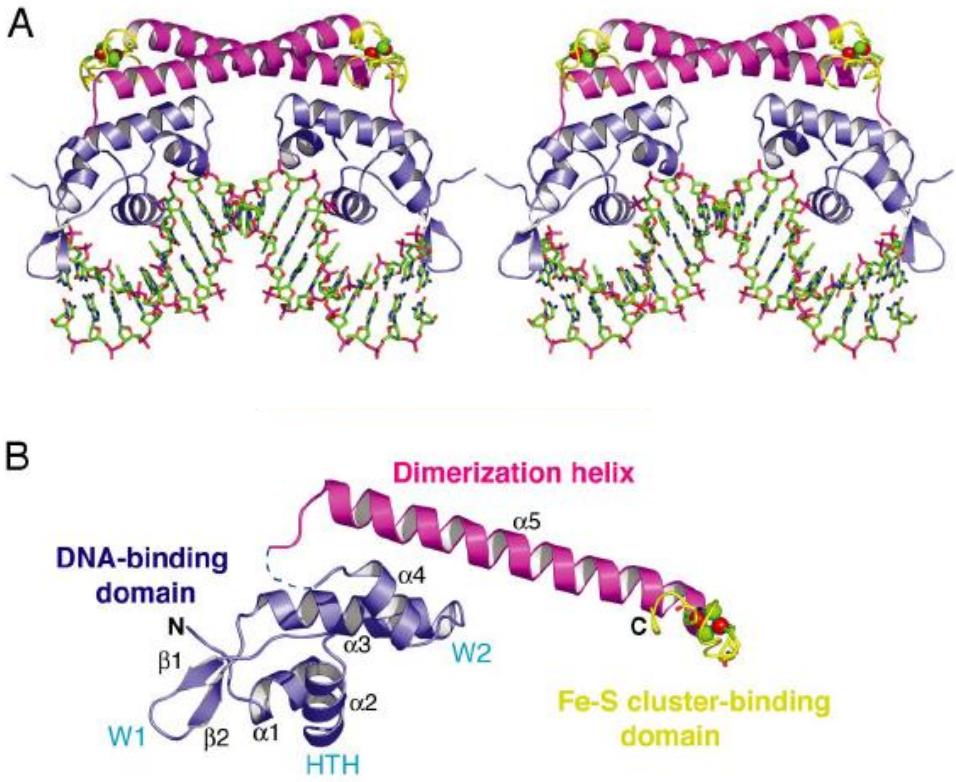


Figure 2-4: Structure of the SoxR-DNA complex. The overall structure of the complex is shown in A and the structure of the SoxR monomer consisting of five alpha helices and two beta sheets is shown in B. (Figure from *31*).

### 2.2.2 $H_2O_2$-Specific Transcription Factor OxyR

OxyR is an *E.coli* transcription factor, which is specifically responsive to $H_2O_2$-stress (*32*). OxyR belongs to the large prokaryotic family of LTTRs. LTTRs typically contain an N-terminal DNA-binding domain comprising a helix-turn-helix motif and two regulatory domains that undergo conformational changes upon binding of a so-called co-inducer. Being 300 amino acids long in length, LTTRs can bind to their own promoter DNA and autoregulate their own transcription (*33*).

Two invariant redox-sensitive cysteines (Cys-199 and Cys-208) in OxyR mediate the redox-dependent reversible conformational transition from the inactive state of OxyR to the active state (*34*) [Fig. 2-5]. Upon oxidation by $H_2O_2$, Cys-199 and Cys-208 form an intramolecular disulfide bond, which activates OxyR (*27*). The active OxyR specifically

regulates genes including *katG*, *trxC*, *gorA* and *grxA* (*35*). *katG* encodes catalase that catalyzes the decomposition of $H_2O_2$ to water and oxygen (*36*). The gene products of *trxC*, *gorA* and *grxA* are components of the thioredoxin and glutaredoxin systems that evolved to reduce disulfide bonds in proteins and preserve the reducing environment in the cytosol (*26*, *37*). All these products devote to diminish $H_2O_2$-triggered damages in cells. Of note, there are several OxyR-independent genes up-regulated upon this stress (*35*), indicating other unknown pathways involved in protecting bacteria from $H_2O_2$-induced damage.

The crystal structures of both the reduced form and oxidized form have been solved [Fig. 2-6] (*34*).

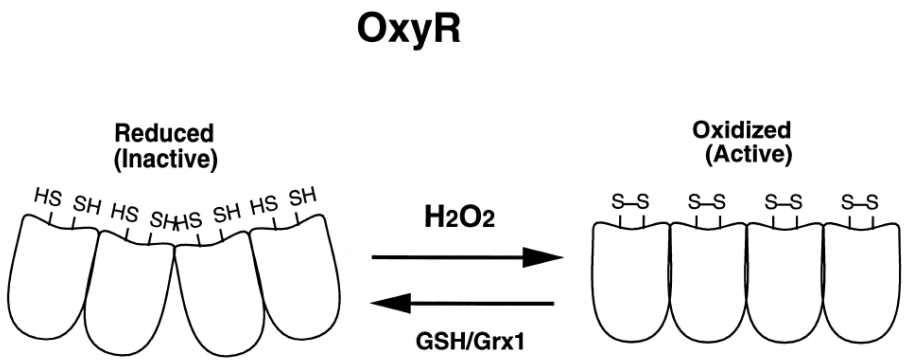


Figure 2-5: Model for OxyR activation and deactivation. OxyR exists as a tetramer. In the reduced form, the Cys-199 and Cys-208 are present as free thiol groups in the monomer. Once exposed to $H_2O_2$, Cys-199 and Cys-208 form an intramolecular disulfide bond leading to a conformational change and OxyR is consequently activated. In the presence of GSH and Grx1, the activated OxyR tetramer containing disulfide bonds can be reduced to form the inactive state. (Figure from *38*).

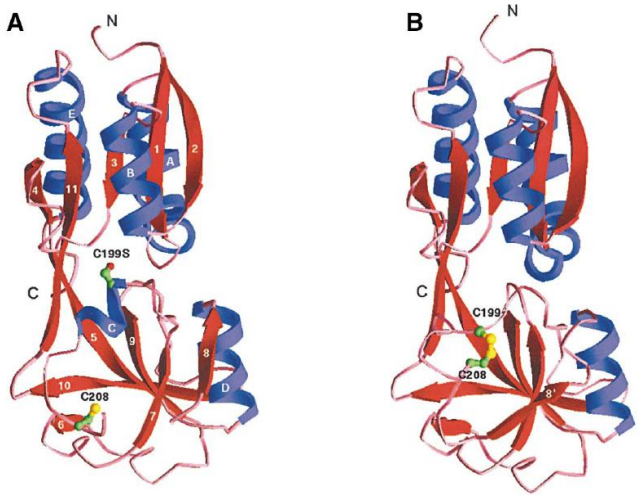


Figure 2-6: Structure of the OxyR regulatory domain. Left is the reduced form of OxyR

monomer (A) and right is the oxidized form (B). The redox-active cysteine-199 and cysteine-208 are shown in yellow and green. The beta stands are shown in red and alpha helices in blue. In the reduced form, Cys-199 and Cys-208 are present as free thiols, but in the oxidized form, they form a disulfide bond. (Figure from *34*).

### 2.2.3 HOCl-Responsive Transcription Factor YjiE

In contrast to $O_2^-$ and $H_2O_2$, HOCl nonspecifically oxidizes various macromolecules and causes wide damage to cells (*6*). However, the cellular response to this highly reactive oxidant has not been intensively studied yet. It has been reported that HOCl can trigger the heat shock response and *soxR* activation (*39*). The redox-regulated *E. coli* chaperone Hsp33 is specifically activated by HOCl, which oxidizes the C-terminal cysteines to intramolecular disulfide bonds and unfolds the C-terminal domain, thereby activating Hsp33 (*22*). Active Hsp33 efficiently protects cellular proteins from irreversible aggregation and increases the viability of *E. coli* cells during HOCl stress (*22*, *23*). Nevertheless, no specific HOCl-responsive transcriptional regulator had been identified in any organism.

Our lab identified the first HOCl-responsive *E.coli* transcription factor YjiE by a genomic library screen to confer HOCl resistance to *E. coli* cells (*7*). Although YjiE was described as cell density-dependent motility repressor, QseD (*40*), cells expressing *yjiE*, in our hand, did not show any effect on bacterial motility but highly resistance to HOCl compared to the cells lacking *yjiE* (*7*). YjiE is conserved in proteobacteria and eukaryotes. Like OxyR, YjiE belongs to the family of LTTRs. Conserved in LTTRs, YjiE comprises an N-terminal DNA binding domain, the co-inducer domain, and the C-terminal oligomerization domain (*41*). However, different from most LTTRs, which usually form dimers and tetramers such as OxyR (*34*), CysB (*42*), NAC (*43*), YjiE is a dodecamer and forms mainly hexagonal ring-like structure (*7*, *44*) [Fig. 2-7]. In cells, this dodecameric state likely serves as the storage form of YjiE, which dissociates to small oligomers including dimers and tetramers upon HOCl challenge and DNA-binding (*44*). YjiE specifically regulates 48 genes upon exposure to HOCl (*44*). These genes encode proteins involved in methionine biosynthesis (e.g., *metN*, *metK*), iron acquisition (e.g., *entC*, *entH*, *fecCDE*), metabolism (e.g., *pflB*, *cysH*), and transport (e.g.,

*oppBD*, *manYZ*) (*44*). Since HOCl preferentially oxidizes methionines and consequently depletes them (*3*, *6*), up-regulation of genes involved in methionine biosynthesis supplies the methionine pool for protein synthesis. Furthermore, elevated free iron levels in cells cause increased generation of ROS and subsequent oxidative damage (*45*). Therefore, down-regulation of genes responsible for iron acquisition reduces the iron load in cells and accordingly abates cell suffering from oxidative stress.

Despite that YjiE confers HOCl-resistance by regulating genes that eliminate HOCl-derived damage, the question of how YjiE is activated in cells upon HOCl stress is still open.

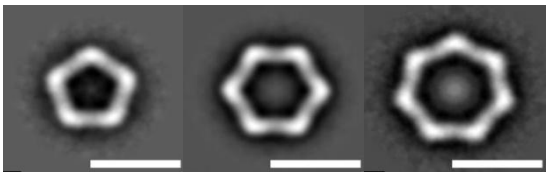

Figure 2-7: YjiE structures observed by transmission electron microscopy. A main population of YjiE forms hexagonal ring structure (75 %) in addition to pentagonal (15 %) and heptagonal ring structure (10 %). (Figure from *44*).

## 2.3 Objectives

Studying bacterial response to oxidative stress, this PhD work focuses on i) unraveling the activation mechanism of the HOCl-responsive transcription factor YjiE and ii) exploration of new proteins participating in the bacterial defense against oxidative stress, above all, $H_2O_2$ stress.

### 2.3.1 Unraveling the Activation Mechanism of YjiE

Typically, LTTRs are activated by a co-inducer, which leads to the activation or repression of LTTR-regulated genes (*41*). For example, the LTTR CysB is activated by its

co-inducer N-acetylserine to regulate genes involved in cysteine biosynthesis (*46*) and BenM, with two effectors benzoate and muconate bound, turns to be transcriptionally active (*47*). On the other hand, modification of amino acids upon stress could also modulate the activity of LTTR. For example, $H_2O_2$ oxidizes the active site cysteines to form disulfide bond and thereby activates OxyR (*34*).

Being an LTTR, YjiE could be activated either by binding of the co-inducer or by modification of conserved amino acids. To elucidate the exact activation mechanism of YjiE, both possibilities were analyzed in this work.

### 2.3.2 Identification of New Proteins Involved in $H_2O_2$ response

The bacterial response to $H_2O_2$ is dominantly driven by activation of the $H_2O_2$-specific transcription factor OxyR (*32*). However, several genes are regulated upon $H_2O_2$ in an OxyR-independent manner (*35*). Examples are *tnaA*, *tnaL*, which encode proteins implicated in amino acid catabolism, and *raiA* that encodes a ribosome associated inhibitor (*35*). This indicates that in addition to the OxyR-mediated pathway, there must be other pathways, which contribute to cellular adaptation to $H_2O_2$ stress. So far, many other proteins have been identified to be involved in the bacterial response to $H_2O_2$. For instance, exposed to $H_2O_2$ in combination with heat, the chaperone Hsp33 becomes active by formation of C-terminal intra-molecular disulfide bonds to protect proteins from unfolding and aggregation (*22*). Bacterial ribonucleases and polynucleotide phosphorylase are responsible for degradation of damaged RNA, in which lesions are introduced due to 8-hydroxyguanine, an $H_2O_2$-oxidized form of guanine (*48*, *49*). In addition, under $H_2O_2$ or HOCl challenge, *ompW*, which encodes a small outer membrane porin, is negatively regulated to prevent the influx of these oxidants (*50*). Furthermore, the quality control systems such as tmRNA system play also a role by rescuing ROS-induced stalled ribosomes (*51*).

In order to shed light on novel bacterial protection mechanisms under oxidative stress, new contributors (proteins) to bacterial resistance to $H_2O_2$ were identified using an *E.coli* genomic library. One novel *E.coli* protein, YifE, without any predicted function was identified

to confer great $H_2O_2$-resistance. To disclose how this protein protects cells from $H_2O_2$-originated insults, this protein was characterized and its potential function in cells was analyzed.

# 3 Material and Methods

## 3.1 Materials

### 3.1.1 Chemicals

| | |
|---|---|
| Acetone | Roth (Karlsruhe, Germany) |
| Acetonitrile | Roth (Karlsruhe, Germany) |
| Acidic Acid | Roth (Karlsruhe, Germany) |
| Agar | Merck (Darmstadt, Germany) |
| Agarose | Serva (Heidelberg, Germany) |
| Ammonium Chloride | Merck (Darmstadt, Germany) |
| Ampicillin | Roth (Karlsruhe, Germany) |
| Arabinose | Sigma (St. Louis, USA) |
| ATTO488 Maleimide | ATTO Tec (Siegen, Germany) |
| Boric Acid | Roth (Karlsruhe, Germany) |
| Bovine Serum Albumin | Sigma (St. Louis, USA) |
| Chloramphenicol | Roth (Karlsruhe, Germany) |
| Diamide | Sigma (St. Louis, USA) |
| Ethanol | Roth (Karlsruhe, Germany) |
| Ethansulfonic Acid (Hepes) | Roth (Karlsruhe, Germany) |
| Ethylendiamintetraacidic Acid (EDTA) | Merck (Darmstadt, Germany) |
| Formaldehyde | Roth (Karlsruhe, Germany) |
| Hi-Di™ Formamide | Applied Biosystems (Manchester, UK) |
| Glycerin | Roth (Karlsruhe, Germany) |
| Hydrogen Peroxide (H2O2) | Sigma (St. Louis, USA) |
| Imidazole | Sigma (St. Louis, USA) |
| Isopropyl-β-D-Thiogalaktopyranosid (IPTG) | Roth (Karlsruhe, Germany) |
| Kanamycin | Roth (Karlsruhe, Germany) |
| LB-Medium (Lennox) | Roth (Karlsruhe, Germany) |
| Magnesium Chloride Hexahydrate | Merck (Darmstadt, Germany) |
| β-Mercaptoethanol | Merck (Darmstadt, Germany) |
| Methanol | Roth (Karlsruhe, Germany) |
| Methionine | Sigma (St. Louis, USA) |
| Milk Powder | Roth (Karlsruhe, Germany) |
| Paraquat | Sigma (St. Louis, USA) |
| Potassium Chloride | Merck (Darmstadt, Germany) |
| Protease Inhibitor HP | Serva (Heidelberg, Germany) |
| Roti®-Phenol pH4 | Roth (Karlsruhe, Germany) |
| [35S]Methionine | Hartmann Analytic (Braunschweig, Germany) |

| | |
|---|---|
| Sodium Carbonate | Roth (Karlsruhe, Germany) |
| Sodium Dihydrogen Phosphat Monohydrate | Merck (Darmstadt, Germany) |
| Sodium Dodecyl Sulfate (SDS) | Merck (Darmstadt, Germany) |
| Sodium Chloride | Merck (Darmstadt, Germany) |
| Sodium Hydroxide | Merck (Darmstadt, Germany) |
| Sodium Hypochlorite (NaOCl) | Sigma (St. Louis, USA) |
| Sodium Thiosulfate | Merk (Darmstadt, Germany) |
| Spectinomycin | Roth (Karlsruhe, Germany) |
| Sucrose | Sigma (St. Louis, USA) |
| Tetracycline | Roth (Karlsruhe, Germany) |
| Trichloroacetic Acid | Roth (Karlsruhe, Germany) |
| Tris-(Hydroxymethyl)-Aminomethan (Tris) | Roth (Karlsruhe, Germany) |
| Tween20 | Merck (Darmstadt, Germany) |

All other chemicals not listed here are provided either by Merck (Darmstadt, Germany) or by Roth (Karlsruhe, Germany).

### 3.1.2 Size and Molecular Mass Standards

| | |
|---|---|
| pEQgold 1 kb DNA Ladder | Peqlab (Erlangen, Germany) |
| Mark12TM Unstained Standard | Invitrogen (Calsbad, USA) |
| GeneScan™-500 LI™Size Standard | Applied Biosystems (Manchester, UK) |

### 3.1.3 Enzymes and Antibodies

| | |
|---|---|
| *BamH*I-Restriction Enzyme | New England Biolabs (Ipswich, England) |
| Catalase | Sigma (St. Louis, USA) |
| DNase I (Powder) | Roche (Mannheim, Germany) |
| RNase free DNase I (1 U/µl) | New England Biolabs (Ipswich, England) |
| *Dpn*I-restriction enzyme | New England Biolabs (Ipswich, England) |
| *Go-taq* DNA Polymerase | Promega (Madison, USA) |
| *Hind*III-Restriction Enzyme | New England Biolabs (Ipswich, England) |
| Lysozyme | Sigma (St. Louis, USA) |
| *NdeI*-restriction enzyme | New England Biolabs (Ipswich, England) |
| *Phusion* High-Fidelity DNA Polymerase | New England Biolabs (Ipswich, England) |
| *Pwo* DNA Polymerase | Roche (Mannheim, Germany) |
| *Pfu* DNA Polymerase | Stratagen (La Jolla, USA) |
| T4-DNA Ligase | Promega (Madison, USA) |
| Thrombin (bovine, high activity) | CalBiochem (Merck, Darmstadt, Germany) |
| Monoclonal IgG-Peroxidase Conjugate against Rabbit-IgG (Goat) | Sigma (St. Louis, USA) |

| | |
|---|---|
| Polyclonal Serum against YjiE | Pineda (Berlin, Germany) |
| Polyclonal Serum against YifE | Pineda (Berlin, Germany) |
| Monoclonal Anti-poly-Histidine (mouse) | Sigma (St. Louis, USA) |
| Monoclonal IgG-Peroxidase Conjugate against Mouse-IgG | Sigma (St. Louis, USA) |
| Monoclonal Anti-Acetylated-Lysine (mouse) | Cell Signaling (Danvers, USA) |

### 3.1.4 Kits

| | |
|---|---|
| Wizard® SV Gel and PCR Clean-Up System | Promega (Madison, USA) |
| Wizard® Plus SV Minipreps System | Promega (Madison, USA) |
| SV Total RNA Isolation System | Promega (Madison, USA) |
| Brilliant III Ultra-Fast SYBR® Green QRT-PCR Master Mix | Agilent (Santa Clara, USA) |
| ECL-Western Blot Detection System | Amersham (Amersham, UK) |
| Oxyblot™ Protein Oxidation Detection Kit | Millipore (Billerica, USA) |

### 3.1.5 Chromatography

| | |
|---|---|
| His-Trap FF Column (5 ml) | GE Healthcare (Amersham, UK) |
| Q-Sepharose FF Column (5 ml) | GE Healthcare (Amersham, UK) |
| Superdex 75 Column (330 ml) | GE Healthcare (Amersham, UK) |
| Superose 6 Column (24 ml) | GE Healthcare (Amersham, UK) |
| NAP5 Desalting Column (5 ml) | GE Healthcare (Amersham, UK) |
| PD10 Desalting Column (10 ml) | GE Healthcare (Amersham, UK) |
| Bischoff NPS C18 (0.232 ml) | GE Healthcare (Amersham, UK) |
| Biosuite 450 (8 µm) | GE Healthcare (Amersham, UK) |
| Chromolith® RP-8e (100-4.6 mm) | Merck (Darmstadt, Germany) |
| Hitrap NHS activated HP Column (1 ml) | GE Healthcare (Amersham, UK) |

### 3.1.6 Additional Materials

**Tubes, 96-well plates, Petri Dishes**

| | |
|---|---|
| Cryo Tube (1.5 ml) | Nalgene (Roskilde, Denmark) |
| PCR Reaction Tube (0.2 ml) | Nerbe Plus (Winsen/Luhe, Germany) |
| Reaction Tube (0.5 ml, 1.5 ml, 2 ml) | Nerbe Plus (Winsen/Luhe, Germany) |
| Greiner Tube (15 ml, 50 ml) | Greiner&Söhne (Nürtingen, Germany) |
| 96-Well Sterile Microtiter Plate | Sarstedt (Nümbrecht, Germany) |
| Petri Dish (94 mm) | Greiner&Söhne (Nürtingen, Germany) |
| Beckman Centrifuge Tube (ref. 326819) | Beckman Coulter (Krefeld, Germany) |

**Cuvettes**

| | |
|---|---|
| Plastic Cuvette 10 x 4 x 45 mm | Aktiencompany (Nuembrecht, Germany) |
| Fluorescence Cuvette 105.250-QS | Hellma (Muellheim, Germany) |

**Membranes, Filters, Centricons**

| | |
|---|---|
| Sterile Filter (0.2 µm) | Zefa (Munich, Germany) |
| Cellulose Acetate Filter (0.45 µm) | Sartorius Stedim (Göttingen, Germany) |
| Cellulose Nitrate Filter (0.2 µm) | Whatman (Maidstone, UK) |
| Centricon YM10 (MWCO 10kDa) | Millipore (Bedford, USA) |
| Microcon® Centrifugal Filter Units | Millipore (Bedford, USA) |

**Precasted Gels, Western Blot Materials**

| | |
|---|---|
| Imobiline Dry Strip pH 4-7, 12 cm | GE Healthcare (Amersham, UK) |
| TBE-Gel (6 %) | Invitrogen (Carlsbad, USA) |
| Tris-Tricine Gel (10-20 %) | Invitrogen (Carlsbad, USA) |
| Tris-Tricine Gel (16.5 %) | Bio-Rad (Munich, Germany) |
| Serva Gel™ Neutral pH7.4 Gradient | Serva (Heidelberg, Germany) |
| Immobile-P (PVDF)-Membrane | Millipore (Bedford, USA) |
| Filter Paper | Whatman (Maidstone, UK) |
| X-Omat AR Film (XAR-5, 13 x 18 cm) | Kodak (Rochester, USA) |

**RNase free materials**

| | |
|---|---|
| RNase Inhibitor Plus (40 U/µl) | Promega (Madison, USA) |
| RNase Free Reaction Tube (1.5 ml) | Eppendorf (Hamburg, Germany) |
| RNase Free Pipette Tips | Eppendorf (Hamburg, Germany) |
| RNase Zap™ Cleaning Agent | Sigma (St. Louis, USA) |
| qRT-PCR 96-Well Plate | Nerbe Plus (Winsen/Luhe, Germany) |
| Sealing Film for qRT-PCR 96-Well Plate | Nerbe Plus (Winsen/Luhe, Germany) |

## 3.2 Plasmids, Strains, Constructs and Primers

Table 2-1: Plasmids used in this work

| Plasmid Name | Parental Plasmid | Insert | Resistance | Comment |
|---|---|---|---|---|
| pJW2 | pBAD22 | | Amp200 | NcoI restriction site mutated to *BamH*I |
| pUC18 | | | | Lab stock |
| pKD3 | | | | Lab stock; Datsenko and Wanner (2000) |
| pKD46 | | | | Lab stock; Datsenko and Wanner (2000) |

| | | | | |
|---|---|---|---|---|
| pKMG9 | pJW2 | *yjiE* | | from K. Gebendorfer |
| pKMG10 | pJW2 | promoter-*yjiE* | Amp200 | from K. Gebendorfer |
| pYL22 | pET28a(+) | *yifE* | Kan100 | via *Nde*I/*Hind*III |
| pYL23 | pJW2 | *yifE* | Amp200 | via *Nde*I/*Hind*III |
| pYL24 | pJW2 | promoter-*yjiE*_S204A | Amp200 | via *Nde*I/*Hind*III |
| pYL25 | pJW2 | promoter-*yjiE*_M206A | Amp200 | via *Nde*I/*Hind*III |
| pYL26 | pJW2 | promoter-*yjiE*_R208A | Amp200 | via *Nde*I/*Hind*III |
| pYL27 | pJW2 | promoter-*yjiE*_S228A | Amp200 | via *Nde*I/*Hind*III |
| pYL28 | pJW2 | promoter-*yjiE*_S229A | Amp200 | via *Nde*I/*Hind*III |
| pYL29 | pJW2 | promoter-*yjiE*_M230A | Amp200 | via *Nde*I/*Hind*III |
| pYL30 | pJW2 | promoter-*yjiE*_S231A | Amp200 | via *Nde*I/*Hind*III |
| pYL31 | pJW2 | promoter-*yjiE*_K235A | Amp200 | via *Nde*I/*Hind*III |
| pYL32 | pJW2 | promoter-*yjiE*_L223A | Amp200 | via *Nde*I/*Hind*III |
| pYL33 | pJW2 | promoter-*yjiE*_L234A | Amp200 | via *Nde*I/*Hind*III |
| pYL34 | pJW2 | promoter-*yjiE*_E232A | Amp200 | via *Nde*I/*Hind*III |
| pYL35 | pJW2 | promoter-*yjiE*_Y205A | Amp200 | via *Nde*I/*Hind*III |
| pYL36 | pJW2 | promoter-*yjiE*_G207A | Amp200 | via *Nde*I/*Hind*III |
| pYL43 | pJW2 | promoter-*yjiE*_A204-208 | Amp200 | via *Nde*I/*Hind*III |
| pYL46 | pJW2 | promoter-*yjiE*_A228-235 | Amp200 | via *Nde*I/*Hind*III |
| pYL47 | pET28a(+) | *yjiE*_A204-208 | Amp200 | via *Nde*I/*Hind*III |
| pYL62 | pUC18 | *yjiE* | Amp200 | via *BamH*I |
| pYL64 | pJW2 | *yjiE*_M206I | Amp200 | via *Nde*I/*Hind*III |
| pYL65 | pJW2 | *yjiE*_M230I | Amp200 | via *Nde*I/*Hind*III |
| pYL66 | pJW2 | *yjiE*_M284I | Amp200 | via *Nde*I/*Hind*III |
| pYL72 | pJW2 | *yjiE*_M206Q | Amp200 | via *Nde*I/*Hind*III |
| pYL73 | pJW2 | *yjiE*_M230Q | Amp200 | via *Nde*I/*Hind*III |
| pYL74 | pJW2 | *yjiE*_M284Q | Amp200 | via *Nde*I/*Hind*III |
| pYL77 | pET11a | *yjiE*_M206Q | Amp200 | via *Nde*I/*BamH*I |
| pYL79 | pET11a | *yjiE*_M206I | Amp200 | via *Nde*I/*BamH*I |
| pYL83 | pET11a | *yjiE*_M230I | Amp200 | via *Nde*I/*BamH*I |
| pYL84 | pET11a | *yjiE*_M230Q | Amp200 | via *Nde*I/*BamH*I |
| pYL90 | pET11a | *yjiE*_M284I | Amp200 | via *Nde*I/*BamH*I |
| pYL91 | pET11a | *yjiE*_M284Q | Amp200 | via *Nde*I/*BamH*I |
| pYL94 | pJW2 | *yifE*_K15A | Amp200 | via *Nde*I/*Hind*III |
| pYL95 | pJW2 | *yifE*_K15R | Amp200 | via *Nde*I/*Hind*III |
| pYL96 | pJW2 | *yifE*_K15Q | Amp200 | via *Nde*I/*Hind*III |

Abbreviation: 200 µg/ml Ampicillin (Amp200), 100 µg/ml Kanamycin (Kan100).

Table 2-2: Strains used in this work

| Strain Name | Genetic Marker | Resistance | Quelle/Reference |
|---|---|---|---|
| XL1blue | *△(mcrA)183 △(mcrCB-hsdSMR-mrr)173 endA1 supE44 thi-1 recA1 gyrA96 lac [F'proAB lacI$^q$Z△M15 Tn10 (Tet$^R$)]* | (Tet35) | Lab stock; Stratagene (La Jolla, USA) |
| XL10Gold | *endA1 glnV44 recA1 thi-1 gyrA96 relA1 lac Hte Δ(mcrA)183 Δ(mcrCB-hsdSMR-mrr)173 tet$^R$ F'[proAB lacI$^q$ZΔM15 Tn10(Tet$^R$ Amy Cm$^R$)]* | (Tet35, Cm25) | Lab stock; Stratagene (La Jolla, USA) |
| MC4100 (BB7222) | *F- araD139△(argF-lac) U169 rspL150 relA1 flb85301 deoC1 ptsF25 rbsR* | | Lab stock; Tomoyasu et al., 2001 |
| BB7224 | *BB7222 rpoH::Km* | Kan100 | Lab stock; Tomoyasu et al., 2001 |
| C600 | *thr leu thi lac4 rpsL supE (F$^-$)* | | Lab stock; *E.coli* stock center |
| BL21(DE3) gold | *F$^-$ ompT hsdS(rB- mB-) dcm$^+$ Tatr gal λ(DE3) endA The* | | Lab stock; Stratagene (La Jolla, USA) |
| JW212 | BB7224 pUC18 | Amp200 | Lab stock |
| JW230 | BB7224 pUC18-library clone_*yjiE* | Amp200 | Lab stock |
| YLe112 | BB7224 pBAD22 | Amp200 | this work |
| YLe113 | BB7224 pBAD22-promoter-*yjiE* | Amp200 | this work |
| YLe126 | BB7224 pYL24 | Amp200 | this work |
| YLe127 | BB7224 pYL25 | Amp200 | this work |
| YLe128 | BB7224 pYL26 | Amp200 | this work |
| YLe129 | BB7224 pYL27 | Amp200 | this work |
| YLe130 | BB7224 pYL28 | Amp200 | this work |
| YLe131 | BB7224 pYL29 | Amp200 | this work |
| YLe132 | BB7224 pYL30 | Amp200 | this work |
| YLe133 | BB7224 pYL31 | Amp200 | this work |
| YLe134 | BB7224 pYL32 | Amp200 | this work |
| YLe135 | BB7224 pYL33 | Amp200 | this work |
| YLe137 | BB7224 pYL34 | Amp200 | this work |
| YLe165 | BB7224 pYL35 | Amp200 | this work |
| YLe166 | BB7224 pYL36 | Amp200 | this work |
| YLe173 | BB7224 pYL43 | Amp200 | this work |
| YLe176 | BB7224 pYL46 | Amp200 | this work |
| YL179 | BL21(DE3) pYL47 | Kan100 | this work |
| YLe210 | BB7224 pUC18-*yjiE* | Amp200 | this work |
| YLe218 | C600 *yjiE::Cm* pBAD22 | Amp200 | this work |
| YLe219 | C600 *yjiE::Cm* pBAD22-*yjiE* | Amp200 | this work |
| YLe220 | C600 *yjiE::Cm* pYL64 | Amp200 | this work |
| YLe221 | C600 *yjiE::Cm* pYL65 | Amp200 | this work |

| | | | |
|---|---|---|---|
| YLe222 | C600 *yjiE::Cm* pYL66 | Amp200 | this work |
| YLe228 | C600 *yjiE::Cm* pYL72 | Amp200 | this work |
| YLe229 | C600 *yjiE::Cm* pYL73 | Amp200 | this work |
| YLe230 | C600 *yjiE::Cm* pYL74 | Amp200 | this work |
| YLe247 | BL21(DE3) pYL77 | Kan100 | this work |
| YLe248 | BL21(DE3) pYL79 | Kan100 | this work |
| YLe253 | BL21(DE3) pYL83 | Kan100 | this work |
| YLe254 | BL21(DE3) pYL84 | Kan100 | this work |
| YLe268 | BL21(DE3) pYL90 | Kan100 | this work |
| YLe269 | BL21(DE3) pYL91 | Kan100 | this work |
| YLe245 | MC4100 *yifE::Cm* | (Cm25) | this work |
| YLe278 | MC4100 *yifE::Cm* pBAD22 | Amp200 | this work |
| YLe279 | MC4100 *yifE::Cm* pYL23 | Amp200 | this work |
| YLe280 | MC4100 *yifE::Cm* pYL94 | Amp200 | this work |
| YLe281 | MC4100 *yifE::Cm* pYL95 | Amp200 | this work |
| YLe282 | MC4100 *yifE::Cm* pYL96 | Amp200 | this work |
| YLe287 | BL21(DE3) *yifE::Cm* pYL22 | Kan100 | this work |

Abbreviation: 25 µg/ml tetracycline (Tet25), 35 µg/ml chloramphenicol (Cm35), 200 µg/ml Ampicillin (Amp200), 100 µg/ml Kanamycin (Kan100).

Table 2-3: Primers used in this work.

| **Primer Name** | **Sequence 5' → 3'** | **Assay** |
|---|---|---|
| *yifE*-Fw | ggaattccatatggcggaaagctttacgacgac | cloning |
| *yifE*-Rv | cccaagcttggatccttaatcgtcagaatcggtgtag | |
| Del-*yifE*-Fw | gaattaggagcgtgcaggatggcggaaagcttttgtgtaggctggagctgctc | generation of *yifE* deletion strain |
| Del-*yifE*-Rv | catttcgccctttttattaatcgtcagaatccatatgaatatcctccttag | |
| Ctr-*yifE*-Fw | cagatagagcgattcagccgc | |
| Ctr-*yifE*-Rv | gaacactgatccatctgggg | |
| QC1-*yjiE*_S204A-Fw | gaattacagccgcaacgcgtacatggggcgattg | site-directed mutagenesis |
| QC1-*yjiE*_S204A-Rv | gaatcgccccatgtacgcgttgcggctgtaattc | |
| QC2-*yjiE*_Y205A-Fw | cagccgcaactccgcgatggggcgattg | |
| QC2-*yjiE*_Y205A-Rv | caatcgccccatcgcggagttgcggctg | |
| QC3-*yjiE*_M206A-Fw | gccgcaactcctacgcggggcgattgattaatc | |
| QC3-*yjiE*_M206A-Rv | gattaatcaatcgccccgcgtaggagttgcggc | |
| QC4-*yjiE*_G207A-Fw | cgcaactcctacatggcgcgattgattaatcgc | |
| QC4-*yjiE*_G207A-Rv | gcgattaatcaatcgcgccatgtaggagttgcg | |
| QC5-*yjiE*_R208A-Fw | ctcctacatgggggcgttgattaatcgcacc | |
| QC5-*yjiE*_R208A-Rv | ggtgcgattaatcaacgcccccatgtaggag | |
| QC6-*yjiE*_S228A-Fw | gcacctttttgtcgcgtcgatgagcgagc | |
| QC6-*yjiE*_S228A-Rv | gctcgctcatcgacgcgacaaaaaaggtgc | |

| | | |
|---|---|---|
| QC7-*yjiE*_S229A-Fw | cctttttgtctctgcgatgagcgagcttttaaag | |
| QC7-*yjiE*_S229A-Rv | ctttaaaagctcgctcatcgcagagacaaaaaagg | |
| QC8-*yjiE*_M230A-Fw | ctttttgtctcttcggcgagcgagcttttaaag | |
| QC8-*yjiE*_M230A-Rv | ctttaaaagctcgctcgccgaagagacaaaaaag | |
| QC9-*yjiE*_S231A-Fw | ctttttgtctcttcgatggcggagcttttaaagcag | |
| QC9-*yjiE*_S231A-Rv | ctgctttaaaagctccgccatcgaagagacaaaaaag | |
| QC10-*yjiE*_E232A-Fw | gtctcttcgatgagcgcgcttttaaagcaggttg | |
| QC10-*yjiE*_E232A-Rv | caacctgctttaaaagcgcgctcatcgaagagac | |
| QC11-*yjiE*_L233A-Fw | cttcgatgagcgaggcgttaaagcaggttgcc | |
| QC11-*yjiE*_L233A-Rv | ggcaacctgctttaacgcctcgctcatcgaag | |
| QC12-*yjiE*_L234A-Fw | cgatgagcgagcttgcgaagcaggttgccctc | |
| QC12-*yjiE*_L234A-Rv | gagggcaacctgcttcgcaagctcgctcatcg | |
| QC13-*yjiE*_K235A-Fw | gatgagcgagcttttagcgcaggttgccctcgac | |
| QC13-*yjiE*_K235A-Rv | gtcgagggcaacctgcgctaaaagctcgctcatc | |
| QC14-*yjiE*_M206Q-Fw | gccgcaactcctaccaggggcgattgattaat c | |
| QC14-*yjiE*_M206Q-Rv | gattaatcaatcgcccctggtaggagttgcggc | |
| QC14-*yjiE*_M206I-Fw | gccgcaactcctacatcgggcgattgattaatc | |
| QC14-*yjiE*_M206I-Rv | gattaatcaatcgcccgatgtaggagttgcggc | |
| QC15-*yjiE*_M230Q-Fw | ctttttgtctcttcgcagagcgagcttttaaag | |
| QC15-*yjiE*_M230Q-Rv | ctttaaaagctcgctctgcgaagagacaaaaaag | |
| QC15-*yjiE*_M230I-Fw | ctttttgtctcttcgatcagcgagcttttaaag | |
| QC15-*yjiE*_M230I-Rv | ctttaaaagctcgctgatcgaagagacaaaaaag | |
| QC16-*yjiE*_M284Q-Fw | cggatgaatacccgccagaatcccgttgccgaac | |
| QC16-*yjiE*_M284Q-Rv | gttcggcaacgggattctggcgggtattcatccg | |
| QC16-*yjiE*_M284I-Fw | cggatgaatacccgcatcaatcccgttgccgaac | |
| QC16-*yjiE*_M284I-Rv | gttcggcaacgggattgatgcgggtattcatccg | |
| *tufB*3-Fw | gtctaaagaaaagtttgaacgtacaaaaccg | quantitative Real-Time PCR |
| *tufB*301-Rv | cgtccatctgcgcagcaccggtgatc | |
| *yjiE3*-Fw | ggatgactgtggtgcgattttgcataatattg | |
| *yjiE*301-Rv | gttgcgcgtaatcgctgccgccacg | |
| *metN*3-Fw | gataaaactttcgaatatcaccaaagtgttcc | |
| *metN*301-Rv | caaaaacagtacgcgaagagagcagg | |
| *16sRNA*9-Fw | gagtttgatcatggctcagattgaacgc | |
| *16sRNA*307-Rv | gtcatcctctcagaccagctagggatc | |
| *23sRNA*7-Fw | gcgactaagcgtacacggtggatgcc | |
| *23sRNA*-Rv | gacgcttccactaacacacacactg | |
| *fecD*3-Fw | gaaaattgcgctggttattttcatcaccc | |
| *fecD*301-Rv | gtagagcccccacagaggccaggc | |
| *marR*3-Fw | ggttaatcagaagaaagatcgcctgcttaacg | |
| *MarR*301-Rv | gcaggtcctggccaactaattgatggc | |
| *5sRNA*2_Fw | gcctggcggcagtagcgcggtggtccc | |
| *5sRNA*300_Rv | ctgcttaatttgatgcctggcagtttatggcg | |

| | | |
|---|---|---|
| *yifE*3_Fw | ggcggaaa gctttacgac gactaatcg | |
| *yifE*301_Rv | cctgcggtttaccgccggaaagggtg | |
| *marA*3_Fw | gtccagac gcaatactga cgctattac | |
| *marA*301_Rv | caaagtaatttttgaaggttcgggtcag | |
| AF488-*metN*-106-Fw | AF488 – attgatttagacgtctggatgccttaac | DNase I footprint |
| *metN*+52-Rv | tggtgcgggtgccctgg | |

## 3.3 Media and Buffers

### 3.3.1 Cultivation Media for *E.coli*

**$LB_0$-Medium** (Lysogeny Broth)
20 g LB-Medium (powder) in 1 liter $H_2O$
For Plates: add 15 g Agar per liter

**5x LB-Medium**
100 g/l LB

**SOB-Medium** (Super Optimal Broth)
20 g Bacto Trypton
5 g Yeast Extract
0.58 g NaCl
0.19 g KCl
in 1 l $H_2O$

**M9 Minimal Medium**

M9 salts (5x):
64 g $Na_2HPO_4$
15 g $KH_2PO_4$
2.5 g NaCl
5 g $NH_4Cl$
(All salts were dissolved in 1 liter $H_2O$ and autoclaved.)

For 1x M9 Medium:
778 ml sterile $H_2O$
0.1 ml 1 M $CaCl_2$ (sterile)
200 ml 5x M9 Salts (sterile)
2 ml 1 M $MgSO_4$ (sterile)
20 ml 20 % (w/v) glucose (sterile)
1 ml 10 % (w/v) thiamine (sterile)
10 ml amino acid stocks (4 mg/ml, in $H_2O$)

All components including amino acids stocks used to prepare 1x M9 minimal medium were sterile filtrated.

| | |
|---|---|
| Top Agar: | 20 g/l LB Medium<br>7.5 g/l Agar<br>10 mM $MgSO_4$<br>5 mM $CaCl_2$, |

### 3.3.2 Antibiotic Stocks

| | |
|---|---|
| Kanamycin Stock | 100 mg/ml in $H_2O$ |
| Ampicillin Stock | 200 mg/ml in $H_2O$ |
| Spectinomycin Stock | 30 mg/ml in $H_2O$ |
| Chloramphenicol Stock | 35 mg/ml in Ethanol |
| Tetracycline Stock | 10 mg/ml in $H_2O$<br>35 mg/ml in Ethanol |

### 3.3.3 Buffers for Molecular Biological Methods

| | |
|---|---|
| DNA Loading Buffer (10x): | 50 % (v/v) Glycerin<br>0.025 % (w/v) Bromphenol Blue<br>0.025 % (w/v) Xylencyanol |
| EMSA Loading Buffer: | 40 mM Tris<br>4 mM EDTA<br>0.2 % (w/v) Bromphenol Blue<br>25 % (v/v) Glycerin<br>pH 8.4 |
| TAE Buffer (50x): | 2 M Tris/Acetate<br>50 mM EDTA<br>pH 8.0 |
| TBE Buffer (10x): | 0.89 M Tris<br>0.02 M EDTA<br>0.89 M Boric acid |
| DNA Elution Buffer: | 0.1 % (w/v) SDS<br>1 mM EDTA<br>10 mM Magnesium Acetate<br>500 mM Ammonium Acetate<br>pH 8.0 |

| | |
|---|---|
| DNase I Footprint Buffer: | 10 mM $KH_2PO_4$, pH 7.5<br>100 mM KCl<br>2.5 mM $MgCl_2$<br>0.5 mM $CaCl_2$<br>10 % (v/v) Glycerin<br>1 mM DTT *(freshly added)* |

### 3.3.4 Buffers for Protein Chemical Methods

| | |
|---|---|
| 2D-Electrophoresis Lysis Buffer:<br>(100 ml) | 7 M Urea<br>2 M Thiourea<br>1 g Serdolit MB-1<br>15 mM DTT<br>4 % (w/v) Chaps<br>0.5 % (w/v) Pharmalyte 3-10 |
| Colloidal Coomassie (for 2D-gels): | 10 % (w/v) Ammonium sulfate<br>0.1 % (w/v) Coomassie G-250<br>2 % (v/v) Phosphoric acid<br>20 % (v/v) Methanol |
| Laemmli Buffer (5x): | 300 mM Tris / HCl<br>10 % (w/v) SDS<br>50 % (w/v) Glycerin<br>0.05 % (w/v) Bromphenole Blue<br>5 % (v/v) ß-Mercaptoethanol<br>pH 7.5 |
| SDS-Running Buffer (10x): | 0.25 M Tris<br>2 M Glycin<br>1 % SDS |
| Western Blot Transfer Buffer: | 25 mM Tris<br>190 mM Glycin<br>20 % (v/v) MeOH |
| Phosphate Buffered Saline:<br>(PBS; 10 x) | 40 mM $Na_2HPO_4$<br>160 mM $NaH_2PO_4$<br>1.15 M NaCl<br>pH 7.4 |

| | |
|---|---|
| PBS-T: | 1 x PBS<br>0.1 % (v/v) Tween 20 |
| Tris-Tricine Running Buffer (10x): | 1 M Tris<br>1 M Tricine<br>1 % (w/v) SDS |
| Fairbanks A: | 25 % (v/v) Isopropanol<br>10 % (v/v) Acetic Acid<br>0.05 % (w/v) Serva Blue R-250 |
| Fairbanks D: | 10 % (v/v) Acetic Acid |

### 3.3.5 Buffers for Protein Purification, Crystallization and Analyses

| | |
|---|---|
| Cell lysis Buffer : | 50 mM $NaH_2PO_4$<br>300 mM NaCl<br>10 mM Imidazole<br>pH 7.5 |
| His-A Buffer: | 50 mM Tris<br>300 mM NaCl<br>10 mM Imidazole<br>pH 7.5 |
| His-B Buffer: | 50 mM Tris<br>300 mM NaCl<br>750 mM Imidazole<br>pH 7.5 |
| Dilution Buffer: | 10 mM $NaH_2PO_4$<br>5 mM EDTA<br>pH 7.5 |
| Q-Sepharose-A Buffer: | 10 mM $NaH_2PO_4$<br>pH 7.5 |

| | |
|---|---|
| Q-Sepharose-B Buffer: | 10 mM $NaH_2PO_4$<br>600 mM NaCl<br>pH 7.5 |
| Gel-Filtration-A Buffer: | 10 mM $NaH_2PO_4$<br>400 mM NaCl<br>pH 7.5 |
| Gel-Filtration-B Buffer: | 10 mM Tris<br>200 mM NaCl<br>pH 8.0 |
| Crystallization Buffer: | 10 mM Tris<br>20 mM NaCl<br>pH 7.5 |
| HPLC Buffer:<br>(analytical gel filtration) | 40 mM Hepes<br>150 mM KCl<br>pH 7.5 |
| YjiE Storage Buffer: | 9.5 mM $NaH_2PO_4$<br>366 mM NaCl<br>5 % (v/v) Glycerin<br>pH 7.5 |
| RP-HPLC-A Buffer: | 5 % (v/v) Acetonitrile<br>0.1 % (v/v) Trifluoroacetic Acid (TFA) |
| RP-HPLC-B Buffer: | 95 % (v/v) Acetonitrile<br>0.1 % (v/v) TFA |
| $TAKM_7$ (10x): | 500 mM Tris, pH 7.5 at 37°C<br>700 mM $NH_4Cl$<br>300 mM KCl<br>70 mM $MgCl_2$ |

All the buffers were filtered before use. In the case of YjiE purification, the pH value of all buffers was adjusted to 7.5, whereas for YifE purification, the pH value was adjusted to 8.0.

## 3.4 Devices

**Incubators**

| | |
|---|---|
| Thermostat Plus | Eppendorf (Hamburg, Germany) |
| Thermomixer Comfort | Eppendorf (Hamburg, Germany) |
| Incubator Unimax1010 | Biometra (Göttingen, Germany) |
| Incubator Certomat BS1 | Sartorius Stedim Biotech (Göttingen, Germany) |

**Gel Documentation System**

| | |
|---|---|
| ImageQuant 300 | GE Healthcare (Amersham, UK) |
| Typhoon 9200 | GE Healthcare (Amersham, UK) |

**Chromatography**

| | |
|---|---|
| Äkta-FPLC with Fraction Collector Frac900 | Amersham Bioscience (Amersham, UK) |
| Shimadzu HPLC Device LC-20AT: | Shimazu (Düsburg, Germany) |
| Degasser DGU-20A3 | |
| UV/VIS Detector SPD20-A | |
| Fluorescence Detector RF-10AXL | |
| Fraction Collector FRC-10A | |

**Centrifuges and Cell Disruption Apparatus**

| | |
|---|---|
| Avanti J-25 Centrifuge (JA-10/25 Rotor) | Beckman Coulter (Krefeld, Germany) |
| Centrifuge Fresco17 | Eppendorf (Hamburg, Germany) |
| Centrifuge Universal 16R | Hettich (Tuttlingen, Germany) |
| Centrifuge Mikro20 | Hettich (Tuttlingen, Germany) |
| Constant Cell Disruption Apparatus Basic Z | Constant System (Northants, UK) |
| Bead Mill | Retsch (Haan, Germany) |
| Optima™Max-E Ultracentrifuge (MLS 50 roter) | Beckman Coulter (Krefeld, Germany) |

**Gel electrophoresis and Blotting devices**

| | |
|---|---|
| Xcell SureLock Mini Cell | Invitrogen (Carlsbad, USA) |
| BlueVertical™Mini Slab Gel System BV102 | Serva (Heidelberg, Germany) |
| 2D-Electrophresis | Amersham (Amersham, UK) |
| 1st dimension: IPGphor; | |
| 2nd dimension: Ettan Dalt II System | |
| Fast Blot Apparatur B44 | Biometra (Göttingen, Germany) |

**Spectrophotometer**

| | |
|---|---|
| Nanodrop ND-1000 Spectromerter | Peqlab (Erlangen, Germany) |
| Jasco FP-6500 Fluorescence Spectrometer | Jasco (Groß-Umstadt, Germany) |
| UV-Vis Spectrophotometer | Amersham (Amersham, UK) |

**Other devices**

| | |
|---|---|
| PCR Thermocycler Primus 25 | Peqlab (Erlangen, Germany) |
| Stratagene Mx3000P | Agilent (Santa Clara, USA) |
| Gene Pulser Xcell Electrophoration Device | Sartorius (Göttingen, Germany) |
| Lab Scale 1601 004 | Sartorius (Göttingen, Germany) |
| Jasco J-715 Circulardichroismus Spectropolarimeter | Jasco (Groß-Umstadt, Germany) |
| Ice maker | Ziegra (Isernhagen, Germany) |
| Image Scanner III (for 2D gels) | GE Healthcare (Amersham, USA) |
| Kodak Biomax Western Blot Cassette | Sigma (St. Louis, USA) |
| Optimax TR Developing Machine | MS Lab Device (Heidelberg, Germany) |
| Vortex-Genie 2 Vortexer | USA Scientific (Ocala, USA) |
| Freezer U725 Innova (-80°C) | New Brunswick Scientific (Nürtingen, Germany) |
| Microtiter Plate Reader | Biotek (Bad Friedrichshall, Germany) |

## 3.5 Computer Programs

| | |
|---|---|
| Adobe Photoshop 9.0 | Adobe Inc (San Jose, USA) |
| Microsoft Office 2007 | Microsoft (Redmon, USA) |
| OriginPro 8.0 | Originlab (Northhampton, USA) |
| LC Solution | Shimadzu (Düsburg, Germany) |
| Unicorn 4.0 | Pharmacia (Amersham, USA) |
| Image Quant TL | GE Healthcare (Uppsala, Sweden) |
| Image J | GE Healthcare (Uppsala, Sweden) |

## 3.6 Molecular Biology Methods

### 3.6.1 Cultivation and Storage of *E.coli*

Generally, *E.coli* cells except for BB7224 (*rpoH::Km*) were inoculated from glycerin stock cultures into $LB_0$ medium (± antibiotic) and cultivated at 37°C with shaking (140 rpm). The *E.coli* strain BB7224, due to the lack of heat shock response gene *rpoH*, was cultivated at 30°C with shaking (140 rpm).

To follow the cell growth, the optical density value of the culture at 600 nm wavelength was measured ($OD_{600}$; $OD_{600}$ = 1 corresponding to approx. 8 x $10^8$ cells/ml).

For long-term storage, 700 µl cultures were mixed with 1 ml sterile 20 % (v/v) glycerin and the glycerin stock culture was stored at -80°C.

Culture stocks were generated by mixing over-night cultures with sterile 20 % (v/v) glycerin at the ratio of 1:1 and distributed into 100 µl-aliquots, which were then stored at -80°C. 10 µl of an aliquot were used to prepare overnight cultures.

## 3.6.2 Amplification of Gene Fragments by Polymerase Chain Reaction

### 3.6.2.1 Standard Polymerase Chain Reaction

The polymerase chain reaction (PCR) is a widely used technique to amplify a gene fragment in the presence of a DNA template, deoxyribonucleic acids (dNTPs), primers and a DNA polymerase. The PCR reaction is composed of three steps. In the first step, the double-stranded DNA template is melted (denaturation), so that the DNA primers can anneal to the denatured DNA in the next step (annealing). Then the DNA polymerase adds the nucleotides from 5'-end to 3'-end to finally give rise to a completely new synthesized DNA fragment (elongation). Based on the principle, cycling of the reactions could result in a high copy number of the target genes.

In this work, *Go-taq* polymerase, *Pwo* polymerase and *Phusion* polymerase were used to amply DNA fragments. Because *Go-taq* polymerase does not exhibit the proof reading activity, it was mostly used in the cases, in which the misreading was acceptable, for example the control PCR to analyze the inserts genes cloned into plasmids. In contrast, *Pwo* and *Phusion* polymerase possess the proof reading activity. Therefore, they were generally used for cloning and generation of DNA fragments for *in-vitro* studies.

Standard PCR Mixture:

| | |
|---|---|
| template | 1 µl |
| buffer (10x) | 5 µl |
| dNTPs (10 mM) | 1 µl |
| forward primer | 0.2 µl |
| reverse primer | 0.2 µl |
| DMSO | 0.5 µl |
| DNA polymerase | 0.25 - 1 µl |
| $ddH_2O$ | add to 50 µl |

(*Go-taq* polymerase: 0.25 µl; *Pwo* polymerase: 1 µl; *Phusion* polymerase: 0.4µl)

Reaction Cycling:

| | | | |
|---|---|---|---|
| denaturation | 95°C | 1 min | 5x |
| annealing | 55°C | 30 sec | |
| elongation | 72°C | 1 min | |
| denaturation | 95°C | 1 min | 30x |
| elongation | 72°C | 1.5 min | |

### 3.6.2.2 Site-Directed Mutagenesis by QuikChange™ PCR

By this means, the amino acids of interest can be replaced by others. The point mutations can be introduced at the desired positions on target genes through QuikChange™ PCR.

Using a pair of complementary primers with the desired mutations in the middle, and a desired plasmid as template, the whole plasmid DNA with a mutation was replicated with the assistance of *Pfu* polymerase. After the thermal cycling reaction, the PCR products were directly treated with *Dpn*I endonuclease that digests the parental DNA template upon the specificity for methylated and hemimethylated DNA isolated from almost all *E.coli* strains and transformed into XL1blue electrocompetent cells.

QuikChange™ PCR Mixture:

| | |
|---|---|
| template | 20-50ng |
| buffer (10x) | 5 µl |
| dNTPs | 1 µl |
| forward primer | 125 ng |
| reverse primer | 125 ng |
| Pfu polymerase | 1 µl |
| dd$H_2O$ | add to 50 µl |

Reaction Cycling:

| | | | |
|---|---|---|---|
| denaturation | 95°C | 30 sec | |
| denaturation | 95°C | 30 sec | |
| annealing | 55°C | 1 min | 18x |
| elongation | 68°C | 7 min | |

*Dpn*I Digestion:

0.5 µl *Dpn*I (New England Biolabs, 20 U/µl) was added to the PCR products (50 µl) and the mixture was incubated at 37°C for 1 hour. 2 µl of the digested DNA were transferred into 50 µl XL1blue electrocompetent cells. In need, the *Dpn*I digested DNA could be precipitated by ethanol (s. 3.6.5) prior to transformation.

### 3.6.3 Purification and Restriction Enzyme Digestion of DNA Fragments

The amplified DNA fragments were analyzed by 1 % (w/v) agarose gel electrophoresis (120 V, approx. 30-60 min, in 1x TAE buffer) and DNA intercalated by ethidium bromide was visualized under UV-light. The bands corresponding to the DNA of interest were cut out and the DNA fragments were isolated using the PCR purification kit. In case, the DNA fragment was specifically amplified during PCR, resulting in only one DNA band of the correct size on 1 % (w/v) agarose gel, the PCR product could be directly purified using PCR purification kit (Progema).

The purified gene fragments as well as the plasmids used for ligation were then digested with restriction enzymes at 37°C for 2 hours. Both the plasmid DNA and the gene fragments were then separated on 1 % (w/v) agarose gels and purified. The concentration of DNA was

determined with the Nanodrop spectrometer.

Preparative Digestion:

| | |
|---|---|
| DNA | 40 µl |
| per restriction enzyme | 1 µl |
| buffer (10x) | 5 µl |
| $ddH_2O$ | add to 50 µl |

### 3.6.4 Ligation

The purified and enzyme treated DNA fragments were cloned into the prepared plasmid with the help of T4-Ligase.

Ligation Mixture:

| | |
|---|---|
| plasmid | 10 fmol |
| DNA fragment | 30 fmol |
| ligation Buffer (10x) | 2 µl |
| T4-Ligase | 1 µl |
| $ddH_2O$ | add to 20 µl |
| (100 fmol = 66 x size in bp of DNA) | |

The Mixture was incubated at 16°C without shaking overnight.

### 3.6.5 DNA Precipitation

Concentration or isolation of DNA from solutions can be achieved by DNA precipitation. 2.5 volumes of 100 % ethanol and 1/10 volume of sodium acetate pH 5.5 were well mixed with DNA solutions. During the incubation (-20°C, >1 h), DNA was precipitated. Separated by centrifugation (4°C, 13300 rpm, 30 min) and washed twice with 70 % (v/v) ethanol, the DNA pellet was dried at 37°C.

## 3.6.6 Transformation of *E.coli*

### 3.6.6.1 Preparation of Electrocompetent Cells

The overnight culture of *E.coli* was 1:50 diluted into fresh LB and cultivated at 37°C with shaking until $OD_{600}$ value of 0.5. Then the cells were harvested by centrifugation (8°C, 5000 rpm, 10 minutes) and the cell pellets were washed three times with ice-cold sterile 10 % (v/v) glycerin to remove all medium. Resuspended in 1 ml 10 % (v/v) glycerin (sterile), the cells suspension was aliquoted into 100 µl- fractions, frozen in liquid nitrogen and stored at -80°C.

### 3.6.6.2 Electroporation

2 µl ligation products were mixed with 50 µl electrocompetent cells on ice and the whole mixture was transferred into the pre-cooled 1 ml-cuvettes (Biorad). The cells were electroporated (program: *E.coli* 1.8 kV, 25 µF, 200 Ω) and immediately resuspended within 1 ml LB medium. The culture was then incubated at 37°C (30°C for BB2774, or the strains carrying plasmid pKD46 or pCP20) with shaking (750 rpm) for one hour. Finally, the cells were plated onto the LB plates containing antibiotics and cultivated at 37°C or 30°C overnight.

If the transformation efficiency was extremely low, the ligation product could be precipitated (s. 3.6.5) and the DNA pellet was applied for transformation.

### 3.6.6.3 Chemical Transformation

The whole ligation DNA (20 µl) was incubated with the commercially available ultracompetent cells XL10Gold (200 µl) on ice for 30 minutes. The DNA was forced into cells by applying a heat shock at 42°C for 30 seconds. The mixture was immediately cooled down on ice for 2 minutes and 1 ml SOB medium was added. The culture was then incubated (37°C, 750 rpm, 1 h) and plated onto the LB plates containing antibiotics.

## 3.6.7 Plasmids Isolation and Confirmation of Positive Clones

### 3.6.7.1 Plasmids Isolation

Plasmids were isolated from 5 ml overnight cultures with Wizard® Plus SV Minipreps Kit (Promega), following the protocols provided by the manufacturer, with the variation that DNA was finally eluted within 50 µl nuclease free water.

### 3.6.7.2 Analysis of Selected Clones

Plasmids of selected clones were isolated and analyzed either by the control PCR or by the analytical restriction enzyme digestion.

The control PCR was carried out as the standard PCR (s. 3.6.2.1), but cells, in this case, were applied as template. The PCR products were analyzed by 1 % (w/v) agarose gel electrophoresis.

Analytical restriction enzyme digestion was performed by mixing plasmids with restriction enzymes. After incubation at 37°C for 2 hours, the inserted gene fragments were analyzed by 1 % (w/v) agarose gel electrophoresis.

Analytical Digestion Mixture:

| | |
|---|---|
| plasmid | 5 µl |
| per restriction enzyme | 0.3 µl |
| buffer (10x) | 1 µl |
| dd$H_2O$ | add to 10 µl |

### 3.6.7.3 DNA Sequencing

The gene of interest cloned into a plasmid was sequenced to verify a positive clone. For sequencing at the GATC Company (Konstanz, Germany), 30 µl plasmid (30-100 ng/ul) and, if needed, 30 µl primers (10 pmol/µl) were required.

## 3.6.8 Construction of in-frame *yifE* Deletion Strain

### 3.6.8.1 Wanner Method

This approach was developed by Datsenko and Wanner (2000) to generate the in-frame single gene knockout (*52*). In principle, an FRT-flanked antibiotic selection marker gene is introduced into bacteria carrying the temperature sensitive plasmid pKD46, which encodes λ Red recombinase. This recombinase catalyzes the DNA exchange based on homologous recombination. As a result, the target gene is replaced by the selection marker gene, creating an in-frame deletion.

#### 3.6.8.1.1 Amplification of Antibiotic Selection Marker Gene

The FRT-flanked chloramphenicol resistance gene *cat* was amplified by PCR using pKD3 as template and *Phusion* polymerase (s. 3.6.2.1), and purified using the PCR purification kit (Promega). Precipitated by ethanol (s. 3.6.5), the dried DNA pellet was resuspended in 10 µl sterile water and kept on ice for transformation.

#### 3.6.8.1.2 Preparation and Transformation of Competent Cells Carrying pKD46

The *E.coli* strain MG1655 carrying pKD46 was cultivated in SOB medium supplemented with ampicillin and 0.1 % (w/v) arabinose at 30°C, 140 rpm for 4 hour. The electrocompetent cells were then prepared (s. 3.6.6.1). The prepared PCR product described above was transferred into the cells by electroporation (s. 3.6.6.2). The *yifE* deletion clones were selected on LB plates with chloramphenicol and confirmed by the control PCR (s. 3.6.7.2).

### 3.6.8.2 Phage P1 -Mediated Transduction

When bacterial virus P1 infects bacteria (donor), it can occasionally encapsulate some pieces of bacterial DNA. These DNA pieces can subsequently be released and integrated into the chromosome of a second bacterial strain (receptor), infected by P1 phage. As a result,

a DNA fragment in the receptor is replaced by the one from the donor. Taken advantage of this property of P1 phage, an *E.coli* deletion strain can be constructed by replacing the gene of interest by an antibiotic resistance cassette, a selectable marker for the deletion strain.

3.6.8.2.1 Preparation of P1 Phage Lysate

5 ml overnight cultures of MG1655 *yifE::Cm* were centrifuged (room temperature, 5000 rpm, 10 min) and the cell pellets were resuspended within 500 µl buffer (10 mM $MgSO_4$, 5 mM $CaCl_2$). Then 100 µl cell suspensions were respectively incubated with 100 µl, 10µl, 1 µl and 0 µl as control at 37°C without shaking for 30 minutes. To each sample, 2-3 ml of top agar were added, shortly mixed and poured onto the LB plates. After 4-6 hours, the plaques were observed, but cells should not be completely lysed. The top agar was scraped off into 15 ml tubes. Adding 200 µl chloroform and immediately 1 min vortexed, the mixture was centrifuged (room temperature, 5000 rpm, 20 min). The supernatant, P1 phage lysate, was transferred into a cyro tube, then 100 µl chloroform were added, and stored at 4°C.

3.6.8.2.2 Determination of Phage Titer

100 µl of any overnight culture were mixed with 2-3 ml pre-warmed top agar and poured onto a LB plate. The plate was incubated (room temperature, 30 min) until the top agar was firm. The P1 phage lysate was serially ($10^{-0}$, $10^{-2}$, $10^{-4}$, $10^{-6}$, $10^{-8}$) diluted. 5 µl each were spotted onto the top agar and incubated at 37°C overnight. The number of plaques was counted and based on the dilution factor and the loading volume (5 µl), the titer in the original lysate could be calculated, which should be at least $5x10^6$ plaque forming unit/µl.

3.6.8.2.3 P1 Phage Transduction

5 ml overnight cultures of MC4100 were centrifuged (room temperature, 5000 rpm, 10 min) and the cell pellet was resuspended within 500 µl buffer (10 mM $MgSO_4$, 5 mM $CaCl_2$). The P1 phage infected MC4100 cells by mixing 100 µl cell resuspensions with 10 µl and 3 µl

P1 lysates respectively, and incubating at 37°C without shaking for 30 minutes. Then 1 ml LB medium supplemented with 100 mM sodium citrate was added to inhibit further attachment of P1 phages to cells and allow the transductant MC4100 cells to grow. After incubation at 37°C with shaking (750 rpm) for 3 hours, the cells were plated onto the chloramphenicol containing LB plates supplemented with 100 mM sodium citrate. The surviving clones were analyzed by the control PCR (s. 3.6.7.2) to examine the in-frame replacement of *yifE* with *cat*.

#### 3.6.8.3 Removal of Chloramphenicol Resistance Marker Gene

Electrocompetent cells of MC4100 *yifE::Cm* were generated (s. 3.6.6.2) and transformed with the plasmid pCP20, carrying the temperature-inducible Flp recombinase gene *flp* and the ampicillin selection marker gene, by electroporation (s. 3.6.6.3). 500 µl LB medium were added and after incubation (30°C, 750 rpm, 1 h), the cells were plated onto the LB plate with ampicillin and cultivated overnight at 30°C. At this temperature, *flp* was induced and the recombinase Flp was produced in cells, catalyzing the excision of the FRT-flanked *cat*. On the following day, the picked colonies grew on an antibiotic free LB plate overnight at 43°C, at which the Flp production was inactivated and pCP20 was flipped out. Each growing colony was transferred onto both the LB plates (± ampicillin) and the LB plates with chloramphenicol. The clones, growing on the antibiotic free LB plate but not on the antibiotic containing LB plates, were analyzed by the control PCR (s. 3.6.7.2) to verify the removal of the selection marker gene *cat*.

### 3.6.9 Isolation of RNA from *E.coli* cells

#### 3.6.9.1 Preparation of Cell Cultures

In the study of YjiE activation mechanism, cells were cultivated in LB medium (± antibiotics, ± 1 % (w/v) arabinose if needed) to $OD_{600}$ of 0.4-0.5 and treated with HOCl at different concentrations (0-3 mM) for 10 minutes at room temperature in 1.5 ml tubes. 5x LB medium was immediately added to quench the remaining HOCl and 2 ml cultures were

centrifuged (room temperature, 5000 rpm, 5 min). The supernatant was removed quickly and pellets were frozen in liquid nitrogen and stored at -80°C.

In the study of YifE function, cells were cultivated to $OD_{600}$ of 0.4 and stressed with HOCl at different concentrations (0-3.25 mM) for 10 minutes (in flasks, 37°C, 140 rpm). After quenching the remaining HOCl, 2 ml cultures were spun (13300 rpm, 2 min, room temperature) to obtain the cell pellets, which were then frozen and stored at -80°C. Alternatively, the cell cultures were challenged with tetracycline (5 µg/ml) in the flasks at 37°C with shaking (140 rpm). At the different time points (0, 10, 25, 40, 60 minutes), 2 ml cultures were removed to prepare the cell pellets.

#### 3.6.9.2 RNA Isolation

The total RNA was isolated from *E.coli* cells using SV Total RNA Isolation Kit (Promega) according to the manufacturer's instructions.

Alternatively, RNA was extracted from mixtures by phenol-chloroform. 200 µl Roti®-Phenol pH4 were added to the same volume of samples and inverted 10 times. After centrifugation (14000 rpm, room temperature, 5 min), 200 µl chloroform were added, inverted and centrifuged again under the same condition. The aqua phase containing RNA was transferred carefully to a new safe-lock tube and subsequently precipitated by ethanol as for DNA precipitation (s. 3.6.5) at -80°C, overnight. After centrifugation (4°C, 13300 rpm, 30 min), the RNA pellet was washed twice with ice-cold 70 % (v/v) ethanol and resuspended within a small volume of nuclease free water. The concentration was measured using Nanodrop spectrometer.

### 3.6.10 Quantitative Real Time PCR

Quantitative real time PCR (qRT-PCR) is a powerful and sensitive assay to quantitatively detect RNA levels. Different from traditional PCR, a reverse transcriptase is required here to reversely transcribe the RNA of interest to its complementary DNA (cDNA). This newly synthesized cDNA is then amplified as in traditional PCR. The PCR products can be

fluorescently detected by binding of a fluorescent dye, in this case SYBR®Green, to the double-stranded DNA.

qRT-PCR Mixture:

| | |
|---|---|
| 2x SYBR® Green master mix | 10 µl |
| DTT (100 mM) | 0.2 µl |
| reference dye | 0.3 µl |
| (1:500 diluted in nuclease free water) | |
| forward primer (3.3 µM) | 1 µl |
| reverse primer (3.3 µM) | 1 µl |
| nuclease free water | add to 17 µl |
| template (40-50 ng/µl) | 2 µl |
| reverse transcriptase (RT) | 1 µl |
| (in no RT-control: 1µl nuclease free water instead of RT) | |

(DTT, reference dye stock, 2x SYBR® Green master mix and RT were provided in the Brilliant III Ultra-Fast SYBR® Green QRT-PCR Master Mix Kit).

Cycling:

| | | | |
|---|---|---|---|
| reverse transcription | 50°C | 10 min | |
| denaturation | 95°C | 3 min | |
| denaturation | 95°C | 20 sec | ] 40x |
| annealing&elongation | 60°C | 30 sec | |
| melting | 95°C | 1 min | ] 140x |
| | 25°C | 30 sec | |

## 3.7 Protein Chemical Methods

### 3.7.1 SDS-Polyacrylamid Gel Electrophoresis (SDS-PAGE)

Proteins can be separated using SDS-gel electrophoresis. The samples were firstly mixed with reducing Laemmli buffer (1x or 5x) and loaded to neutral gradient gel (Serva) or 10-20 % tris-tricine gels (Invitrogen), which were run at 35 mA (per gel) for 70 min (tris, glycin neutral gel, Serva) or for 3.5 hours (tris-tricine gel, Invitrogen). The gels could be stained with Coomassie and destained with 10 % (v/v) acetic acid, or stained by silver staining.

## 3.7.2 Western Blot and Dot Blot

### 3.7.2.1 Western Blot

Western blotting can be used to detect the target protein, despite of tiny amount, in a protein mixture. After separation by SDS-PAGE, the proteins were transferred onto a PVDF membrane (per blot: 200 mA for 1 hour) or nitrocellulose membrane (1.5 mA/cm$^2$, 1 hour). The membrane was then saturated with pre-warmed milk powder (5 % w/v in PBS-T buffer) for 20 min to prevent unspecific binding of antibodies to the membrane. After washing, the membrane was incubated with the primary antibody for 45 min at room temperature (anti-YjiE antibody, anti-His antibody) or overnight at 4°C (anti-acetylated lysine antibody, purified anti-YifE antibody). Washed with PBS-T buffer three times, the membrane was incubated with the second antibody at room temperature for 45 min. After wash, the detection was performed using the ECL-Detection System.

Dilution Grade for Antibodies:

| | |
|---|---|
| polyclonal antibody against YjiE (purified) | 1:4000 |
| antibody against His-tag | 1:2000 |
| polyclonal antibody against YifE (purified) | 1:4000 |
| monoclonal antibody against acetylated lysine | 1:1000 |
| monoclonal peroxidase conjugate against rabbit IgG | 1:4000 |
| monoclonal peroxidase conjugate against mouse IgG | 1:4000 |

(The antibodies were diluted with PBS-T buffer containing 1 % w/v milk powder or 5 % w/v BSA, and used only twice.)

### 3.7.2.2 Dot Blot

Dot blotting is a simpler and quicker technique than western blotting. Protein solutions were dotted onto nitrocellulose (NC) membrane. After the solutions were completely absorbed into the membrane and dried, the proteins were fixed in 5 % (v/v) acetic acid. After wash with water, it can be incubated with the primary and secondary antibodies and developed as described above (s. 3.7.2.1).

### 3.7.3 Determination of the Protein Concentration with Bradford Assay

Bradford assay is a rapid and relatively accurate method commonly used to determine the total protein concentration. The assay is based on a shift of absorbance maximum from 465 nm to 595 nm caused by binding of Coomassie Brilliant Blue to protein. 900 µl Bradford (1:5 diluted) were incubated with 100 µl diluted samples at room temperature for 10 minutes and the absorbance was measured at 595 nm. Using the Bradford standard curve generated with BSA in different concentrations, the corresponding protein concentration could be calculated.

### 3.7.4 Ellman's Assay

The Elman's assay is used to determine the amount of free thiol groups in proteins. The Ellman's reagent, 5,5'-dithio-bis (2-nitrobenzoic acid) (DTNB), can react with the free sulfhydryl groups and convert to a conjugate with proteins through a mixed disulfide and a 2-nitro-5-thiobenzoic acid, the colored species produced in this reaction, which has a high extinction at 412 nm.

In this experiment 100 µg proteins were mixed with 100 mM Tris (pH 7.77) with the final volume of 1 ml. After adding 30 µl DTNB (4 mg / ml), the mixture was incubated at room temperature for 20 min and $OD_{412}$ was measured. The free thiol groups can then be calculated according to the Lambert-Beer law ($E = c \times d \times \varepsilon$; E: extinction, c: concentration [M], d: light path in the sample [cm], DTNB: 13600 [$M^{-1}xcm^{-1}$] in 0.1 M K-phosphate buffer, pH 8.0).

### 3.7.5 Protein Precipitation by Trichloroacetic Acid (TCA)

100 % (w/v) ice-cold TCA was well mixed with protein solutions to the final concentration of 15 % (w/v). After incubation (-20°C, >1 h), the samples were centrifuged (13300 rpm, 4°C, 30 min) and the pellets were washed twice with acetone and dried at 37°C.

### 3.7.6 Two-Dimensional Electrophoresis

In the first dimension, proteins are separated upon their isoelectric point (pI). Thereby, a pH gradient is generated in a gel strip. At all pH values other than their isoelectric point value, proteins will be charged and move towards the opposite charged side. Only at the isoelectric point, proteins carry a neutral charge so that they do not move any more but are focused at that point. In the second dimension, proteins are further separated upon their molecular weights on a SDS-PAGE.

To prepare the 2D-samples, 6 ml cultures ($OD_{600}$ = 0.5) were harvested by centrifugation (5000 rpm, 4°C, 5 min) and washed once with 10 ml ice-cold sterile water to remove salts. Then, the supernatant was completely removed and the cell pellet was resuspended in 1.5 ml 2D-lysis buffers (500 µl x … ml cells x…OD) and stored at -80°C. For cell lysis, samples were frozen and thawed four times. After incubation with shaking (400 rpm) at 20°C for one hour, cell debris was separated by centrifugation (13300 rpm, 4°C, 45 min). The supernatants were transferred into new tubes and centrifuged again (13300 rpm, 4°C, 45 min). Finally, the supernatant could be used for 2D-electrophoresis.

After separation on the first dimension, the strip was equilibrated with DTT for 15 min and then with iodoacetamide for 15 min. The second dimensional separation was performed on the neutral gradient gel (Serva), which gel was stained with colloidal Coomassie/Coomassie and destained with 10 % acetic acid. Finally, gels were scanned at 300 Dpi.

Program for the First Dimension:

| | | |
|---|---|---|
| pH gradient | 4 – 7 | |
| temperature | 20°C | |
| run program | 30 V | 6 h |
| | 60 V | 6 h |
| | 200 V | 1 h |
| | 500 V | 1 h |
| | 1000 V | 1 h |
| | 1000 – 8000 V | 0.5 h |
| | 8000 V | 10 h |

## 3.8 Protein Purification

### 3.8.1 Protein Expression and Generation of Cell Lysate

*E.coli* strain BL21(DE3)/BL21(DE3) *yifE::Cm* carrying the required plasmid was used for gene expression and protein purification. Cells were inoculated from glycerin culture stocks into 1.5 l LB media with requiring antibiotics and incubated at 37°C overnight (about 15 hours) without shaking. Then the culture was incubated at 25°C for 1 hour (for wild type YjiE/YjiE mutants) or at 37°C (for wild type YifE) with shaking (125 rpm). After inducing target protein production for 4 hours (wild type YjiE/YjiE mutants) or 2 hours (wild type YifE), the cells were harvested by centrifugation (6000 rpm, 20 min, 7°C) and the cell pellets were resuspended in the lysis buffer supplemented with protease inhibitor HP (1:200) and *DNase* I (Roche). Cells were disrupted by french press at 2 kbar and centrifuged at 7°C, 20000 rpm for 30 minutes. The cell lysate was filtrated (0.2 µm-filter) and used for purification.

### 3.8.2 Affinity Chromatography

The His-trap fast flow column (max. pressure: 0.3 MPa, GE Healthcare) was equilibrated with His-A buffer. The lysate was loaded onto the column and the column was washed with His-A buffer (5x column volumes) to remove the nonspecifically bound proteins. The protein of interest was eluted using His-B buffer (gradient 0-100 %: 10 x column, at 100 % His-B buffer: 5x column volumes) in 2.5 ml-fractions.

### 3.8.3 Anion Exchange Chromatography

Due to the high salt concentration in the eluted protein solution, which could interfere with the Q-Sepharose chromatography, this protein solution was diluted with dilution buffer to a final salt concentration of 200 mM (for wild type YjiE) or with Q-seph A buffer to 125 mM salt concentration (for wild type YifE). After equilibration with Q-sephA buffer, the diluted protein solutions were loaded onto the column (max. pressure: 0.3 MPa) and the column was then washed with Q-seph A buffer (5x column volumes). Target proteins were eluted with Q-seph

B buffer (gradient 0-100 %: 10x column volumes, at 100 % Q-seph B buffer: 5x column volumes) in 2 ml-fractions.

### 3.8.4 Removal of His-tag Through Thrombin Digestion

Thrombin (18.75 units per mg protein) was added to the protein solution and incubated at 4°C for 42 hours.

### 3.8.5 Size Exclusion Chromatography

The Superdex 75 gel filtration column was washed ($H_2O$: 1 x column volume, 0.5 M NaOH: 1 x column volume, $H_2O$: 1 x column volume; max. pressure: 0.3 MPa) and equilibrated with gel filtration A buffer (for YjiE/YjiE mutants) or gel filtration B buffer (for YifE). Concentrated to a final volume of 10-15 ml, proteins were loaded on the column and separated using the same buffer in 3.5 ml-fractions.

For quick purification of His-tagged YjiE, after the affinity chromatography, the eluate was applied to PD10 column, pre-equilibrated with gel-filtration-A buffer, to remove the imidazole and fractionated. The protein concentration in each fraction was measured by Nanodrop spectrometer and the fractions containing YjiE were collected.

To obtain the purified His-tagged YifE, omitting thrombin digestion, all the three chromatographic methods were used.

## 3.9 Purification of Primary Antibody

N-hydroxysuccinimide (NHS) can react with amine at low pH. Due to this property, the column packed with NHS can be used to nonspecifically immobilize proteins at low pH.

To purify anti-YifE antibody, Hi-Trap NHS activated HP column (1 ml, GE healthcare) was activated with 1 mM HCl (7ml) and 2 ml lysates ($A_{280}$=28) were loaded onto the column. After

incubation (room temperature, 10 min), further 2 ml lysates were loaded and incubated again (room temperature, 10 min). Then, the column was washed with 6 ml buffer 1 (0.5 M ethanolamine, 0.5 M NaCl, pH 8.3), 6 ml buffer 2 (0.1 M sodium acetate, 0.5 M NaCl, pH 4), again 6 ml buffer 1 and incubated (room temperature, 15 min). After wash with 6 ml buffer 2 and 6 ml buffer 1, the column was equilibrated with buffer 3 (10 mM $NaH_2PO_4$/pH 7.5, 150 mM NaCl). 350 µl anti-YifE serums were diluted with 650 µl buffer 3 and loaded onto the column. After incubation (room temperature, 15 min), 1 ml buffer 3 was applied to the column and the flow through was collected, corresponding to the purified anti-YifE antibody, which was analyzed by western blot (s. 3.7.2.1).

## 3.10 Protein Labeling With Fluorescence Dye

Free cysteines in proteins can be labeled by fluorescence dye such as ATTO488 via maleimide linker that modifies the thiol group in the cysteine. Since the exclusive cysteine in the purified YifE was reduced according to Ellman's assay (s. 3.7.4), the DTT treatment was not required. Otherwise, proteins need to be reduced by DTT before labeling. YifE was mixed with ATTO488 maleimide (dissolved in DMSO) in the molar ratio of 1:5 and incubated at 4°C overnight with shaking. NAP5 column was used to remove free dyes and the degree of labeling (DOL) was calculated by measuring the free thiols in samples using Ellman's assay (s. 3.7.4).

## 3.11 Nucleic Acid Binding Assays

### 3.11.1 Electrophoretic Mobility Shift Assays (EMSA)

Binding of protein to DNA leads to a slower migration of the DNA-protein complex than the free DNA on a non-denaturing gel. According to this observation, EMSA technique has been developed to analyze protein-DNA interactions.

C-terminal His-tagged wild type YjiE isolated from unstressed cells (YjiE-$His_C$), 2 mM

HOCl stressed cells (YjiE-$His_C$-HOCl; provided by Katharina Gebendorfer), HOCl treated cell lysates (YjiE-$His_C$-$HOCl_{lysate}$; 30 µM HOCl, 5 min, on ice) as well as from untreated cell lysate mixed with HOCl treated LB medium (YjiE-$His_C$-$HOCl_{LB}$; 45 ml cell lysate + 10 ml 1.5 mM HOCl treated LB) were firstly centrifuged (13300 rpm, 4°C, 15 min) and the concentrations were determined. For each reaction (15 µl), 100 ng DNA (5'-AlexaFuor488 labeled *yjiE* promoter DNA of 158 bp) was incubated with the proteins at the molar ratio of 1:6, 1:30 and 1:58 in the presence of 1 µg BSA at room temperature for 20 minutes. Adding 2 µl EMSA loading buffers, the samples were analyzed by electrophoresis (6 % TBE gel, 150 V, 50 minutes) and the fluorescence signals were scanned.

### 3.11.2 Fluorescence Anisotropy

Fluorescence anisotropy (FA) can provide information on the size of proteins or the rigidity of molecular environments and is commonly used to study protein-protein interaction or in this case DNA-protein interaction. Excited by polarized light, the fluorophores emit polarized fluorescence. In solution, the fluorophores are flexible and the fluorescence polarization is affected only by the movement of fluorophores such as rotation. Upon binding of a macromolecule to a fluorophore, the rotational motion is slowed down, leading to an increase in fluorescence anisotropy.

In the study of YjiE activation mechanism, wild type YjiE/YjiE mutants were centrifuged (4°C, 13300 rpm, 15 min) and the concentrations were determined. The proteins were than mixed with 3'-AlexaFuor 488 labeled MetN promoter of 158 bp (3'-AF488-MetN158) and the degassed buffer (10 mM sodium phosphate pH7.5, 5 % v/v glycerin). To analyze the DNA binding ability of the reduced proteins, wild type YjiE/YjiE mutants were treated with 1mM DTT at 37°C for 2 hour before mixing with DNA.

In the study of YifE function regarding nucleic acid binding, ATTO488 labeled YifE (ATTO488-YifE, s. 3.9) was incubated with single-stranded DNA (ssDNA provided by Katharina Gebendorfer: Fw-NdeI-plac-*yjiE* of 90 base, Rv-FRT-*yjiE* of 99 base), double-stranded DNA (dsDNA: *yjiE* promoter DNA of 102 bp, qRT-PCR product of *metB* of

300 bp) and RNA isolated from wild type and *yifE* deletion strains.

FA Mixture:

| | |
|---|---|
| wt YjiE/YjiE mutants | 2 µM |
| 3'-AF488-MetN158 | 10 nM |
| buffer | add to 130 µl |
| | |
| ATTO488-YifE | 10 pmol |
| gel-filtration-B Buffer | 29.5 µl |
| RNase Inhibitor Plus (40 U/µl) | 0.5 µl |
| ssDNA/dsDNA/RNA | 10 pmol/10 pmol/7 µg |

Conditions:

| | |
|---|---|
| excitation | 488 nm |
| emission | 515 nm |
| temperature | 37°C (for YjiE)/25°C (for YifE) |

### 3.11.3 DNase I Footprinting Assay

DNase I footprinting assay is an essential technique to explore the DNA-protein interaction (*53*). Once a protein binds to DNA, this protein-bound DNA fragment is protected by DNase I cleavage. Using the fluorescently end-labeled DNA, the digested DNA fragments can be separated by gel electrophoresis or chromatography and the cleavage pattern can be detected, revealing the protein binding sites on its target DNA.

#### 3.11.3.1 Preparation of DNA

Fluorescent labeled DNA (3'/5'-AF488 MetN158) was generated by PCR (s. 3.6.2.1) and purified by PCR purification kit (Promega). Separated on 6 % TBE gel (150V, 50 min), the bands corresponding to the PCR product were cut out and incubated overnight in the DNA elution buffer at 55°C without shaking (in dark). By this means, the DNA was extracted from the gel slices. The supernatant was then transferred into a new 1.5 ml tube. After washing the gel slice twice with the DNA elution buffer, all the supernatants were collected and applied to

ethanol precipitation (s. 3.6.5). Finally the DNA pellet was resuspended within a small volume of water to obtain a highly concentrated DNA sample and the concentration was measured using Nanodrop spectrometer.

#### 3.11.3.2 Preparation of Proteins

Wild type YjiE-$His_C$-HOCl was centrifuged (4°C, 13300 rpm, 15 min) to remove the potential aggregates and the concentration was measured. After treated with DTT (1 mM, 37°C) and subsequently centrifuged (4°C, 13300 rpm, 15 min), the protein concentration was measured.

#### 3.11.3.3 DNase I Cleavage

The prepared DNA and protein was mixed at different molar ratios(1:0, 1:10, 1:30) in the presence of BSA (5 µg/ml) and incubated at 25°C for 15 minutes. Then, 1 µl diluted DNase I (New England Biolab; dilution factor: 1:0, 1:70, 1:85, 1:100) was added. After incubation at 25°C for 10 minutes, the DNase I was inactivated by heating (95°C, 10 min). The DNA fragments were mixed with 35 µl membrane binding solution, purified using PCR purification kit (Promega) and eluted within 50 µl nuclease free water.

Mixing 5 µl purified DNA fragments with 10 µl formamid, which inhibits the formation of the secondary structures of DNA, and 0.1 µl standard, the samples were prepared for footprint mapping analysis carried out in Gene Center, Ludwig-Maximilians-Universität München (Munich, Germany).

## 3.12 Reversed Phase Chromatography

Reversed Phase high performance liquid chromatography (RP-HPLC) uses twp phases, a non-polar stationary phase and a polar mobile phase, to separate the organic molecules according to their hydrophobic properties. The polar molecules with little affinity to

hydrophobic matrix are eluted relatively earlier than the non-polar molecules.

The column Bischoff NPS C18 (0.232 ml) was equilibrated with RP-buffer 1. Proteins (YjiE-$His_C$-HOCl and YjiE-$His_C$) were mixed with the storage buffer, acetonitrile (ACN) and 10 % (v/v) TFA to the concentration of 0.05 µg/µl in 10 % ACN, 1 % TFA. 65 µl protein samples were injected onto the column and eluted with the gradient (5 % (v/v) ACN, 10 min; 5-95 % (v/v) ACN, 40 min). The column was regenerated in 5 % (v/v) ACN. The absorption at 280 nm and 214 nm as well as the fluorescence were recorded.

## 3.13 Pull-down Assays

### 3.13.1 Protein Pull-down Assays

10 µl NTA-Ni sepharose beads (GE Healthcare) were washed three times with 40 mM Hepes buffer (pH 7.5) and saturated/incubated with YjiE-$His_C$ at room temperature with shaking for 30 minutes. After washing, 400 µl cell lysates of the *yjiE* deletion strain (25 µg/µl) supplemented with protease inhibitor HP were added and further incubated at 4°C with shaking for 1 hour. Alternatively, the Ni-beads were incubated together with YjiE-$His_C$ and cell lysate (4°C, shaking, 1 h). As control, the Ni-beads were incubated with cell lysate alone. After removing the supernatant, the beads were washed twice with buffers containing the increasing concentrations of imidazole (10-50 mM). The proteins were eluted with the buffer containing 750 mM imidazole and separated by SDS-PAGE. The protein bands of interest were cut out and the proteins, which could be the potential interaction partner of YjiE, were extracted, digested and identified by mass spectroscopy.

### 3.13.2 RNA Pull-down Assay

150 µl NTA-Ni magnetic beads (Qiagen) were washed three times with PBS buffer and then incubated with an excess amount of N-terminal His-tagged YifE (YifE-$His_N$) (3 µg protein per 10 µl beads suspension) in the presence of protease inhibitor HP (4°C, shaking, 1 h). After discarding the supernatant and washing twice with PBS buffer supplemented with

protease inhibitor HP, protein-coupled beads were prepared.

5 ml MC4100 *yifE*$^{-}$ cultures ($OD_{600}$ 0.4) were harvested and lysed in 250 µl lysis buffer (lysis buffer per ml: 1x PBS, 1 mM DTT, 5 µl protease inhibitor HP, 40 Unit RNase Inhibitor Plus , 5 Unit RNase free DNase I, 100 µg/ml lysozyme). Incubated at 37°C for 8 minutes to digest *E.coli* genomic DNA, the lysate was supplemented with 1 mM ATP and applied to the YifE coupled beads. After incubation (4°C, shaking, 1 hour), the supernatant was removed and the beads were washed twice with PBS buffer supplemented with protease inhibitor (1:200) and RNase Inhibitor Plus (1:1000). Eluted with 250 µl PBS buffer containing 500 mM imidazole and RNase Inhibitor Plus (1:1000), 230 µl eluate were subjected to phenol-chloroform treatment (s.3.6.9.2) to extract the potential target RNA of YifE. The RNA was analyzed by qRT-PCR using various primers (s. 3.6.10).

## 3.14 Viability Assay and Recovery Assay

### 3.14.1 Viability Assay

Exposed to various stresses, the cell viability was analyzed by calculating the colony forming unit (cfu). *E.coli* cells overexpressing wild type *yjiE*/*yjiE* mutants under 0.1 % (w/v) arabinose induction were cultivated to $OD_{600}$ of 0.46. 500 µl cultures were mixed with 125 µl LB medium in 2 ml tubes and subjected to HOCl (0-6 mM). After incubation (room temperature, 10 min), 500 µl 5x LB medium were added to quench the remaining HOCl. The cell suspension was serially diluted with LB medium (dilution factor 1:10) and 5 µl of each dilution step were spotted onto LB plates. After incubation overnight, the cfu was calculated.

In the case of $H_2O_2$/paraquat stress, 50 µl cells were diluted into 950 µl/450 µl LB medium in 2 ml tube and stressed with $H_2O_2$ (6 mM)/paraquat (1, 2, 3 mM) at 37°C with shaking (700 rpm) for 90 minutes/75 minutes. In the case of diamide stress, 10 ml cultures were treated with 5 mM diamide at 37°C, 140 rpm for 2 hours. The cells were then serially diluted and spotted onto LB plates as described above.

### 3.14.2 Recovery Assay

Wild type MC4100 and MC4100 *yifE*$^-$ were cultivated to the exponential growth phase ($OD_{600}$ 0.4-0.5) and diluted with LB medium into 96-well plates with final $OD_{600}$ of 0.1 (HOCl/$H_2O_2$ stress) or 0.05 (antibiotic stress). HOCl/$H_2O_2$ or various antibiotics with different concentrations were added and the absorption at 600 nm was measured every 5 minutes by microtiter plate reader.

| | |
|---|---|
| HOCl concentrations in wells: | 0, 2.0, 2.25, 2.5, 2.75, 3.0 mM |
| $H_2O_2$ concentrations in wells: | 0, 2.25, 2.5, 2.75, 3.0, 3.25 mM |
| chloramphenicol concentrations in wells: | 0, 1.0, 1.5, 2.0, 2.5, 3.0 µg/ml |
| tetracycline concentrations in wells: | 0, 0.2, 0.4, 0.8, 1.0 µg/ml |
| kanamycin concentrations in wells: | 0, 0.5, 1.0, 1.5, 2.0, 2.5 µg/ml |
| spectinomycin concentrations in wells: | 0, 1.0, 2.0, 4.0, 6.0, 8.0 µg/ml |

## 3.15 Structural Analysis Methods

### 3.15.1 Circular Dichroism Spectroscopy

Circular dichroism (CD) is a property of optical active molecules to differently absorb left and right handed polarized light. It plays an important role in the structural investigation of optical active biological macromolecules such as proteins and DNA, which are composed of optically active elements. Such molecules can adopt different types of three-dimensional structures, thus each type of molecules produces a distinct CD spectrum. A common use of this technique is to analyze the protein secondary structures (helices, sheets, turns and random coils) according to the CD spectra, because different types of secondary structures give rise to a characteristic shape and magnitude of CD spectrum. In the far UV (170 nm- 250 nm), alpha helix shows two characteristic minima at 208 and 222 nm while β-sheet structure shows a less intense signal with a single minimum at 218 nm. Ellipticity is used to scale the quantitative content of secondary structure and it can be converted into mean residue ellipticity following the formula.

$$\Theta_{MRW} = \Theta \times 100 \times M / (d \times c \times N_{aa})$$

$\Theta_{MRW}$: mean residue ellipticity
$\Theta$: obtained ellipticity
M: molecular mass [g/mol]
D: layer thickness [cm]
c: concentration [mg/ml]
$N_{aa}$: number of amino acids

Wild type YjiE/YjiE mutant was mixed with the gel filtration A buffer supplemented with methionine (2.5 mM) and the degassed samples were measured in far-UV region. Additionally, the thermal transition could be measured by CD spectroscopy, since the ellipticity is temperature- independent.

Far-UV-CD Spectrum Conditions:

| | |
|---|---|
| wave length | 260-195 nm |
| sensitivity | 100 mdeg (standard) |
| scan modus | 20 nm/min |
| reaction time | 4 sec |
| band width | 1 nm |
| repeat | 16 |
| temperature | 20 °C |

Thermal Transition Conditions:

| | |
|---|---|
| temperature | 20-80°C |
| wave length | 222 nm |
| sensitivity | 100 mdeg (standard) |
| heating rate | 0.2°C |
| delay | 0 |
| reaction time | 4 sec |
| band width | 1 nm |

### 3.15.2 X-Ray Crystallography

Since many materials can form crystals, X-ray crystallography becomes a fundamental means to study the atomic and molecular structures of biological molecules such as proteins and DNA.

His-tagged YifE was purified (s. 3.8) with the variation that the crystallization buffer, instead of gel filtration B buffer, was used for the size exclusion chromatography. The freshly purified protein was concentrated by Centricon (exclusion size: 10 kDa) to 25 mg/ml and applied to a crystallization screen, which was carried out in the group of Professor Michael Groll at the Technische Universität München, Department Chemie (Munich, Germany).

## 3.16 Oligomerization Analysis Methods

### 3.16.1 Analytical Size Exclusion HPLC of Cell Lysate

In order to analyze the oligomerization status of YifE *in vivo*, analytical gel filtration HPLC was performed using cell lysate. 1.5 l culture of BL21(DE3) carrying pET28(a)-YifE was incubated without shaking at 37°C overnight (15 hours) and then at 37° with shaking (146 rpm, 45 min). The production of His-tagged YifE was induced by IPTG (100 µM, 37°C, 30 min). The cell lysate was prepared as for purification (s. 3.8) and the total protein amount was determined by Bradford assay (s. 3.7.3). 120 µg proteins were loaded onto the superpose 6 column (max. pressure: 2.3 MPa) and 0.25 ml-fractions were collected in the 96-well plate. The proteins in each elution faction were precipitated by adding TCA (s. 3.7.5). Finally, the proteins were separated by SDS-PAGE and the His-tagged YifE were detected by western blot using monoclonal antibody specifically against His-tag.

### 3.16.2 Analytical Ultracentrifugation

In order to analyze the oligomerization states of purified His-tagged YifE, the analytical ultracentrifugation (aUC) based on sedimentation velocity was performed. In this case, the sedimentation coefficient s is determined, which is used to characterize the behavior of proteins during centrifugation and provides information about the molecular weight and shape of proteins. Sedimentation coefficient is defined via the following formula.

$$s = M ( 1 – \bar{u} \rho ) / f$$

s: sedimentation coefficient [S]
M: molecular weight
ū: partial specific volume of the molecule
ρ: density of solution
f: fictional coefficient

The purified His-tagged YifE was diluted with gel-filtration B buffer to the absorption at 280 nm of 0.7 and 500 µl samples were applied to analytical ultracentrifugation.

## 3.17 Carbonylation Assay

The carbonyl groups in proteins can react with 2,4-dinitrophenylhydrazine (DNPH) to form protein-bound 2,4-dinitrophenylhydrazones (*54*). This derivate is detected by anti-dinitrophenyl antibodies, allowing a quantitative determination of carbonylations (*54*).

2 ml cells (± HOCl) at the exponential growth phase were centrifuged (5000 rpm, room temperature, 10 min) and the cell pellets were resuspended in 1x Laemmli buffer, freshly supplemented with 1.5 % (v/v) β-mercaptoethanol, (200 µl 1x Laemmli per 1 ml culture of $OD_{600}$=1). Mixed with the same volume of 1x DNPH/1x derivation control solution, the samples were incubated at room temperature for 15 minutes. To stop the reaction, 3/4 volume of the neutralization buffer was added. The samples were then separated by SDS-PAGE (s. 3.7.1) or 2D-PAGE (s. 3.7.6) and the carbonyl groups were detected by western blot (s. 3.7.2.1) using anti-dinitrophenyl antibodies (primary antibody: 1:150; secondary antibody: 1:300; room temperature, 1 h). All reagents including the antibodies were provided in the Oxyblot™ protein oxidation detection kit (Millipore).

## 3.18 Sucrose Gradient Centrifugation

Based on the density, macromolecules can be separated in a sucrose gradient during

centrifugation.

### 3.18.1 Preparation of the Sucrose Gradient

50 % (w/v) sucrose stock solution was generated by dissolving sucrose in the buffer: 20 mM Hepes pH 7.5, 150 mM $NH_4Cl$, 1 mM $MgCl_2$ (dissociation condition)/10 mM $MgCl_2$ (association condition), and diluted with the same buffer to the different sucrose concentrations (10 %, 20 %, 30 %, 40 %, 50 %). The sucrose gradient was created by firstly loading 750 µl 50 % sucrose solution into a Beckman centrifuge tube, then carefully overlaying with the next diluted sucrose solution (e.g., 40 %) until the sucrose solution with the least density (10 %). The gradient was equilibrated at 4°C, overnight.

### 3.18.2 Preparation of Cell Lysates

Wild type/*yifE*$^-$ strains were cultivated to $OD_{600}$ of 0.35 and harvested by centrifugation (5000 rpm, room temperature, 10 min). Resuspended within the lysis buffer (1 ml per $OD_{600}$=1; lysis buffer: 20 mM Hepes pH 7.5, 6 mM $MgCl_2$, 30 mM $NH_4Cl$, 1:1000 RNase free DNase I, 1:1000 RNase Inhibitor Plus, 1:200 protease inhibitor HP, 2 mM Tcep), cells were disrupted by glass beads (2 min 30/sec + 2 min break on ice, repeated five time). After centrifugation (4°C, 13300 rpm, 30 min), the supernatant (lysate) was transferred into a new tube and the absorptions at 260 nm (nucleic acid) and 280 nm (protein) were measured.

### 3.18.3 Sucrose Gradient Ultracentrifugation

The 95 µl lysate (A260=2U) supplemented with RNase Inhibitor Plus (40 Unit) was loaded onto the sucrose gradient and sedimented at 4°C, 50000 g for 17 hours (rotor: MLS50, Beckman Coulter).

To analyze the distribution/location of YifE, the sucrose gradient was pumped out from the bottom of the tube and fractionated in 96-well plate (1 drop/well). The absorption at 254 nm in each well was measured using Nanodrop spectrometer. The proteins in the fractions of

interest were precipitated by TCA (s. 3.7.5). The acetone washed protein pellets were dried, resuspended within 1x Laemmli reducing buffer and analyzed by SDS-PAGE (s. 3.7.1) and western blot (s. 3.7.2.1).

## 3.19 Ribosome Binding Assay

This assay was performed in the group of Professor Marina Rodnina (Max-Planck Institute, Göttingen, Germany) and the materials except the purified YifE were provided there.

200 pmol YifE (in $TAKM_7$ buffer) were mixed with 100 pmol *E.coli* 70S ribosome, in the presence/absence of tetracycline (30 µM). 50 µl mixtures were loaded onto the analytical size exclusion column (Biosuite 450), which was pre-equilibrated with $TAKM_7$ buffer, and separated in the same buffer in 800 µl-fractions. The fractions containing 70S ribosomes were concentrated and applied to dot blot analysis in order to detect YifE (s. 3.7.2.2).

## 3.20 Translation Related Assays

### 3.20.1 [$^{35}$S]Met Incorporation

Wild type MC4100 and MC4100 *yifE*$^-$ cells were cultivated in M9 minimal medium to $OD_{600}$ of 0.25. 1 ml each culture was stressed with/without tetracycline (2 µg/ml) and incubated at 37°C with shaking (800 rpm). Before and 10 minutes after adding 2 µl hot methionine stock (10 mCi/ml, 1000 Ci/mmol), 200 µl cultures were centrifuged (14000 rpm, room temperature, 2 min) and cell pellets were resuspended within 10 µl 1x Laemmli reducing buffer. After heating (95°C, 5 min) and shortly spinning down, the proteins were separated by SDS-PAGE (s.3.7.1) and exposed to a phosphor image screen overnight at room temperature, and the radioactivity was analyzed.

## 3.20.2 *In-vitro* Translation Assay

The *in-vitro* translation assay was a powerful method to follow the protein synthesis *in vitro*. This assay was performed in the group of Prof. Dr. Marina Rodnina (Max-Planck Institute, Göttingen, Germany) and all the materials were provided there.

### 3.20.2.1 Initiation Complex and Ternary Complex Formation

The template mRNA, *E.coli* initiation factors (IF), *E.coli* 70S ribosome and $^{3}$H/AF488-double labeled N-formylmethionine tRNA (Q8 BdpFL-Met-tRNA$^{fMet}$) were mixed in $TAKM_7$ buffer containing DTT and GTP with the final magnesium concentration of 7 mM. The initiation complex was formed by incubation at 37°C for 50 minutes. Then, the initiation efficiency was controlled by nitrocellulose filtration, in which the initiation complexes with the double labeled N-formylmethionine tRNA were retained on the membrane, whereas the free initial methionine flowed through. Generally, the initiation efficiency was 60-80 %.

Initiation Complex Formation Master Mix:

| | |
|---|---|
| DTT | 2 mM |
| GTP | 2 mM |
| mRNA | 1.5 µM |
| IF mixture | 0.75 µM |
| 70S ribosome | 0.75 µM |
| Q8 BdpFL-Met-tRNA$^{fMet}$ | 0.5 µM |

(The mRNA used coded for the first 75 amino acids of HemK.)

In order to load GTP onto the elongation factor (EF), *E.coli* elongation factor Tu (EF-Tu) and EF-G (EF-G) were incubated with pyruvate kinase (PK), phosphoenolpyruvate (PEP) in the presence of DTT, GTP, in $TAKM_7$ buffer with the final magnesium concentration of 7 mM (37°C, 15 min). Then the *E.coli* total tRNA was added and further incubated at 37°C for 2 min.

Ternary Complex Fromation Master Mix:

| | |
|---|---|
| DTT | 2 mM |
| GTP | 2 mM |
| PEP | 3 mM |
| PK | 2 % |
| EF-Tu | 84 µM |
| EF-G | 4.8 µM |

#### 3.20.2.2 *In-vitro* translation

The initiation complex (IC)/ternary complex (TC) was mixed with YifE in the presence/absence of tetracycline. The translation was started at 37°C by adding the prepared IC to TC. At different time points (0, 20, 30, 40, 50, 60, 80, 100 sec), samples were taken and mixed with ice-cold NaOH (400 µM) to stop translation. After incubation (37°C, 60 min) and neutralization by adding 2 M Hepes, pH7.5, samples were incubated with 2x loading dye (40°C, 30 min) and analyzed by SDS-PAGE (s. 3.7.1) using 16.5 % tris-tricine gel (Bio-Rad, 100 V, 2 h), and fluorescence image using Typhoon.

### 3.20.3 Dipeptide Formation Assay

This assay has been established in the group of Professor Marina Rodnina (Max-Planck Institute, Göttingen, Germany), and the experiment was carried out there.

The initiation complex coupled with $^{3}$H-labeled N-formylmethionine tRNA (f[$^{3}$H]Met-tRNA$^{fMet}$) was mixed with the ternary complex loaded with $^{14}$C-labeled Phenylalanine tRNA (EF-Tu·[$^{14}$C]Phe-tRNA$^{Phe}$) in the presence of YifE (30µM) and tetracycline at different concentrations (0-100 µM). After short incubation (37°C, 20 sec), ribosomes were filtrated using nitrocellulose membrane and the dipeptides, which were bound to the nitrocellulose membrane, were analyzed in $^{3}$H- and $^{14}$C-channels.

# 4 Results

This part is composed of two sections: i) unraveling the activation mechanism of the HOCl-responsive *E.coli* protein YjiE; ii) identification and characterization of the novel *E.coli* protein YifE involved in the oxidative stress response.

## 4.1 Unraveling the Activation Mechanism of YjiE

### 4.1.1 Analysis of the Involvement of YjiE in Cellular Response to Oxidative Stress

Since YjiE conferred HOCl resistance to *E.coli* cells (*7*), its specificity to HOCl stress became of interest. To test whether YjiE played a role in bacterial responses to other oxidative stresses, the wild type C600 cells and *yjiE* deleted cells (C600 *yjiE::Cm*) were stressed respectively with $H_2O_2$, diamide and paraquat, and their viability was analyzed [Fig. 4-1-A-C].

With increasing concentration of $H_2O_2$, the viability of the wild type and the deletion strain comparably decreased, indicating an YjiE-independent *E.coli* response to $H_2O_2$ [Fig. 4-1-A].

Similarly, upon diamide stress, no difference in viability between the wild type cells and the deletion cells was observed [Fig. 4-1-B]. This suggested that YjiE is not involved in the bacterial response to diamide.

Paraquat could not kill C600 cells efficiently. At 1 mM paraquat, which is commonly used to kill bacteria (*55*), 50 % cells were still viable. Therefore, it was not clear, whether YjiE played a role or not in this case [Fig. 4-1-C].

Based on these observations, it can be concluded that YjiE is not a general oxidative-stress responsive transcription factor, but HOCl-specific.

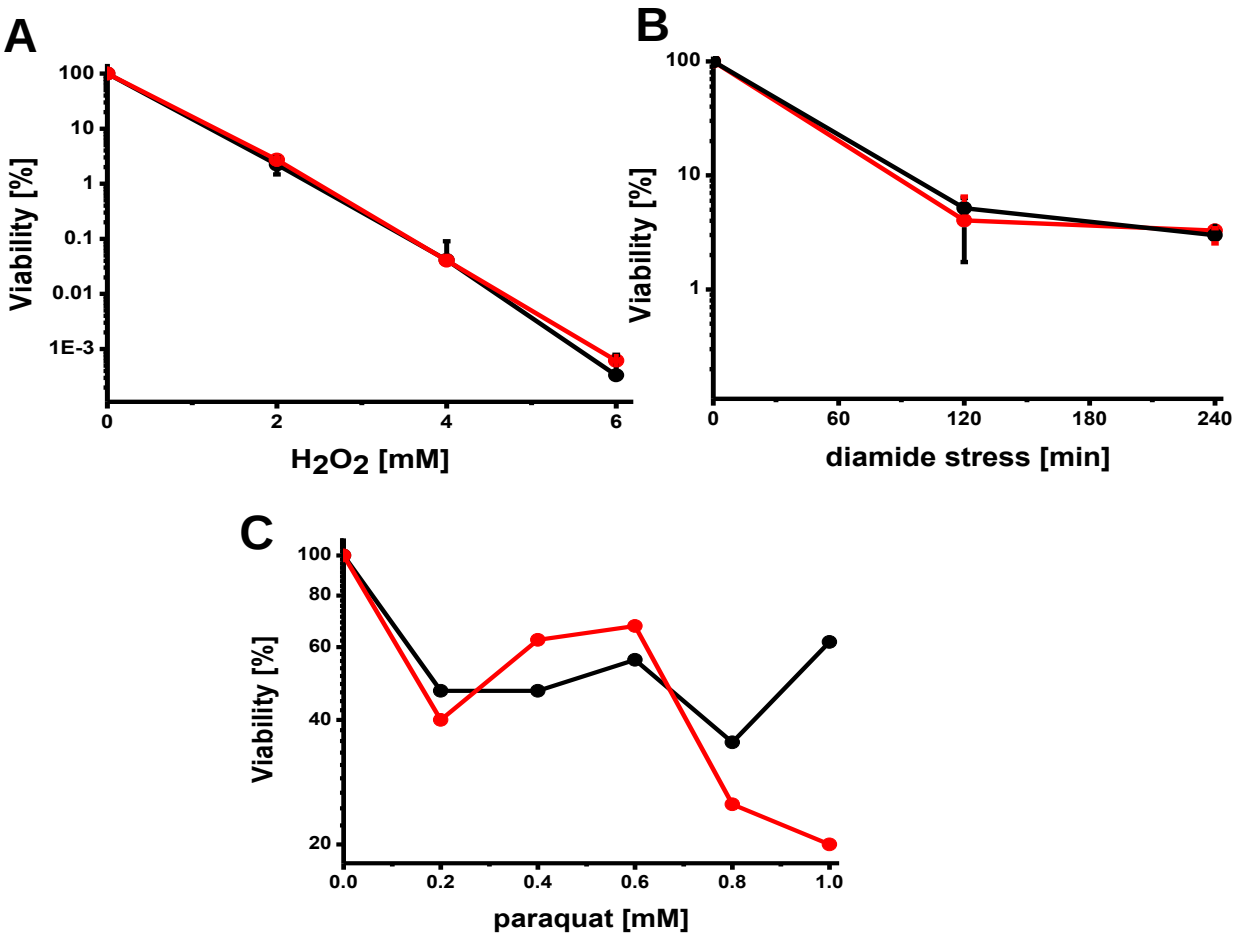


Fig 4-1: YjiE involvement in different oxidative stresses. At the exponential growth phase, wild type cells (red line) and *yjiE* deletion cells (black line) were challenged with A) $H_2O_2$, B) 5 mM diamide, and C) 1 mM paraquat. 50 µl cultures were serially diluted and 5 µl were spotted on LB agar plates (37°C, 20 h). Viability was calculated by counting colony forming unit (cfu) and comparing the cfu of stressed and unstressed cells. The viability of the unstressed cells was set to 100%.

### 4.1.2 Analysis of YjiE mRNA Level and Protein Level upon HOCl Stress

Since YjiE is a HOCl-specific transcription factor, its transcript level and protein level could accordingly change upon HOCl stress. To test this, wild type C600 cells and C600 *yjiE::Cm* cells were cultivated to the exponential growth phase. After exposure to different concentrations of HOCl, cells were harvested and RNA was isolated. The amount of YjiE transcripts was quantified by qRT-PCT using the primers specific for *yjiE*. With increasing HOCl concentrations, the YjiE transcript level (about 1xE-5 ng) remained unaffected [Fig.

4-2-A].

YjiE protein levels were detected by western blot using purified primary antibodies against YjiE. Upon HOCl stress, YjiE protein level slightly increased [Fig. 4-2-B]. This indicated that YjiE does not regulate its own promoter like many LTTRs (e.g., OxyR) and responses to HOCl by increasing the protein level.

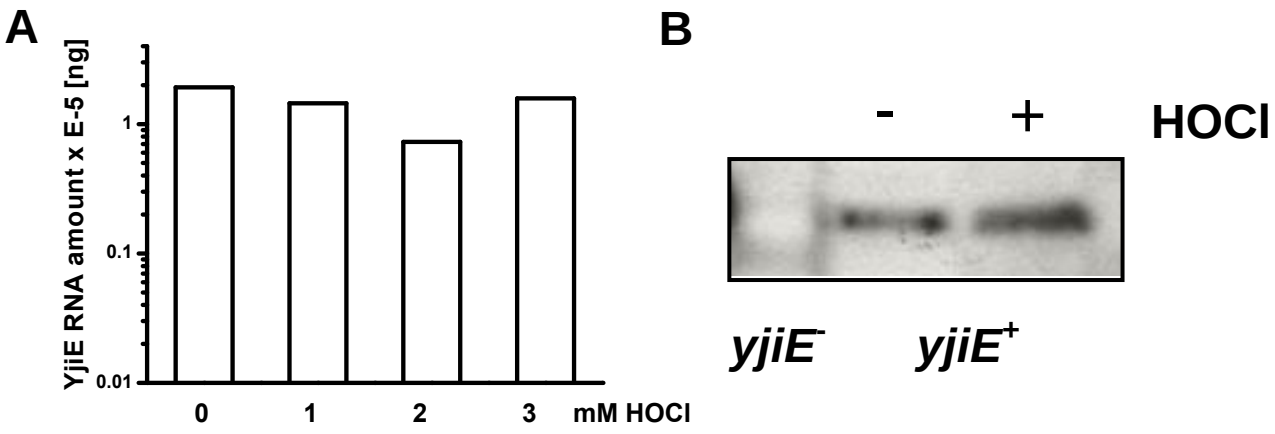


Fig. 4-2: YjiE transcript level and protein level upon HOCl stress. A) Quantification of YjiE mRNA amount using qRT-PCR. 2 ml culture ($OD_{600}$=0.45) was stressed with HOCl (room temperature, 5 min) and quenched with 5x LB medium. RNA was isolated and qRT-PCR was performed. B) YjiE level upon HOCl stress. 8 ml cultures ($OD_{600}$=0.45) were stressed with 2 mM HOCl (room temperature, 5 min). Total proteins were precipitated by TCA and separated by SDS-PAGE. YjiE was detected by western blot using purified antibodies against YjiE.

## 4.1.3 Identification of Inactive YjiE Mutants

### 4.1.3.1 Identification of Conserved Amino Acids in YjiE

Conserved amino acids in YjiE are potentially essential for YjiE activation. In order to identify such amino acids, the amino acid sequence of *E.coli* YjiE was aligned with YjiE from other organisms (Aug. 2010). 69 organisms contain *yjiE*, and in 64 organisms YjiE had been predicted as DNA binding protein (*56*). By a multiple sequence alignment of YjiE from 10 representative species, two hotspot clusters of conserved amino acids (first cluster: 204-208; second cluster: 228-235) in the C-terminal co-inducer domain were revealed, in addition to

many conserved amino acids in the N-terminal DNA binding domain [Fig. 4-3]. Reducing the species number used for alignment resulted in a more pronounced conservation in these clusters [Fig. S1]. Therefore, these two conserved amino acids hotspot clusters were of great interest.

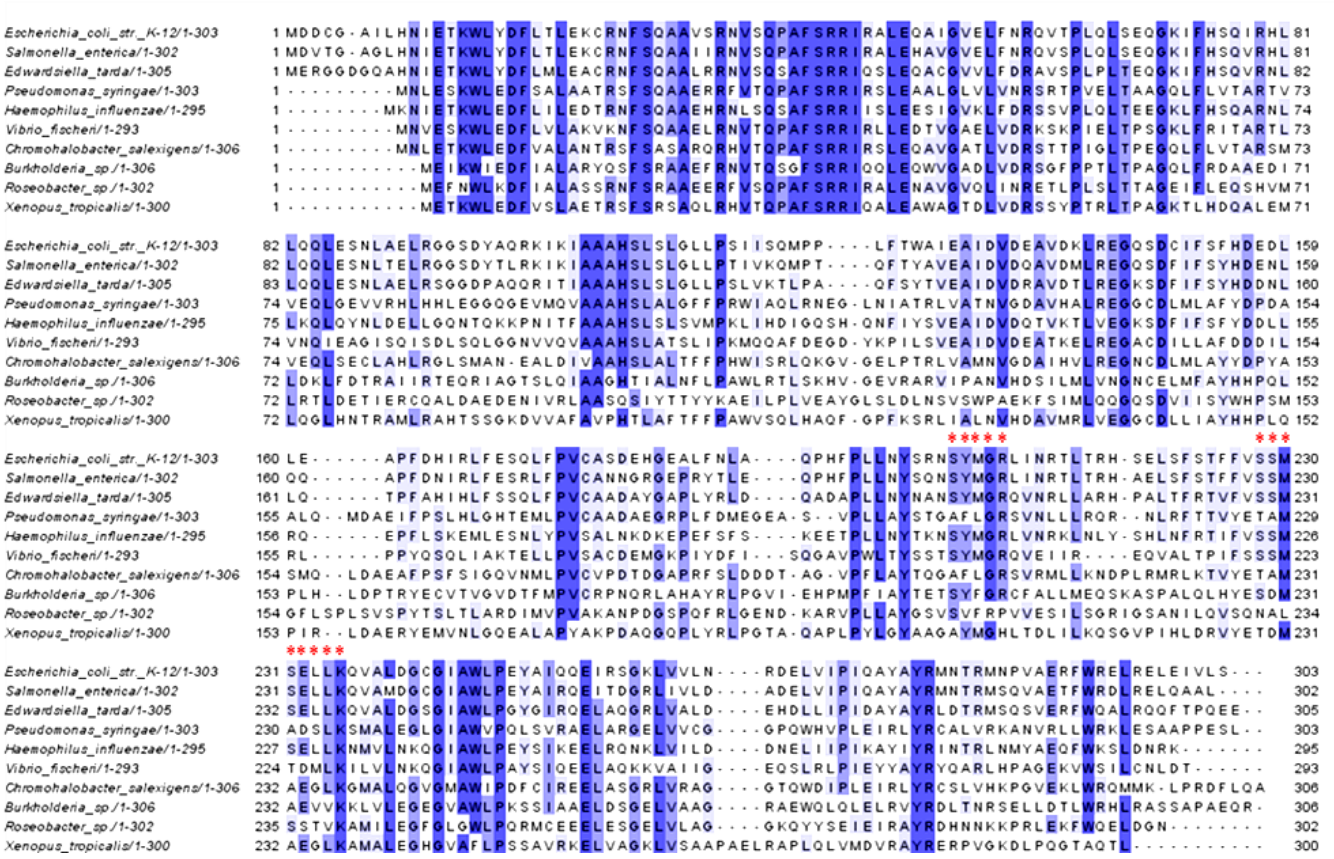


Fig. 4-3: Multiple sequence alignment of YjiE from 10 representative organisms using ClustalW. The conserved amino acids are highlighted in blue and the degree of conservation is proportional to the darkness of the colour. The conserved amino acids in the hotspot clusters are labeled with red stars.

### 4.1.3.2 Identification of YjiE Inactive Mutants *in vivo*

To study the effects of the conserved amino acids on YjiE activity, the amino acids in the two hotspot clusters were substituted with alanine, generating 13 single mutants and 2 cluster mutants (YjiE_A204-208, YjiE_A228-235), in which all single amino acids in either the first or the second cluster were replaced by alanine.

In addition, a triple YjiE mutant, YjiE_L208S, P286S, F291Y, and a single mutant

YjiE_P286S were used for experiments. They were generated during cloning and had been observed to be inactive (triple mutant) and active (YjiE_P286S) (*57*).

In order to identify inactive YjiE mutants, *yjiE*$^-$ cells and cells producing wild type YjiE or the YjiE mutants were stressed with HOCl and their viability was analyzed. The *in-vivo* activity of an YjiE mutant was estimated by its ability to complement the HOCl sensitive phenotype of the *yjiE*$^-$ strain. The active YjiE mutants, which act as wt YjiE, should confer HOCl resistance to *yjiE*$^-$ cells, whereas the inactive mutants should fail to rescue *yjiE*$^-$cells from HOCl killing, leading to a similar viability as *yjiE*$^-$ cells.

However, in all experiments, the *yjiE* expressing strain did not show a strong and reproducible HOCl-resistant phenotype, compared to the *yjiE*$^-$ strain [Fig. 4-4-A]. Using another plasmid (pUC18), in which *yjiE* was constitutively expressed, did also not give rise to a stable and significant HOCl-resistant phenotype [Fig. 4-4-B].

To obtain another readout, the phenotypes of *yjiE*$^+$ and *yjiE*$^-$ cells along the bacterial growth phase were analyzed. Neither at the exponential growth phase ($OD_{600}$=0.55), nor at the stationary growth phase (early/later stationary phase, $OD_{600}$=1.5/4.8), *yjiE*$^+$ cells did show to be firmly HOCl-resistant [Fig. 4-4-C].

Thus, it was very difficult to discriminate between active and inactive mutants, especially since the effect of individual substitutions may not manifest a strong phenotype to start with [Fig. 4-4-D, shown only three mutants].

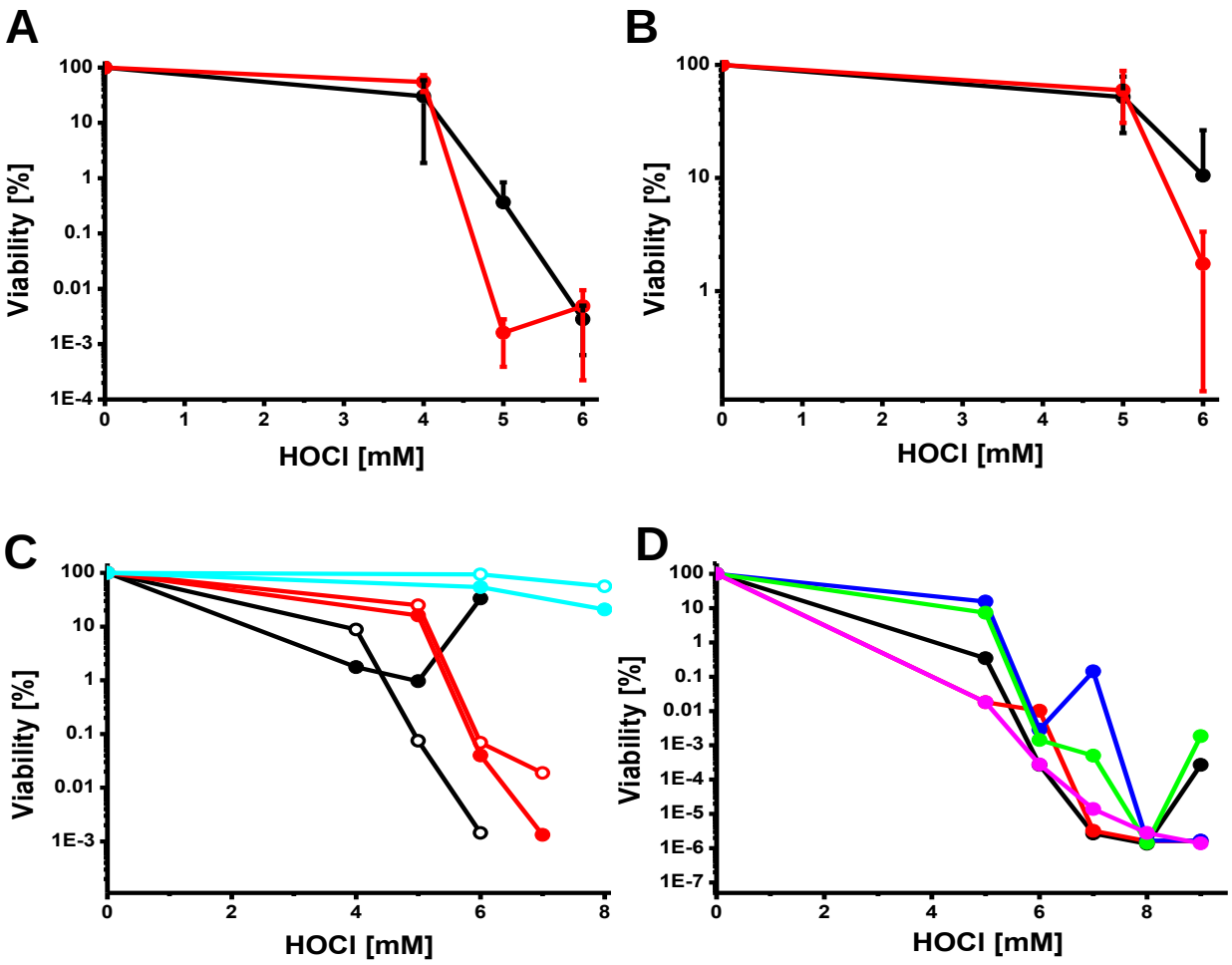


Figure 4-4: Viability of *yjiE*⁻ cells and cells expressing *yjiE* mutants from a plasmid. A) Viability of C600 *yjiE::Cm* harboring an empty pBAD22 plasmid (black line) and the strain expressing wild type *yjiE* (red line); B) Viability of MC4100 *rpoH::Km* harboring an empty pUC18 plasmid (black line) and the strain expressing wild type *yjiE* (red line); C) Viability of wild type C600 (filled circle) and C600 *yjiE::Cm* (open circle) at the exponential phase (black line), the early stationary phase (red line) and the late stationary phase (cyan line); D) Viability of MC4100 *rpoH::Km* (black line) and the strain expressing wild type *yjiE* (red line) or the mutants Y205A (blue line), S231A (green line) and E232A (pink line). Cells were cultivated to $OD_{600}$ of 0.5. 2 ml cultures were treated with different concentration of HOCl (room temperature, 10 min). HOCl was quenched by adding 0.5 ml 5x concentrated LB medium. 50 µl cultures were serially diluted and 5 µl were spotted on LB agar plates (37°C, 20 h). Viability was calculated by counting cfu and comparing the cfu of stressed and unstressed cells. The viability of the unstressed cells was set to 100 %.

### 4.1.3.3 Characterization of YjiE_A204-208

Despite that cells expressing wild type *yjiE* did not exhibit a significant and reproducible HOCl-resistant phenotype, cells producing YjiE_A204-208 stably showed to be more sensitive to HOCl than *yjiE*$^-$ cells in the concentration range of 4-7 mM HOCl [Fig. 4-5]. This implied that this mutant could be inactive, or expression of this mutant could be toxic to cells.

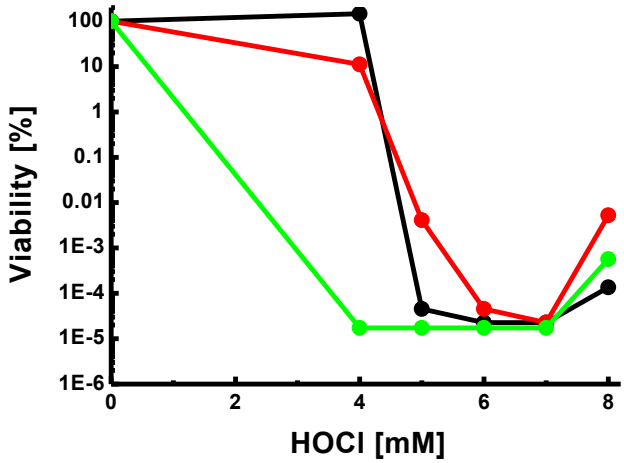


Figure 4-5: Viability of cells expressing YjiE_A204-208. MC4100 *rpoH::Km* cells containing an empty pBAD22 plasmid (black line), the cells producing wild type YjiE (red line) and the mutant YjiE_A204-208 (green line) were cultivated to $OD_{600}$ of 0.46. 500 µl cultures were stressed with HOCl (room temperature, 10 min). HOCl were quenched by adding 5x LB medium. 50 µl cultures were serially diluted and 5 µl were spotted on LB agar plates (37$^o$C, 20 h). Viability was calculated by counting cfu and comparing the cfu of stressed and unstressed cells. The viability of the unstressed cells was set to 100 %.

#### 4.1.3.3.1 YjiE_A204-208 Solubility Test

To test whether the HOCl-hypersensitive phenotype of cells producing YjiE_A204-208 could be attributed to the reduced solubility of this mutant, the solubility of YjiE_A204-208 was first analyzed. Cells overexpressing wild type *yjiE* and this mutant gene were harvested and disrupted by French Press. After centrifugation, the lysates (soluble proteins) and the pellets (insoluble proteins) were analyzed by SDS-PAGE and western blot using YjiE-specific antibodies. Possessing the solubility of 55 % YjiE_A204-208 was almost as soluble as wild type YjiE [Fig. 4-6]. Therefore, the HOCl-hypersensitive phenotype mediated by YjiE_A204-208 did not result from its insolubility but from the loss of wild type function.

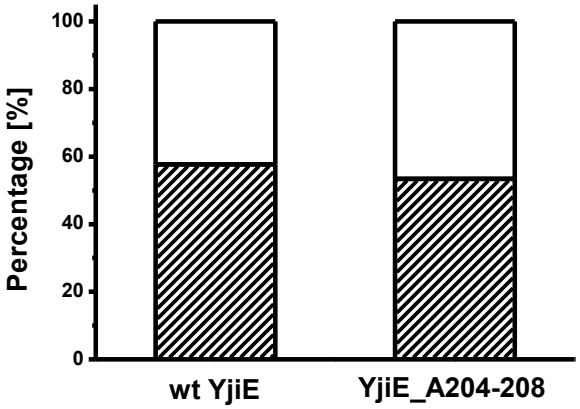


Figure 4-6: Solubility of YjiE_A204-208 and wild type YjiE. The percentage of the soluble protein was indicated as patterned in column and that of the insoluble protein as non-patterned. Cells at the exponential growth phase were harvested and disrupted by French Press. The protein pellet (insoluble proteins) was resuspended in the same volume of $H_2O$ as the volume of lysates. Both soluble and insoluble proteins were precipitated by TCA and analyzed by SDS-PAGE. The soluble and insoluble YjiE were detected by western blot using YjiE-specific antibody.

#### 4.1.3.3.2 Secondary Structure Analysis of YjiE_A204-208

To test whether the structural change of YjiE_A204-208 rendered this mutant inactive, the secondary structure in oxidized and reduced YjiE_A204-208 was analyzed using CD spectroscopy. Both oxidized and reduced YjiE_A204-208 showed similar alpha-helical spectrum as wild type YjiE [Fig. 4-7]. It indicated that oxidation by HOCl *in vitro* does not trigger a significant conformational change in both wild type YjiE and YjiE_A204-208. Owning the similar structure to wild type YjiE, this mutant apparently loses its function by other reasons.

#### 4.1.3.3.3 Thermal Stability of YjiE_A204-208

To test whether the mutant was inactive because of reduced stability, the thermal stability of this mutant was analyzed by thermal transition as measured by CD following the change in signal at 222 nm. The heating-induced unfolding of YjiE_A204-208 was irreversible and the midpoint of transition ($T_m$) was 51°C [Fig. 4-8]. Compared to the $T_m$ of wild type YjiE (60°C)

(*7*), YjiE_A204-208 was less stable than wt YjiE. Thus, the reduced stability could contribute to the inactivity of YjiE_A204-208.

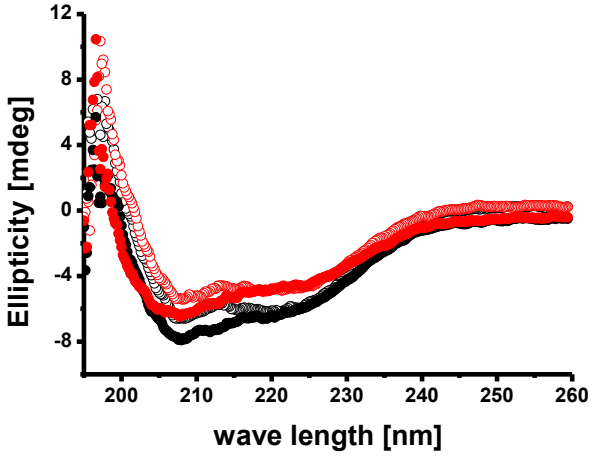


Figure 4-7: CD spectroscopy of YjiE_A204-208 and wild type YjiE. Wild type YjiE (black curve) and YjiE_A204-208 (red curve) were oxidized with 10 fold molar excess of HOCl (25°C, 30 min), which was then quenched by 10 fold molar excess of methionine. In parallel, the proteins were reduced with 1 mM TCEP (37°C, 1 h), which was subsequently removed by NAP5 column. The CD spectra of oxidized protein (open circle) and reduced protein (filled circle) were recorded from 195 nm to 260 nm with the scan rate of 20 nm/min at 20°C. (Figure from *58*).

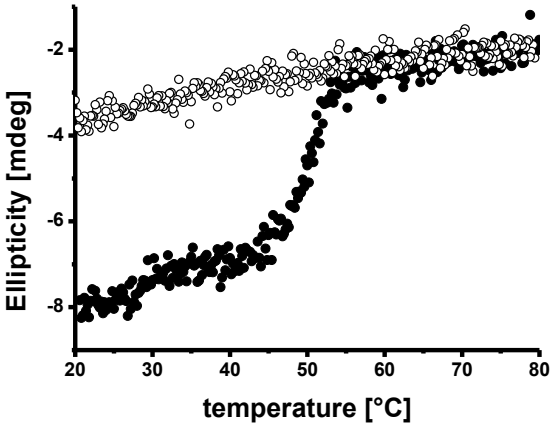


Fig 4-8: Thermal transition of YjiE_A204-208. The thermal transition was recorded at 222 nm with the heating rate of 20°C/h from 20°C to 80°C (filled black circle) and back (open circle). Calculated $T_m$ is 51°C. (Figure from *58*).

4.1.3.3.4 Analysis of 3D Structure and Oligomerization State of YjiE_A204-208

Wild type YjiE predominantly formed 12-mer with hexagonal ring-like structures (*7*). To

test whether the inactive YjiE_A204-208 maintained the 12-meric ring-like structure or not, its structure and oligomerization state were analyzed by TEM and aUC. Similar to wild type YjiE, YjiE_A204-208 mainly formed 12-mer like wild type YjiE and some ring-like structures of YjiE_A204-208 could still be observed by TEM [Fig. S2-3]. However, most of the ring structures appeared disrupted, because the protein massively aggregated during sample preparation for TEM [Fig. S2]. Hence, YjiE_A204-208, being inactive, could still form the 12-meric hexagonal ring-like structure like wild type YjiE.

Taken together, YjiE_A204-208, possesses a similar solubility, secondary structure, oligomerization state and 3D structure as wild type YjiE, but is instable and dysfunctional.

### 4.1.4 Study of YjiE Activation *in vitro*

Compared to YjiE from unstressed cells, YjiE isolated from HOCl stressed cells exhibited strong DNA binding ability and represents the active species (*7*). Since purified YjiE from unstressed cells could not be activated by HOCl *in vitro* (*7*), activation of YjiE seems to takes place exclusively *in vivo*. In this case, YjiE could probably activated by a HOCl-oxidized protein/metabolite in lysates or an HOCl-oxidized component of LB medium. To test these possibilities, the C-terminal His-tagged YjiE was purified from the unstressed cell lysates (YjiE-$His_C$), which were challenged with HOCl *in vitro* (YjiE-$His_C$-$HOCl_{lysate}$), or from unstressed cell lysates premixed with HOCl-treated LB medium (YjiE-$His_C$-$HOCl_{LB}$). The DNA binding ability of these species as well as the active species (YjiE-$His_C$-HOCl) was analyzed by EMSA. However, in contrast to YjiE-$His_C$-HOCl, neither YjiE-$His_C$-$HOCl_{lysate}$ nor YjiE-$His_C$-$HOCl_{LB}$ was able to bind to DNA, indicating that both of them were as inactive as YjiE-$His_C$ [Fig. 4-9].

Furthermore, YjiE could not be in-trans activated. Pre-incubation of YjiE-$His_C$ with cell lysates of HOCl-stressed cells did not restore the DNA binding of inactive YjiE species, YjiE-$His_C$ [Fig. 4-10] (*59*).

All these results suggested that YjiE can exclusively be activated *in vivo*.

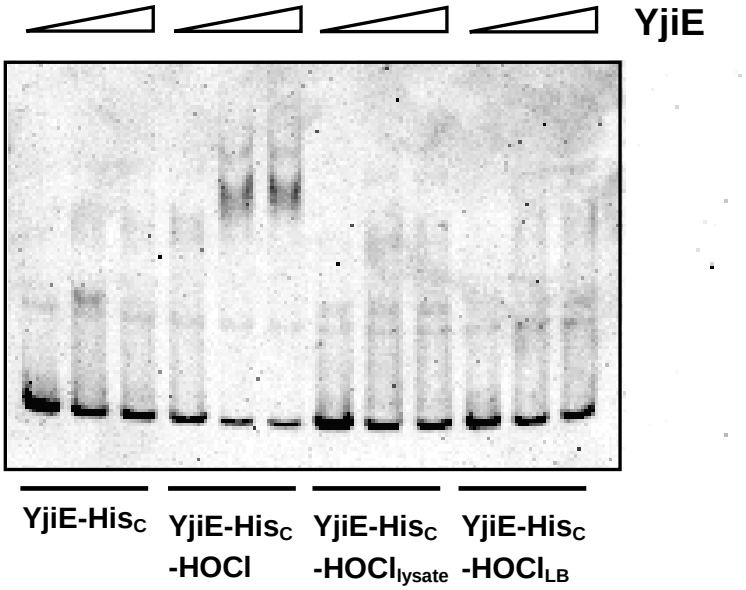


Figure 4-9: DNA binding of YjiE-His$_C$, YjiE-His$_C$-HOCl, YjiE-His$_C$-HOCl$_{lysate}$, YjiE-His$_C$-HOCl$_{LB}$. Proteins were incubated with 5'-AlexaFuor488-labelled *yjiE* promoter DNA of 158 bp at a molar ratio of 60:1, 120:1, 130:1 (protein:DNA) at the room temperature for 10 minutes. The DNA shift was analyzed on 6 % TBE gel electrophoresis (150 V, 50 min), followed by ethidium bromide staining.

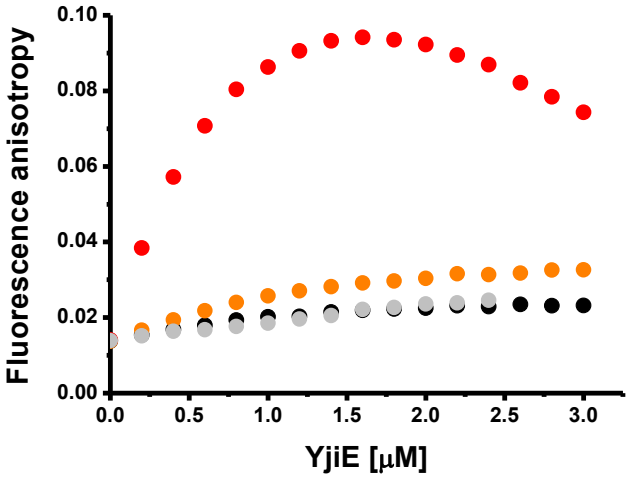


Fig 4-10: DNA binding of YjiE-His$_C$, YjiE-His$_C$-HOCl, *in-vitro* HOCl treated YjiE-His$_C$, and potentially in-trans actived YjiE-His$_C$. Red point: YjiE-His$_C$ purified from 2.75 mM HOCl stressed cells (YjiE-His$_C$-HOCl); orange point: potentially in-trans activated YjiE-His$_C$, purified from a combination suspension of unstressed *yjiE* overexpressing cells and 2.75 mM HOCl stressed non overexpressing cells; grey point: *in-vitro* 2.75 mM HOCl treated YjiE-His$_C$; black point: YjiE-His$_C$ from unstressed cells. The proteins were titrated (200 nM per step) into 10 nM 3'-AlexaFluo488 labeled *metN* promoter DNA (158 bp in length) and the fluorescence anisotropy was monitored. (Figure from *59*).

### 4.1.5 Identification of a Potential Co-inducer Required for Activation of YjiE

LTTRs are typically activated by either binding of a co-inducer (*41*, *46*, *47*), or direct modification of amino acids under certain conditions (*34*). Since YjiE-$His_C$-HOCl, being the active species, showed large DNA binding ability, there could be a potential co-inducer bound. To test this, a large amount of YjiE-$His_C$-HOCl, to which a potential co-inducer should bind stoichiometrically, was applied to reversed phase HPLC. In this chromatographic system, the samples were denatured, so that any organic molecules could be separated according to their hydrophobic character and detected by UV and fluorescence, in case some molecules do not absorb in UV. However, YjiE-$His_C$-HOCl and YjiE-$His_C$ were eluted very similarly at the retention time of 37 minutes with no indication of an additional peak in the sample of the active species [Fig. 4-11-A-B]. This indicated that no co-inducer was bound to YjiE-$His_C$-HOCl in stoichiometric amounts and that the increased DNA binding ability was likely caused by other means.

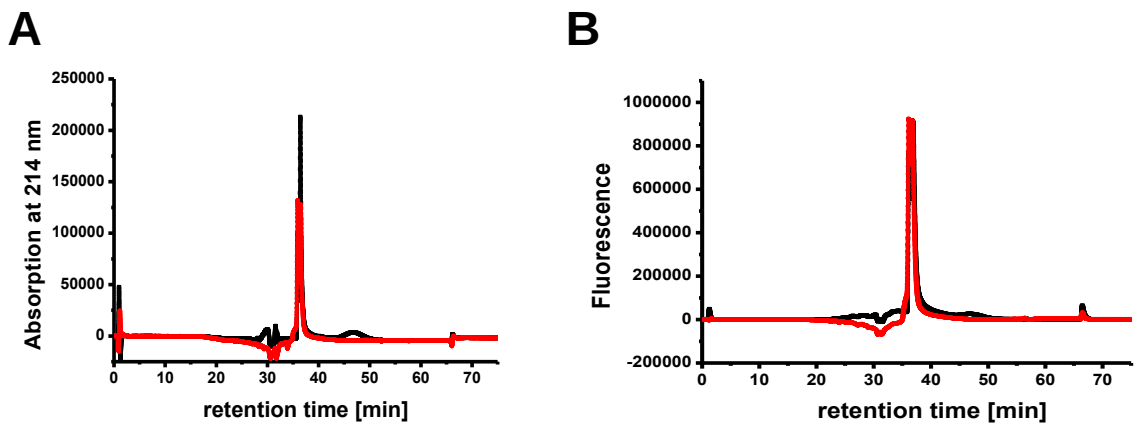


Figure 4-11: Detection and separation of a potentially bound co-inducer by reversed phase HPLC. A) Detection of peptides; B) Detection of fluorescent substances. YjiE-$His_C$ (black curve) and YjiE-$His_C$-HOCl (red curve) were supplemented with 10 % ACN and 1 % trifluoroacetic acid. 3.4 µg proteins were loaded onto a Bischoff NPS C18 column (column volume: 0.232 ml) and eluted with an acetonitrile gradient from 5 % to 95 %.

### 4.1.6 Identification of HOCl Modified Amino Acids Involved in YjiE Activation

The other potential mechanism of YjiE activation is by HOCl-specific modification of amino acids in YjiE. Thus, the potentially modified amino acids in the active species YjiE-$His_C$-HOCl compared with those in the inactive species YjiE-$His_C$ were identified using mass spectroscopy. According to the preliminary results, methionines and cysteines were discovered to be oxidized (i.e., +16 Da adducts) in YjiE-$His_C$-HOCl (*7*, *60*).

In addition, the protein samples for stable isotope labeling by/with amino acids in cell culture (SILAC), a powerful approach to precisely identify modifications on amino acids, were prepared in this work and the isotope labeling efficiency was above 95 % (*60*). However, the collaboration was discontinued, since Dr. Graumann moved to Katar to establish a new facility, and SILAC analysis was not yet finished.

Nevertheless, the multiple sequence alignment, preformed at the beginning, identified Met206 in the first hotspot cluster and Met230 in the second hotspot cluster to be stronger conserved than the remaining methionines and the cysteines. Thus, they were of particular interest. It is known that oxidation of methionine to methionine sulfoxide (Met-SO) by HOCl could inactivate protein such as GroEL (*20*). To investigate the role of methionine oxidation in activation of YjiE, Met206 and Met230 were substituted with Gln and Ile respectively to investigate the role of methionine sulfoxide (Met-SO) in YjiE activity. Glutamine structurally mimics methionine sulfoxide, being the potentially active state, while Ile mimics the reduced Met, being the inactive state (*61*, *62*). As a result, four single mutants (M206I, M230I, M206Q, M230Q) were generated. Given that oxidation of methionine potentially activates YjiE, the Gln mutants (M206Q, M230Q) should be constitutively active, whereas the Ile mutants (M206I, M230I) should remain inactive.

#### 4.1.6.1 Analysis of the Activity of YjiE Methionine Mutants

The *in-vivo* activity of the mutants and wild type YjiE was then examined by analyzing the change in the RNA level of YjiE target genes upon HOCl stress using qRT-PCR.

Constitutively active mutants should show up- or down-regulated RNA levels of YjiE-regulated genes already in the absence of stress, while for inactive mutants the RNA levels should not change upon HOCl stress. In this work, the qRT-PCR procedure was established and all conditions concerning template preparation, and template and primer concentration were optimized. *tufB* encoding EF-Tu was used as house keeping gene, since its RNA level in cells did not alter upon HOCl treatment. According to transcription profile (*44*), *metN* and *metB* were strongly up-regulated, whereas *fecD* and *cydA* strongly down-regulated by YjiE upon HOCl stress. Thus, their RNA levels in *yjiE* deletion cells expressing the mutant genes and wild type *yjiE* (as positive control) were analyzed.

Concerning the RNA levels of the genes *metN*, *metB*, all the non-stressed cells have almost the same RNA levels of these genes [Fig. 4-12-A-B]. This indicated that neither M206Q nor M230Q, both of which supposedly mimic the oxidized state, was constitutively active. After stress, the MetN RNA level significantly increased in the cells expressing wild type YjiE, M230I, 206Q, but not in the case of M206I and M230Q due to their large error bars [Fig. 4-12-A]. The MetB RNA level greatly increased in cells producing M230I, M206Q and M230Q upon HOCl stress, but the level in the positive control did not differ from that in the negative control [Fig. 4-12-B]. Thus, the increase in MetB RNA level seems to be purely a HOCl-effect. This indicated that M230I, which mimics the reduced methionine, was active. The activity of M206I in both cases was unclear.

HOCl exposure did not alter the RNA levels of FecD or CydA in the cells producing wild type or mutant YjiE [Fig. 4-12-C, shown only for FecD] and as a result, the activity of the methionine mutants could not be determined in these cases.

Since qRT-PCR did not show strong and reproducible results, even in the cells producing wild type YjiE (positive control), it was impossible to investigate the activity of the methionine mutants by this means.

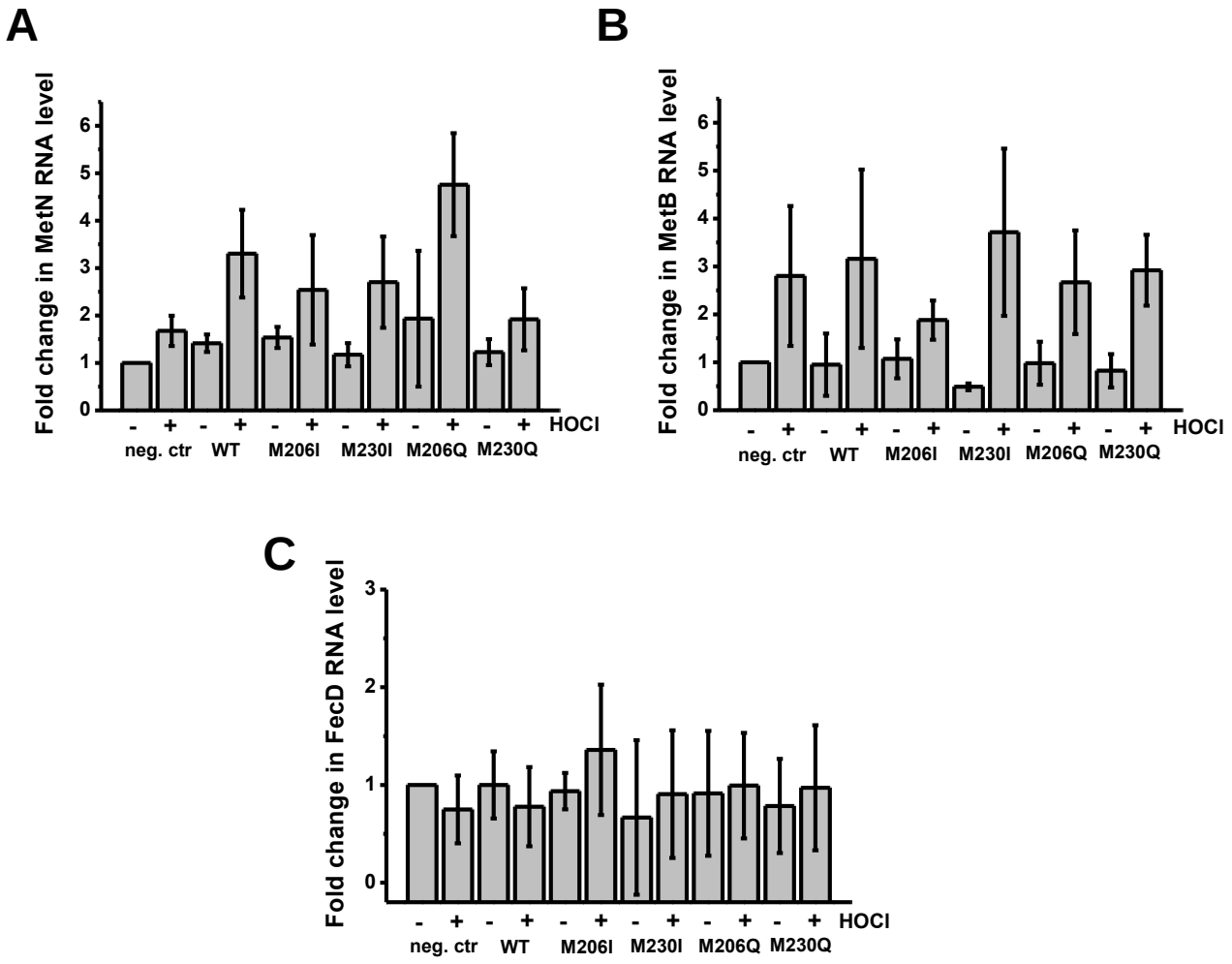


Figure 4-12: Changes in RNA levels of YjiE-regulated genes upon HOCl stress analyzed by qRT-PCR. A) MetN RNA level; B) MetB RNA level; C) FecD RNA level. C600 *yjiE::Cm* cells harboring an empty pBAD22 plasmid (negative control) and the cells over expressing wild type or mutant *yjiE* were cultivated to the exponential growth phase. 2 ml cells were removed and left unstressed or treated with 2 mM HOCl (room temperature, 5 min) and subsequently quenched by adding 0.5 ml 5x LB medium. RNA was isolated and qRT-PCR was performed.

### 4.1.6.2 Analysis of the DNA Binding Ability of YjiE Methionine Mutants

The active YjiE species (YjiE-$His_C$-HOCl) showed a significant DNA binding ability. Thus, the activity of YjiE methionine mutants should be determined by analyzing and comparing their DNA binding ability with that of YjiE-$His_C$-HOCl *in vitro*.

4.1.6.2.1 Fluorescence Anisotropy

C-terminal His-tagged YjiE and Gln- and Ile-mutants (YjiE-$His_C$, M206Q-$His_C$, M230Q-$His_C$, M206I-$His_C$, M230I-$His_C$) were purified and their binding to fluorescent-labeled *metN* promoter DNA was examined. Binding of YjiE to this DNA decreases the rotation of the DNA molecule and results in a change in fluorescence anisotropy (FA). For M206 mutants (M206I, M206Q), the proteins from unstressed cells showed a slightly increased FA compared to inactive wild type YjiE (from unstressed cells), while all the proteins from HOCl exposed cells showed a significantly increased FA. This indicated that M206 had a wild type-like behavior [Fig. 4-13-A]. Similarly, M230I from unstressed or stressed cells showed the same FA as wild type YjiE, whereas M230Q both from unstressed and stressed cells showed the same low FA as inactive YjiE [Fig. 4-13-B]. This indicated that M230I was functional and M230Q might be inactive. Since the qRT-PCR failed to clearly demonstrate the activity of the mutants, these results from FA experiment should be estimated with caution.

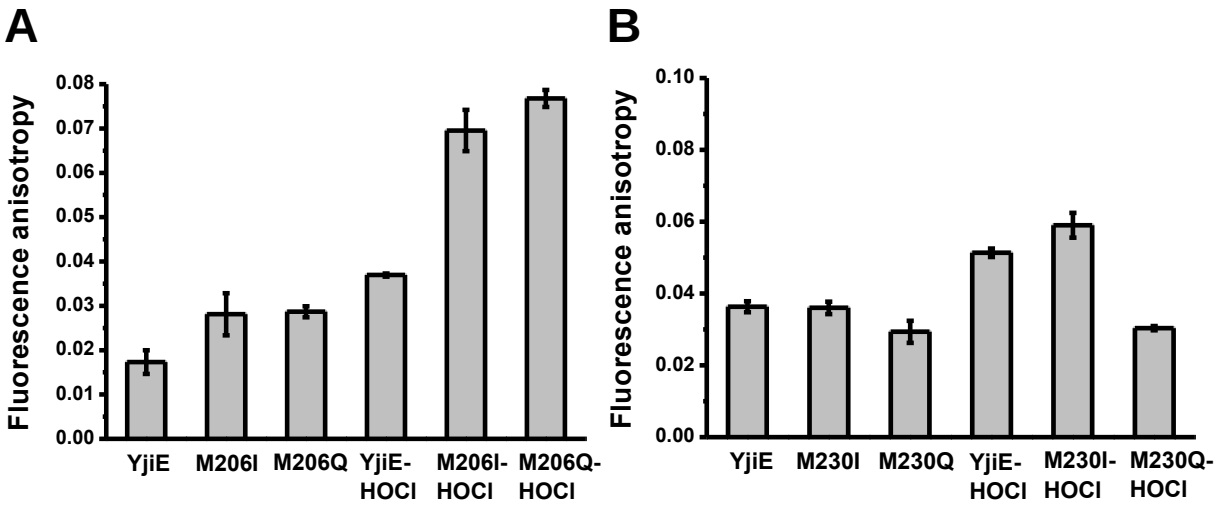


Figure 4-13: Fluorescence anisotropy of His-tagged wild type YjiE and its mutants. A) Met206 mutants; B) Met230 mutants. Proteins were pre-incubated with 1 mM DTT (37°C, 2 h) and then mixed with *metN* promoter DNA (3'-AF488-MetN158) at the molecular ratio of 200:1 (10 nM DNA, 2 µM protein). The fluorescence anisotropy was analyzed at 37°C in YjiE storage buffer.

#### 4.1.6.2.2 DNase I Footprint

DNase I footprint is another approach to detect protein-DNA interaction (*53*). To identify the potential binding site(s) of YjiE on the *metN* promoter, this assay was performed using the active YjiE species. Once YjiE binds to the promoter of *metN*, the bound region in DNA should be protected from DNase I digestion. The purified DNA fragments are then sequenced and the exact binding region can be identified. The conditions for DNase I footprints for two different *metN* promoter DNA (158 bp in length [MetN158] and 315 bp in length [MetN315]), both of which were fluorescent labeled either at the 3'-end or 5'-end, were optimized. However, although initial results looked promising, no region specific for YjiE binding could be identified. In all cases, the apparent binding region of YjiE was near the fluorophores but not sequence-specific (data not shown). Hence, the assay could not be further used to analyze the activity of YjiE methionine mutants.

#### 4.1.6.2.3 Analysis of the DNA-YjiE Interaction using Pull-down Assay

Additionally, the DNA-YjiE interaction could be analyzed by a pull-down assay. In principle, target DNA containing restriction enzyme recognition sites was coupled to beads and then incubated with active YjiE. When YjiE binds to DNA, this complex should be cleaved from beads using the specific restriction enzyme and analyzed by SDS-PAGE. Using this assay, the DNA binding of YjiE and its mutants could be examined. For this purpose, the *metN* promoter DNA linked with multiple *Nde*I restriction sites at the biotin-labeled 3'-end was constructed and the DNA was coupled on the streptavidin-crosslinked beads through the biotin-streptavidin interaction. After incubation with YjiE-$His_C$-HOCl, the DNA-YjiE complex should be cleaved from beads by the restriction enzyme *Nde*I. However, the restriction sites in DNA were inaccessible for *Nde*I, making it impossible to release the DNA-YjiE complex (data not shown). Thus, this assay failed to identify DNA-YjiE interaction and consequently the activity of YjiE mutants.

### 4.1.6.3 Analysis of Carbonylation in the Proteome

Carbonylation is a kind of common modification on proteins aroused by oxidative stress (*17*). Thus, protein carbonyl content in proteome is a marker for cellular oxidative damage. The carbonyl group can react with DNPH, giving rise to a product, which can be recognized by a specific antibody. Since YjiE was shown to confer HOCl resistance to *E.coli* cells (*7*), proteins in could be less carbonylated by HOCl than in *yjiE*$^-$ cells. Thus, the activity of YjiE mutants could be determined by analyzing and comparing the proteomic carbonyl levels in the HOCl-challenged cells expressing mutant *yjiE* and wild type *yjiE* (as control). For this purpose, the carbonyl content in *yjiE*$^+$ and *yjiE*$^-$ cells were first analyzed. The DNPH treated proteins were separated by either 1 dimensional or 2 dimensional gel electrophoresis (here shown only 1 dimensional electrophoresis) and the amounts of the modified carbonyl groups were detected by western blot. Yet, exposed to HOCl, proteins were more carbonylated in *yjiE*$^-$ cells than in the *yjiE*$^+$ cells. In the negative control, in which derivarization control buffer instead of DNPH was added, nothing was detected [Fig. 4-14]. Hence, this assay was not suitable to further determine the activity of YjiE mutants.

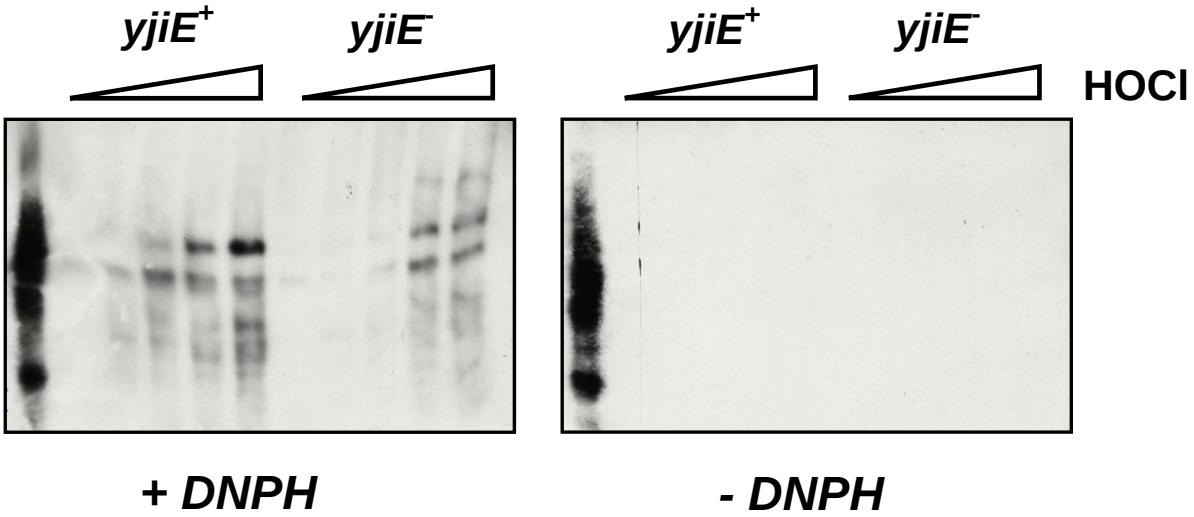


Figure 4-14: Carbonylation level in wild type and *yjiE* deletion strain. C600 cells and C600 yjiE:Cm cells were cultivated to the exponential growth phase and stressed with HOCl (0, 3, 4, 5, 6 mM, room temperature, 10 min). After quenching with 5x LB medium, cells were harvested and resuspended within 1x reducing Laemmli buffer. One half was treated with DNPH and the other half with derivarization control buffer (room temperature, 15 min). After adding the neutralization buffer, the samples were analyzed by SDS-PAGE and western blot.

## 4.2 Identification and Characterization of YifE

### 4.2.1 Discovery of YifE

In order to discover further components/proteins involved in the bacterial response to oxidative stress, a genomic library (*63*), was used to select for $H_2O_2$- resistant clones. In several independent screens, one clone, harboring the complete gene *yifE*, repeatedly showed $H_2O_2$ resistant. Furthermore, the same clone was discovered to be HOCl resistant in the genomic library screening upon HOCl stress (*64*).

*yifE*, located downstream from one *E.coli* ribosomal RNA operon (*rrsC*), encodes a small conserved protein with the molecular weight of 13.13 kDa. It consists of 112 amino acids and has only one cysteine at position 64 (*65*). So far, nothing has been known about its function and structure, making this protein mysterious.

To gain insight into the potential function of YifE, an alignment was performed. Bacterial proteins with similar sequences to YifE were searched using Blast-analysis in the database Swissprot (*66*). Besides hypothetical proteins with unknown function, one *E.coli* protein, 30S ribosomal protein S6, which constitutes a component of the ribosome 30S subunit, showed a limited sequence similarity to YifE. Individually aligning the sequence of YifE with those of other ribosome related proteins, such as Rrf (ribosome recycling factor), Hsp15 (heat shock protein 15 involved in ribosome recycling) and YbeY (the conserved protein involved in translation), revealed a partial sequence similarity to YifE [Fig. 4-15].

On the other hand, the secondary/ternary structure of YifE was predicted using Phyre and PredictProtein programs (*67*, *68*). YifE is composed mainly of alpha helical and coil structure [Fig. 4-16] (*68*). The $\sigma^2$ domain of RNA polymerase sigma factors, which consist of α-helices and coils, turned out as the most structurally relevant protein with an estimated precision of 35% (35% of sequences were truly homolog according to the Structural Classification of Proteins (SCOP) database) (*67*).

Thus, YifE could be a ribosome related protein or a sigma factor.

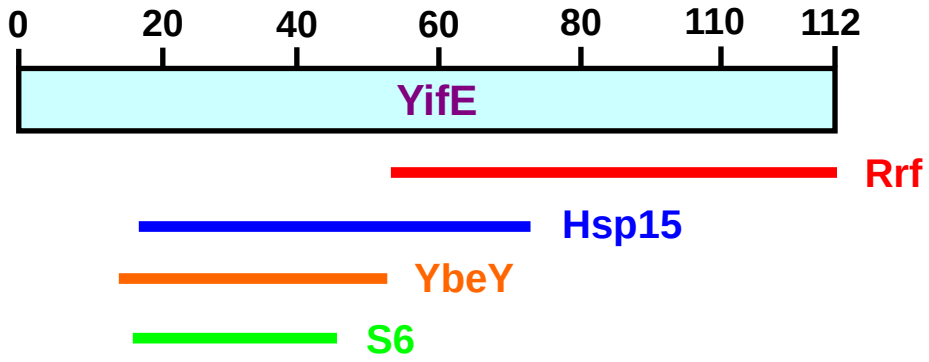


Figure 4-15: Sequence alignment of YifE with ribosome related proteins using Blast. The region of YifE, which shows similar sequence to other proteins, was underlined.

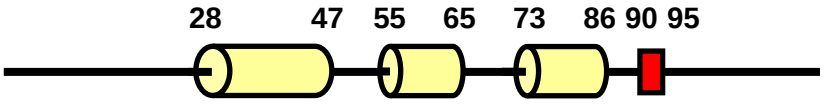


Figure 4-16: Predicted secondary structure in YifE using PredictProtein. The helical structures (helix 1: 28-47; helix 2: 55-65; helix 3: 73-86) were illustrated by yellow cylinders and the sheet structure (90-95) by a red box.

## 4.2.2 Identification of YifE-Mediated Phenotype

### 4.2.2.1 YifE-Mediated Oxidative Stress Resistance

YifE was initially discovered to confer $H_2O_2$ resistance. In the genomic library screenings, cells overexpressing *yifE* exhibited large resistance to $H_2O_2$ stress (in this work) and HOCl stress (*64*). Thus, these oxidative-stress related phenotypes were first confirmed by analyzing the growth of wild type and *yifE* deleted cells in the presence of $H_2O_2$ and HOCl. Deletion of *yifE* rendered *E.coli* cells more susceptible to $H_2O_2$ and HOCl, leading to an inhibited bacterial growth [Fig. 4-17-A-B], while overexpression of *yifE* conferred resistance to both oxidants [Fig. 4-17-C-D]. These observations demonstrated that YifE protects cells from oxidative damages caused by $H_2O_2$ and HOCl.

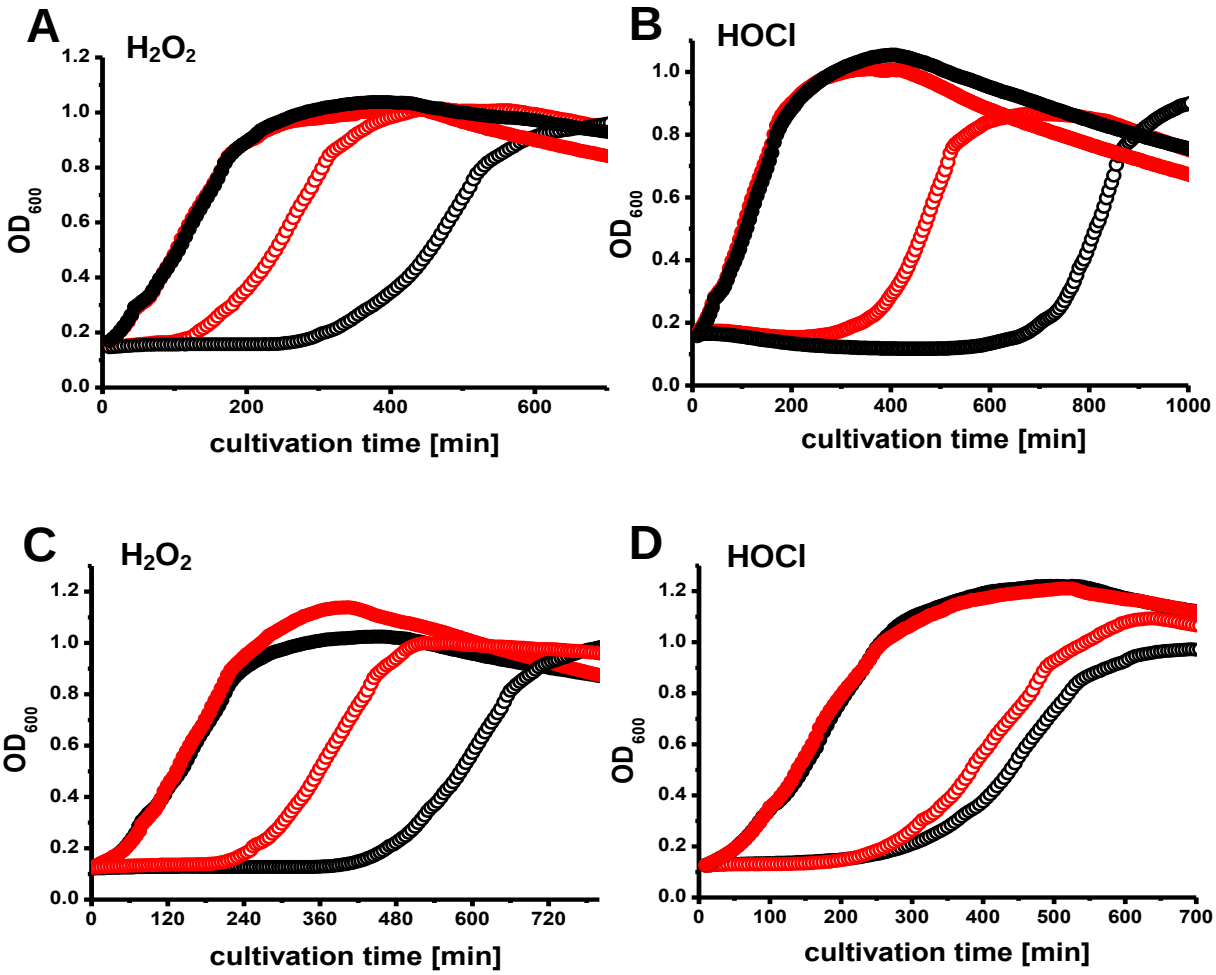


Figure 4-17: Growth of *yifE* expressing strain and *yifE* deleted strain upon oxidative stress. Filled circle: unstressed cells; open circle: stressed cells. Red curve: *yifE* expressing strain; black curve: *yifE* deleted strain. A) Growth of MC4100 and MC4100 *yifE*$^-$ in the presence of 3.25 mM $H_2O_2$; B) Growth of MC4100 and MC4100 *yifE*$^-$ in the presence of 2.25 mM HOCl; C) Growth of MC4100 *yifE*$^-$ containing an empty pBAD22 plasmid and the strain overexpressing *yifE* from a plasmid in the presence of 2.5 mM $H_2O_2$; D) Growth of MC4100 *yifE*$^-$ containing an empty pBAD22 plasmid and the strain overexpressing *yifE* from a plasmid in the presence of 2.75 mM HOCl. Cells were cultivated to the exponential growth phase and diluted with LB medium into 96 well plate ($OD_{600}$=0.05 per well). Oxidants were added and the growth was followed by measuring $OD_{600}$ every 5 minute using a microtiter plate reader.

### 4.2.2.2 YifE-Mediated Antibiotic Resistance

Since YifE showed limited sequence similarity to the ribosomal protein S6, Rrf, YbeY and Hsp15, its involvement in the bacterial response to antibiotics targeting ribosome function

was examined. In this case, various antibiotics, which interfere the ribosome function in different manner were used, such as tetracycline disrupting tRNA decoding (*69*), kanamycin inhibiting translocation (*70*), and chloramphenicol arresting peptidyl transferase activity (*71*). The growth of *yifE*$^{+}$ and *yifE*$^{-}$ cells, which were exposed to these antibiotics, was analyzed. Compared to the *yifE*$^{+}$ strain, the *yifE*$^{-}$ strain was more sensitive to tetracycline, [Fig. 4-18-A], chloramphenicol [Fig. S4-A], spectinomycin [Fig. S4-B], but not to kanamycin [Fig. 4-18-B]. Overexpression of *yifE* from a plasmid partically complemented the tetracycline sensitive phenotype of *yifE*$^{-}$ cells [Fig.4-18-C], while the effects on chloramphenicol, spectinomycin have not been analyzed yet. These results demonstrated that YifE participates in the bacterial defense against some ribosome targeting antibiotics, first of all, tetracycline. This result is in accordance with the YifE-mediated phenotype suggested by the bacterial phenotypic database (*72*).

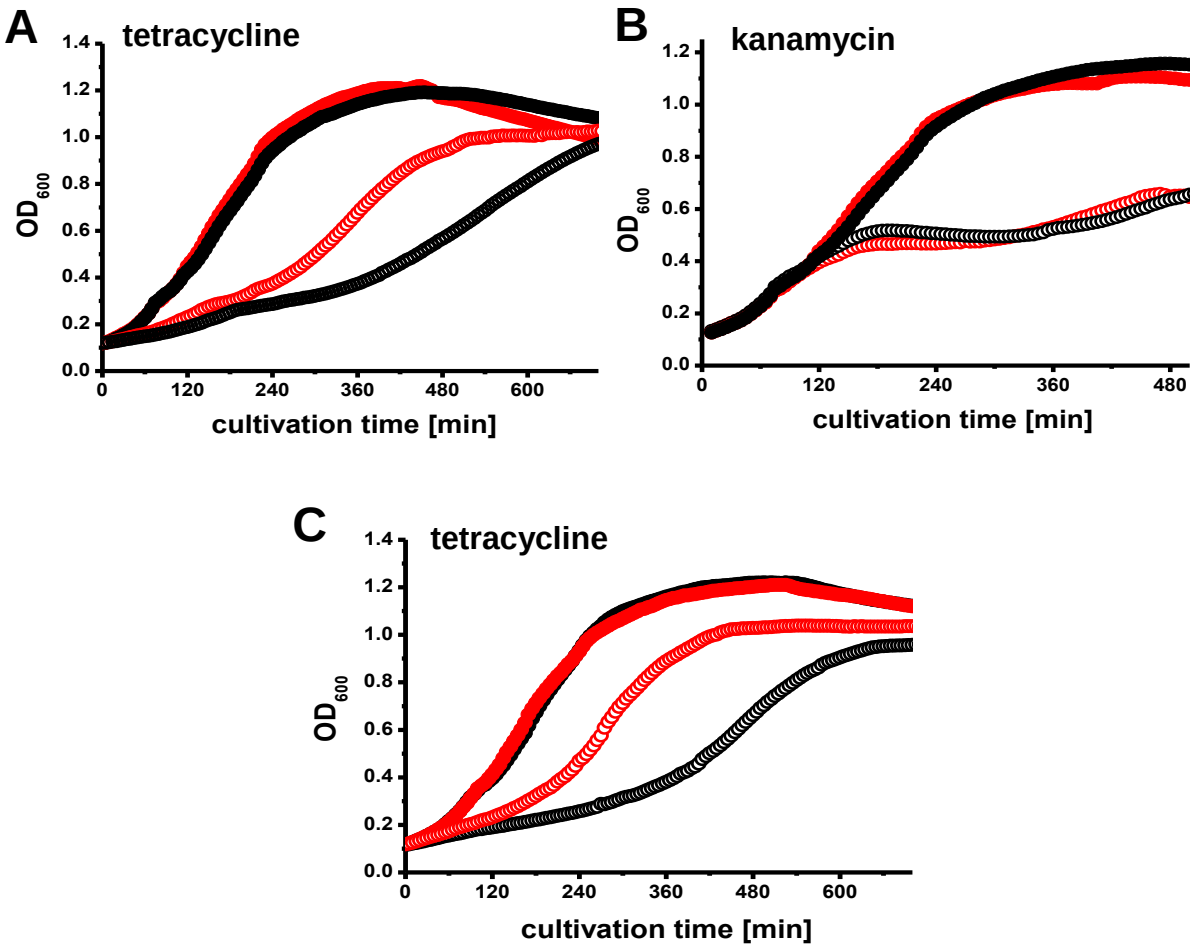


Figure 4-18: Growth of *yifE* expressing strain and *yifE* deleted strain upon antibiotic exposure.

Filled circle: unstressed cells; open circle: stressed cells. Red curve: *yifE* expressing strain; black curve: *yifE* deleted strain. A) Growth of MC4100 and MC4100 *yifE*$^-$ in the presence of tetracycline (0.8 µg/ml); B) Growth of MC4100 and MC4100 *yifE*$^-$ in the presence of kanamycin (1 µg/ml); C) Growth of MC4100 *yifE*$^-$ containing an empty pBAD22 plasmid and the strain overexpressing *yifE* from a plasmid in the presence of tetracycline (1 µg/ml). Cells were cultivated to the exponential growth phase and diluted with LB medium into 96 well plate ($OD_{600}$=0.01 per well). Antibiotics were added and the growth was followed by measuring $OD_{600}$ every 5 minute by a microtiter plate reader.

#### 4.2.2.3 YifE Mediated Phenotype under Non-stress Growth Conditions

To investigate, whether YifE had an effect on bacterial growth under non-stress conditions, *yifE*$^+$ and *yifE*$^-$ cells were cultivated in flasks with chicanes and $OD_{600}$ was measured regularly. These cultivation conditions were different from those for the phenotype analysis mentioned above, under which cells were cultivated in 96-well plates. Compared to *yifE*$^+$ cells, *yifE*$^-$ cells grew at a slightly lower rate. To visualize the growth difference between these two strains, the ratio of $OD_{600}$ value of *yifE*$^-$ cells to *yifE*$^+$ cells was calculated. No matter if in the exponential or the stationary growth phase, the *yifE*$^-$ strain constantly showed a lower value of $OD_{600}$ than the wild type strain by approximately 17 %. This indicated that YifE has already a slight influence on bacterial growth under non-stress conditions [Fig. 4-19].

Regarding that *yifE*$^-$ cells exhibited inhibited growth under stress conditions, this result here suggested that yifE plays a role under non-stress conditions, but upon stresses, the role of YifE became more pronounced.

Since YifE mediated resistant phenotypes in the presence of two different oxidants ($H_2O_2$, HOCl) and three different antibiotics (tetracycline, spectinomycin and chloramphenicol), in the following studies, YifE was analyzed above all under HOCl stress (as representative of oxidative stress) and tetracycline stress (as representative of antibiotic challenge).

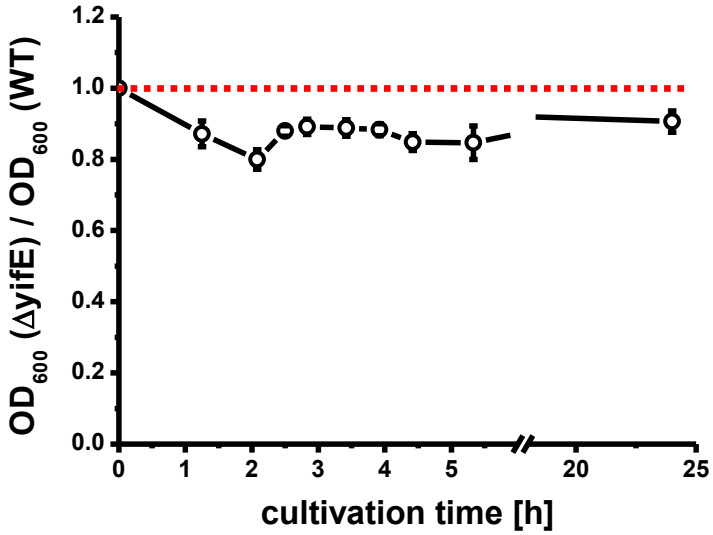


Figure 4-19: Comparison of growth of MC4100 *yifE*$^-$ with MC4100 under non-stressed conditions. Overnight cultures were diluted into fresh LB medium ($OD_{600}$=0.01) and $OD_{600}$ was measured along the growth phase.

### 4.2.3 Analysis of YifE mRNA and Protein Levels upon Stress

Since YifE conferred resistance to oxidative stress and antibiotic challenge, the change in its mRNA and protein levels under such stresses were then analyzed.

RNA was isolated from *yifE*$^+$ and *yifE*$^-$ cells (± tetracycline or HOCl) and the YifE transcript level was analyzed by qRT-PCR using *yifE*-specific primers. In the case of tetracycline challenge, MarA mRNA served as positive control, because *marA* encodes multiple antibiotic resistance protein A, which participates in bacterial resistance to antibiotics including tetracycline (*73*). YjiE mRNA served as negative control, since YjiE is a HOCl-specific transcription factor and its mRNA level should not change upon tetracycline challenge. Upon exposure to tetracycline, MarA transcript levels increased in both *yifE*$^+$ and *yifE*$^-$ cells by almost 4 fold and 2 fold respectively within 1 hour, whereas YjiE transcript level remained unchanged [Fig. 4-20-A]. YifE transcript level, however, increased more significantly than the positive control, by 16 fold within one hour [Fig. 4-20-A].

In the case of HOCl stress, MetN mRNA served as positive control, since it largely increases upon HOCl stress (*44*), while YjiE mRNA as negative control, since its level did not

alter under HOCl stress [Fig. 4-2-A]. Different from tetracycline stress, *yifE* transcript level did not change with the increasing HOCl concentrations as the YjiE control, whereas MetN transcript level significantly increased by maximal 30 fold at 2 mM HOCl [Fig. 4-20-B].

In parallel, cell lysates were prepared and YifE was detected by western blot using purified antibodies specific to YifE [Fig. S5]. The YifE level decreased at the beginning of tetracycline stress by almost 50 %, probably because few proteins were newly synthesized, due to the tetracycline-originated inhibition of translation or the proteins are largely degraded by active proteases. However, the YifE level increased later 3 fold within the next 2 hours, probably due to the massive increase in its mRNA level [Fig. 4-20-C].

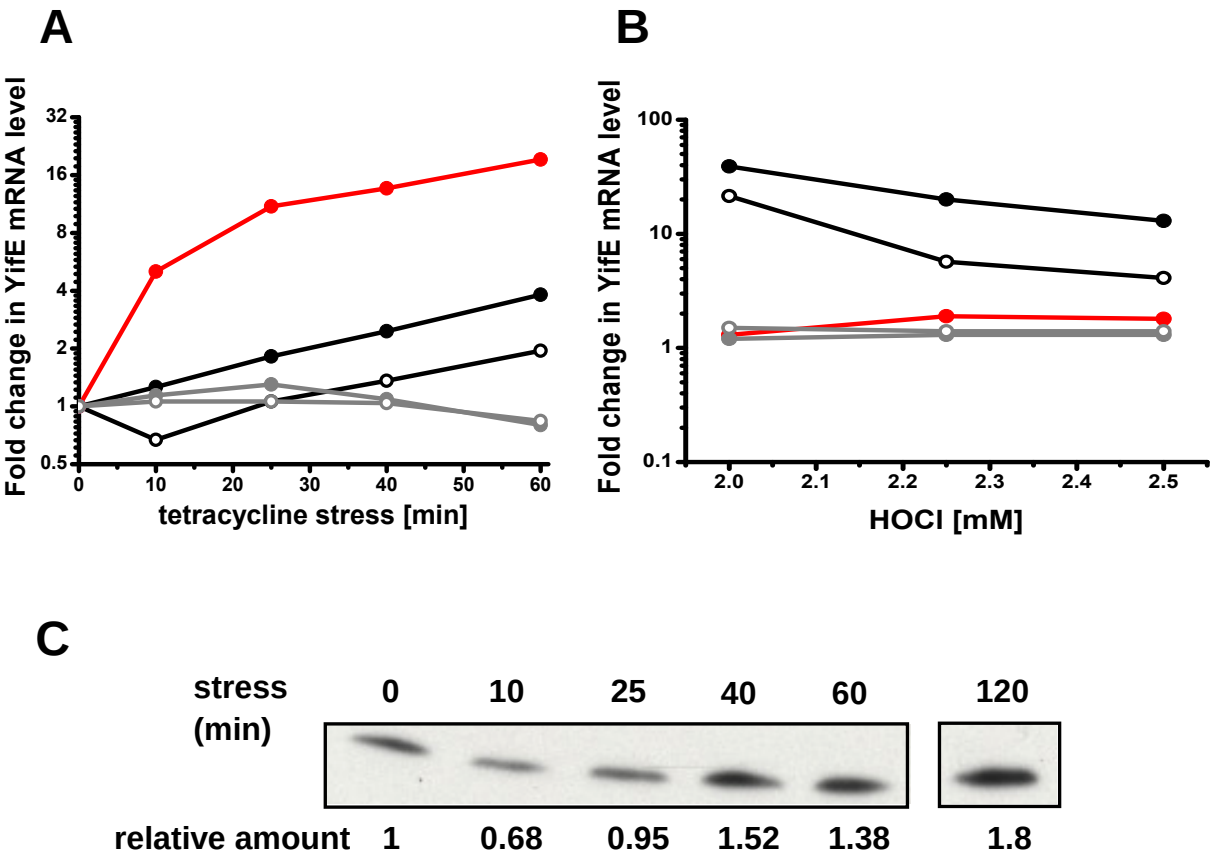


Figure 4-20: YifE mRNA level and protein level upon tetracycline stress. Open circle: *yifE*$^-$ strain, filled circle: *yifE*$^+$ strain; black curve: positive control; grey curve: negative control; red curve: YifE sample. A) YifE mRNA level upon 5 µg/ml tetracycline stress. Positive control: MarA mRNA; negative control: YjiE mRNA. B) YifE mRNA level upon HOCl stress (0, 2.0, 2.25, 2.5 mM). Positive control: MetN mRNA; negative control: YjiE mRNA. RNA was isolated

using SV Total RNA Isolation Kit (Promega) and qRT-PCR was performed. C) YifE protein level upon 5 µg/ml tetracycline stress. To detect YifE protein levels, 1 ml cells were harvested and resuspended within 1x reducing Laemmli buffer (200 µl per 1 ml cells with $OD_{600}$ of 1). After heating (95°C, 10 min), proteins were separated by SDS-PAGE and analyzed by western blot using purified YifE antibody. The band intensity was quantified using Image J and the amount of YifE before stress was set to 1.

## 4.2.4 Structural Characterization of YifE

### 4.2.4.1 Analysis of YifE Secondary Structure

Proteins are made up from three kinds of secondary structural elements: alpha helix, beta sheet and random coil. In a far-UV spectrum, a pronounced double minimum at 208 and 222 nm indicates alpha helical structure, whereas a single minimum at 204 nm or 217 nm reflects random-coil or beta sheet structure, respectively. Using CD spectroscopy, the secondary structure of YifE was analyzed. Due to the extraordinary activity of HOCl, $H_2O_2$ is more convenient for *in-vitro* treatment than HOCl. For both oxidized and reduced YifE, a dominant double minimum at 208 and 222 nm was observed in the CD spectrum, indicating a prominent alpha helical structure [Fig. 4-21]. This result supported the predicted secondary structure of YifE [Fig. 4-16]. Besides, oxidation on YifE did not induce change in its secondary structure [Fig. 4-21].

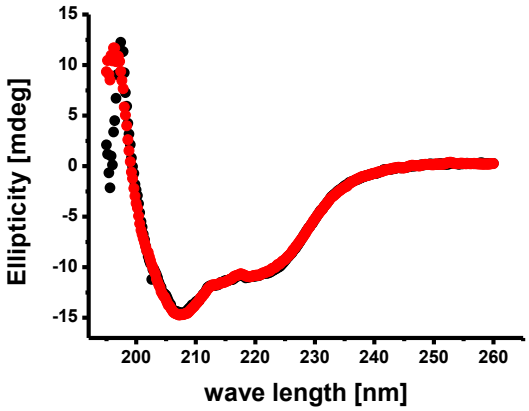


Figure 4-21: CD spectroscopy of oxidized and reduced YifE. YifE was oxidized with 1 mM $H_2O_2$ (37°C, 1 h) and stopped by adding catalase. YifE was reduced with 1 mM TCEP (37°C, 1 h), which was then removed by NAP5 column. The CD spectra of oxidized YifE (red point) and reduced protein (black point) were recorded from 195 nm to 260 nm with the scan rate of 20 nm/min at 20°C. (Figure from *74*).

### 4.2.4.2 Analysis of the Oligomerization State of YifE

#### 4.2.4.2.1 *In-vitro* Analysis

Purified YifE, $H_2O_2$ oxidized and DTT reduced YifE were subjected to analytical size exclusion chromatography (Superose 6, GE Healthcare). All proteins were eluted with the same retention time (37 min) [Fig.4-22-A], which corresponded to the calculated molecular weight of 20 kDa according to the standard curve [Fig. S6]. These results suggested YifE could be a monomer in solution and neither oxidation nor reduction changed its oligomeric state. To further determine the oligomeric state of YifE *in vitro*, analytical ultracentrifugation was performed. YifE sedimented with the sedimentation coefficient of 1.6 S, which reflects a molecular weight of 14 kDa [Fig. 4-22-B]. This demonstrated that the purified YifE is a monomer in solution. Taken together, YifE, no matter if oxidized or reduced, is present as monomer *in vitro*.

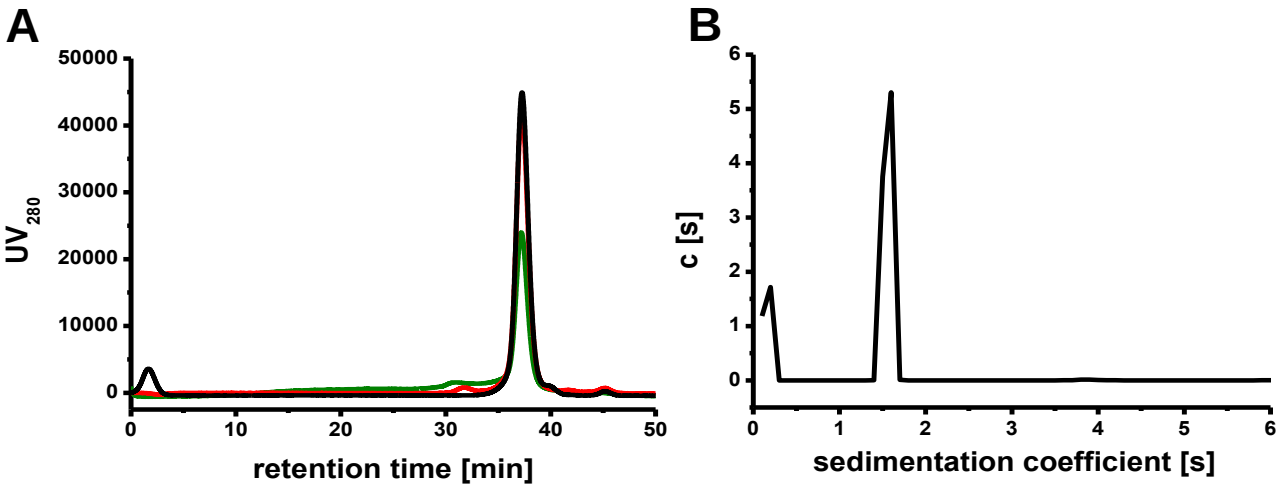


Figure 4-22: Analysis of the oligomerization state of YifE *in vitro*. A) Analysis of oligomeric state by analytical HPLC. 16 µg untreated YifE (green curve), 120 µg 1 mM $H_2O_2$ oxidized YifE (red curve) and 120 µg 1 mM TCEP reduced YifE (black curve) were loaded onto superpose 6 HPLC column (CV: 25 ml). B) Analysis of oligomeric state by analytical ultracentrifugation (42000 rpm, 20°C).

4.2.4.2.2 *In-vivo* Analysis

To explore the oligomeric state of YifE in cells, lysates of cells mildly overproducing His-tagged YifE were prepared. His-tagged YifE was separated by analytical size exclusion chromatography (Superose 6, GE Healthcare) and analyzed by western blot using monoclonal antibodies against His-tag. Most of the His-tagged YifE was eluted at the retention time from 37 minutes to 40 mininutes, corresponding to monomer in cell lysate [Fig. 4-23].

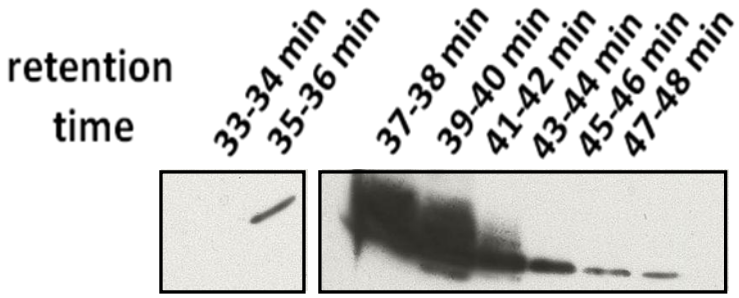


Figure 4-23: Analysis of oligomerization state of YifE *in vivo*. BL21(DE3) cells carrying a pET28a-*yifE* plasmid were cultivated at 37°C, 130 rpm. Production of His-tagged YifE was induced (100 µM IPTG, 37°C, 2 h). The cell lysate was prepared, 120 µg lysate were load onto superpose 6 column (CV: 25 ml) and fractioned (250 µl per fraction). Proteins in each fraction were precipitated by TCA, separated by SDS-PAGE and analyzed by western blot using monoclonal antibodies against His-tag.

### 4.2.4.3 Crystallization of YifE

To determine the 3D structure of YifE, highly concentrated YifE (22 mg/ml, in 10 mM Tris pH 7.5, 20 mM NaCl) was subjected to crystallization screens. Using the classic and classic II suite refill-His solution (Qiagen) crystallization screens including various combination of salts (e.g., magnesium formate, potassium phosphate), buffers with different pH, and precipitates (e.g., ammonium sulfate, sodium chloride), no YifE crystals but salt crystals formed after incubation at 20°C for two months. Thus, this method was so far not suitable to solve the 3D structure of YifE and other methods such as nulear magnetic resonance should be taken into consideration.

### 4.2.5 Investigation of YifE Function

#### 4.2.5.1 Identification of YifE Interaction Partners

According to the sequence alignment and structure prediction, YifE was likely to be a ribosome-related protein or a sigma factor for RNA polymerase. In order to gain insight into the function of YifE, its interaction partners were analyzed by identifying the proteins copurified with YifE and by pull-down assay using YifE-coupled beads. His-tagged YifE was purified by affinity chromatography. Coeluted with YifE, the proteins of interest were identified by mass spectrometry. Among them, a large population was ribosomal proteins [Tab. 4-1]. Besides, the pull-down assays revealed also some ribosomal proteins such as ribosomal protein S1, S4, L2, and elongation factors, in addition to the nonspecifically bound proteins, such as pyruvate dehydrogenase , which were detected in GFP-coupled beads (as control). But so far no subunits of RNA polymerase or RNA polymerase related proteins have been identified in any case. This implied that YifE was most likely to be a ribosome related protein rather than a sigma factor.

Table 4-1: Interaction partners identified by copurification and pull-down assay.

| Protein Name | Function | Method |
|---|---|---|
| RpsA | binding to leader sequence of mRNAs; involvement in tmRNA system | pull-down |
| RpsC | component of 30S ribosomal subunit; helicase activity | co-purification |
| RpsD | assembly of 30S ribosomal subunit; mRNA helicase activity; effects on translation fidelity; direct interaction with 16S rRNA | co-purification pull-down |
| RpsO | component of 30S ribosomal subunit; interaction with 16S rRNA | co-purification |
| RplB | Component of 50S ribosomal subunit; peptidyl transferase center; tRNA binding to A/P site; association of 30S and 50S ribosomal subunits; interaction with 23S and 5S rRNA and aminoacyl-tRNA | co-purification pull-down |
| RplQ | component of 50S ribosomal subunit; interaction with tRNA | co-purification |
| RpmB | assembly of 50S ribosomal subunit | co-purification |
| RusA | pseudouridylation of 16S rRNA at the position 516 (only *in vivo*) | co-purification |
| EF-Tu | tRNA decoding | pull-down |

### 4.2.5.2 Analysis of the Role of YifE in Ribosome Biogenesis and Assembly

To test whether YifE exerts a function in ribosome biogenesis or assembly, the 70S ribosome as well as ribosomal subunits 30S and 50S in *yifE*$^{+}$ and *yifE*$^{-}$ cells were separated using sucrose gradient ultracentrifugation and detected by measuring the absorption at 254 nm. In the sucrose gradient, the ribosomes were separated according to their densities during centrifugation. If YifE influences ribosome biogenesis or assembly, deletion of YifE should give rise to premature or impaired ribosomal subunits or 70S ribosome, which sedimented differently from the mature ribosomal subunits or 70S ribosome (*75*). Under dissociation conditions, 50S ribosomal subunits sedimented to 38-39 % (w/v) sucrose, while 30S ribosomal subunits of low density sedimented to lower concentrations of sucrose (32-33 % w/v) [Fig. 4-24-A]. But the ribosomal subunits sedimented similarly for both *yifE*$^{-}$and *yifE*$^{+}$ cells, indicating that the ribosome biogenesis was not impaired in the *yifE* deletion strain.

Also under association conditions, the 70S ribosome, due to its high density, sedimented to 41-42 % (w/v) sucrose, while 50S ribosomal subunits to 38-39 % (w/v) sucrose and 30S ribosomal subunits to 32-33 % (w/v) sucrose [Fig. 4-24-B]. Since 70S ribosomes in *yifE*$^{-}$ cells sedimented similarly to that in *yifE*$^{+}$ cells [Fig. 4-24-B], it suggested that depletion of *yifE* did not lead to misassembly of the 70S ribosome. Of note, the absorption was irrelevant to the amount of ribosomes.

Taken together, YifE was involved neither in ribosome biogenesis nor assembly.

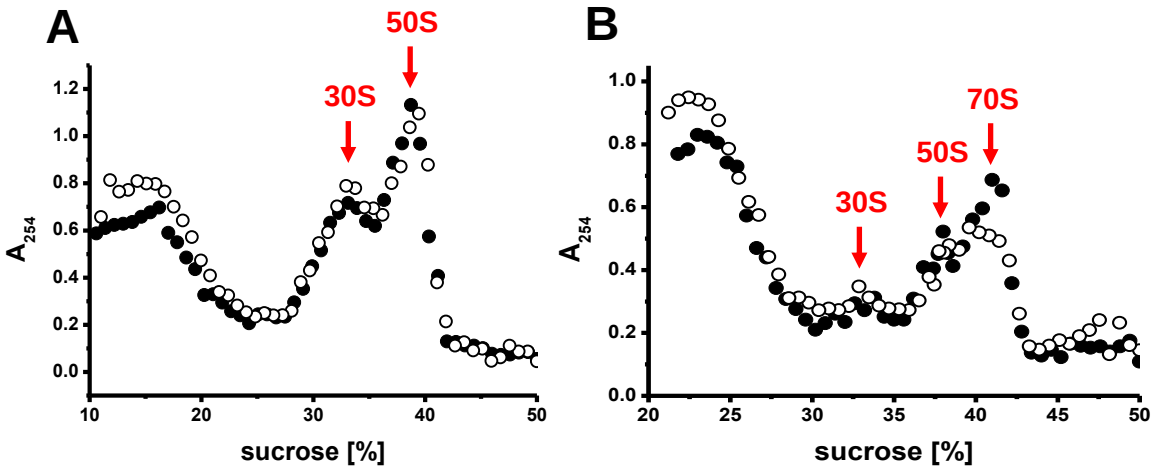


Figure 4-24: Sucrose gradient ultracentrifugation. Ribosomes of MC4100 (filled circle) and

MC4100 *yifE*⁻ (open circle) were separated under A) dissociation conditions (10-50 % (w/v) sucrose gradient in 20 mM Hepes pH 7.5, 150 mM $NH_4Cl$, 1 mM $MgCl_2$) and B) association conditions (20-50 % (w/v) sucrose gradient in 20 mM Hepes pH 7.5, 150 mM $NH_4Cl$, 10 mM $MgCl_2$) by sucrose gradient ultracentrifugation (4°C, 50000 g, 17 h). Cell lysates ($A_{260}$=2 absorption unit) supplemented with 80 U RNaseIn Plus (Promega) were loaded onto the sucrose gradient.

#### 4.2.5.3 Analysis of Ribosome Binding of YifE

Since several ribosomal proteins were identified as YifE interaction partners, the specific binding of YifE to ribosomes was analyzed *in vitro*. Using analytical size exclusion HPLC, the purified 70S ribosome, eluted at the retention time of 10 minutes, and ATTO488 labelled YifE, eluted at the retention time of 17 minutes, could be well separated [Fig. 4-25-A]. Due to the incomplete removal of His-tag, 10 % of the fluorescent labelled YifE still contained His-tag and 90 % were His-tag free. This resulted in two peaks of fluorescent labeled YifE observed on the chromatograph. The small peak represented His-tagged YifE (YifE-$His_C$), whereas the dominant peak represented YifE without His-tag [Fig. 4-25-A]. Incubated with YifE in the presence/absence of tetracycline, 70S ribosomes were separated and YifE bound to 70S ribosomes was detected by western blot. Without tetracycline, there was a small amount of YifE bound to 70S ribosome [Fig. 4-25-B]. But in the presence of tetracycline, a massively increased amount of YifE was associated with 70S ribosome [Fig. 4-25-B].

Additionally, the 30S and 50S ribosomal subunits in the lysates of tetracycline-treated or untreated wild type cells were separated by sucrose gradient ultracentrifugation and YifE bound to these subunits was analyzed by western blot. In both stressed cells and unstressed cells, 50S and 30S ribosomal subunits sedimented quite similarly to 37-38 % (w/v) and 33-34 % (w/v) sucrose respectively [Fig. 4-26-A]. This was reasonable, since tetracycline as well as YifE does not have any effect on ribosome biogenesis. Of note, the absorption here did not reflect the quantity of ribosomal subunits.

Moreover, YifE was detected to be bound to both ribosomal subunits. Under non-stress condition, twice as much as YifE bound to 30S ribosomal subunit were associated with 50S ribosomal subunit [Fig. 4-26-B]. Exposure to tetracycline generally increased the amount of

YifE bound to both ribosomal subunits by 2 fold [Fig. 4-26-B]. However, according to the relative amount of YifE, the tetracycline-induced increase in YifE bound to 30S ribosomal subunit (2.5 fold) was slightly greater than to 50S ribosomal subunit (2 fold). This suggested that YifE is capable of binding to both 50S and 30S ribosomal subunits, preferentially to 50S ribosomal subunit in the absence of stress. Tetracycline triggers an increased amount of YifE associated with ribosomal subunits, especially with 30S ribosomal subunit.

All these results indicated that YifE is able to bind to ribosomes in cells, and tetracycline stress induced more YifE to be bound to ribosomes.

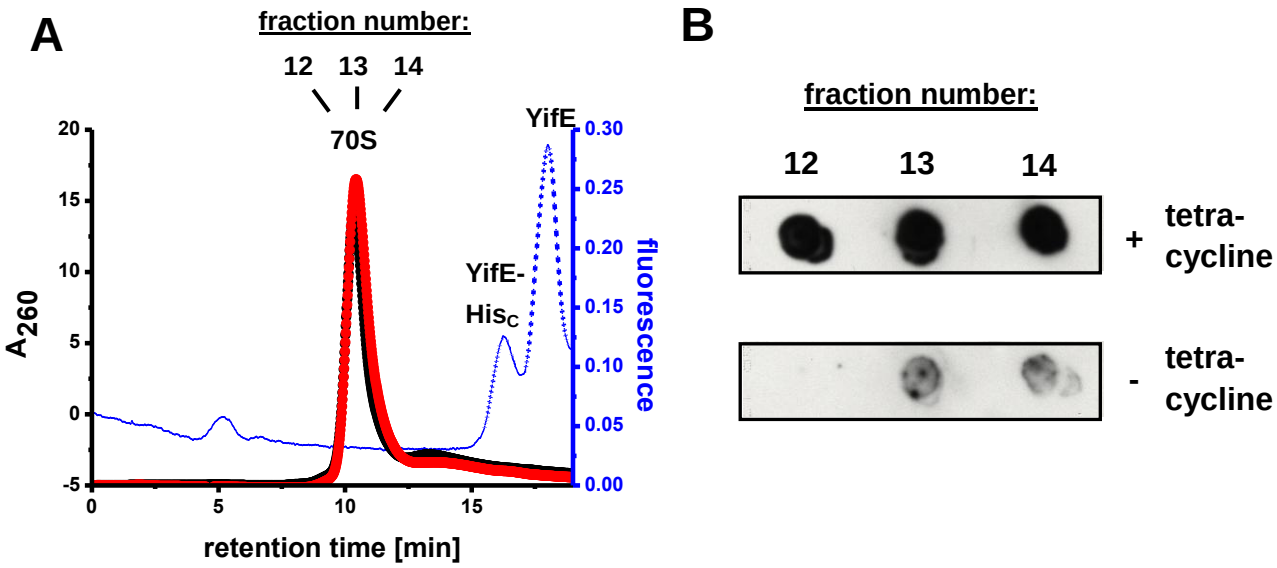


Figure 4-25: Binding of YifE to 70S ribosome. A) Analytical size exclusion HPLC of 70S ribosome and 70S ribosome-YifE mixture. Black curve: 70S ribosome only (100 pmol); red curve: 70S ribosome-YifE mixture (100 pmol 70S ribosome, 200 pmol YifE); blue curve: Atto488 labeled YifE (200 pmol; His-tag cleavage: 90 %). Samples were separated using the column Biosuit 450 (7.8 mm x 30 cm). B) Analysis of YifE bound to 70S ribosome. 100 pmol 70S ribosome were incubated with 200 pmol YifE in the presence/absence of 30 µM tetracycline (37°C, 5 min). Samples were separated and fractionated (800 µl/fraction). YifE in the fractions containing 70S ribosomes was detected by dot blot using purified YifE-antibody.

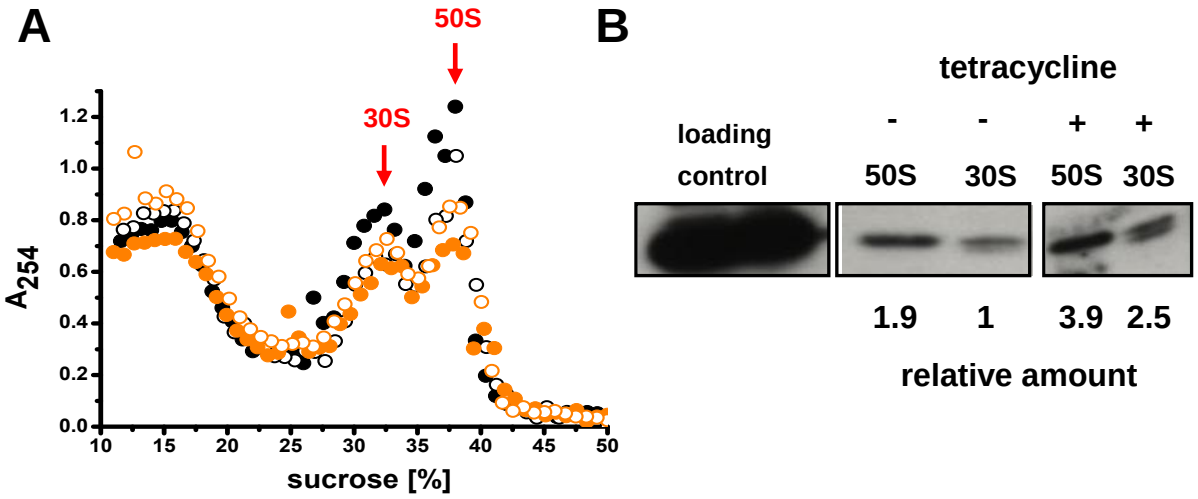


Figure 4-26: Binding of YifE to 50S and 30S ribosomal subunits. A) Sucrose gradient ultracentrifugation. B) Analysis of YifE bound to ribosomal subunits. MC4100 (filled circle) and MC4100 *yifE*$^-$ cells (open circle) were stressed with 5 µg/ml tetracycline (37°C, 140 rpm, 5 min). Ribosomes from stressed cells (orange curve) and unstressed cells (black curve) were separated under dissociation conditions (10-50 % (w/v) sucrose gradient in 20 mM Hepes pH 7.5, 150 mM $NH_4Cl$, 1 mM MgCl) by sucrose gradient ultracentrifugation (4°C, 50000 g, 17 h). Cell lysates ($A_{260}$=2 absorption unit) supplemented with 80 U RNaseIn Plus (Promega) were loaded onto the sucrose gradient. YifE in the fractions containing 50S ribosome and 30S ribosome was detected by western blot using purified YifE-antibody. The western blot slices were from one blot. The band intensity was quantified using Image J and amount of YifE bound to 30S ribosomal subunit under non-stress conditions was set to 1.

### 4.2.5.4 Analysis of Nucleic Acid Binding to YifE

The potential nucleic acid binding ability of YifE was analyzed by fluorescence anisotropy using single-stranded or double-stranded DNA and RNA isolated from *E.coli* cells. Once nucleic acids bind to the fluorescent labeled YifE, it gives birth to an increase in fluorescence anisotropy. In the case of DNA (single-stranded, double stranded), the fluorescence anisotropy did not change significantly, indicating that YifE did not bind to DNA [Fig. 4-27-A]. In contrast, addition of RNA to fluorescent labeled YifE led to a great increase in fluorescence anisotropy, indicating formation of a YifE-RNA complex [Fig. 4-27-A].

To identify the target RNA of YifE, an RNA pull-down assay was performed. RNA bound to the YifE-coupled beads was eluted as RNA-YifE complex, extracted using

phenol-chloroform and identified by qRT-PCR. In this experiment, different primers were used to detect 16S ribosomal RNA, 23S ribosomal RNA, primary transcript of ribosomal RNA as well as TufB RNA. TufB RNA served as random control to assess the binding ability of YifE for any RNA. Conversely, green fluorescence protein (GFP)-coupled beads were used as protein control to estimate unspecific binding of RNA to any protein. In both cases of YifE and GFP, 16S and 23S ribosomal RNA, were detected as predominantly bound species [Fig. 4-27-B]. Further, 13-times more 16S ribosomal RNA was bound to GFP compared to 23S ribosomal RNA, whereas 50-times bound to YifE [Fig. 4-27-B]. This indicated that although 16S RNA, compared to 23S RNA, possesses high affinity to protein, YifE preferentially binds to 16S RNA. In contrast, the amount of TufB and primary transcript of ribosomal RNA was comparably neglectable [Fig. 4-27-B].

Based on these observations, YifE is capable of binding to ribosomal RNAs, preferentially 16S ribosomal RNA.

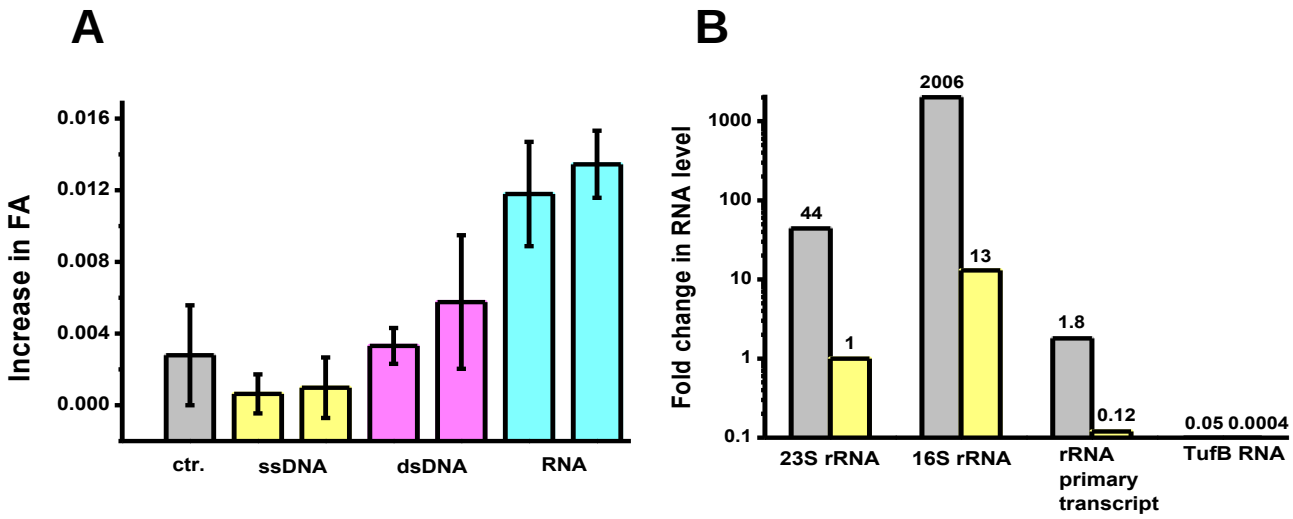


Figure 4-27: Nucleic acid binding ability of YifE. A) Fluorescence anisotropy. 10 pmol ssDNAs (left magenta column: 90 base in length; right magenta column: 99 base in length) and dsDNAs (left cyan column: 102 bp in length; right cyan column: 300 bp in length) and 7 µg pure RNAs isolated from unstressed wild type (red left column) and *yifE* deletion strains (red right column) were titrated to 10 pmol Atto488 labeled YifE (degree of labeling: 90%). B) RNA pull-down assay. YifE-His (grey column) and GFP-His as control (yellow column) were coupled to Ni-NTA beads (4°C, shaking, 1 h). Then cell lysates of MC4100 *yifE*$^-$ cells supplemented with RNaseIn Plus, protease inhibitor HP and DNase I was incubated with protein coupled beads (4°C, shaking, 1 h). After washing, the potential YifE-RNA complex was eluted by high concentration of imidazole (500 mM) and the RNA was extracted by

phenol-chloroform. qRT-PCR was performed. The amount of 23S rRNA bound to GFP-coupled beads was set as reference. The amount of other RNA was calculated by comparison to the reference and the fold change could be determined. These results were from one representative experiment.

### 4.2.5.5 Analysis of YifE-Mediated Effects on Translation

YifE could bind to the ribosome and ribosomal RNAs and it did not have any effect on ribosome biogenesis or assembly. Therefore, the influence of YifE on translation was analyzed next.

#### 4.2.5.5.1 [$^{35}$S]Methionine Incorporation

The translation efficiency of wild type cells (MC4100) and *yifE* deletion cells (MC4100 *yifE*$^-$) was determined by analyzing the level of incorporated radioactive methionine [$^{35}$S]Met into newly synthesized proteins. In *yifE*$^+$ cells, tetracycline challenge diminished the level of the incorporated [$^{35}$S]Met by 20 % [Fig. 4-28]. However, unstressed *yifE*$^-$ cells, compared to unstressed *yifE*$^+$ cells, possessed an reduced level of incorporated [$^{35}$S]Met, about 70 %, [Fig. 4-28]. This indicated that deletion of YifE alone already affected translation. Exposure to tetracycline, the level of incorporated [$^{35}$S]Met dramatically dropped to 30 %, reflecting a severely inhibited protein biosynthesis [Fig. 4-28].

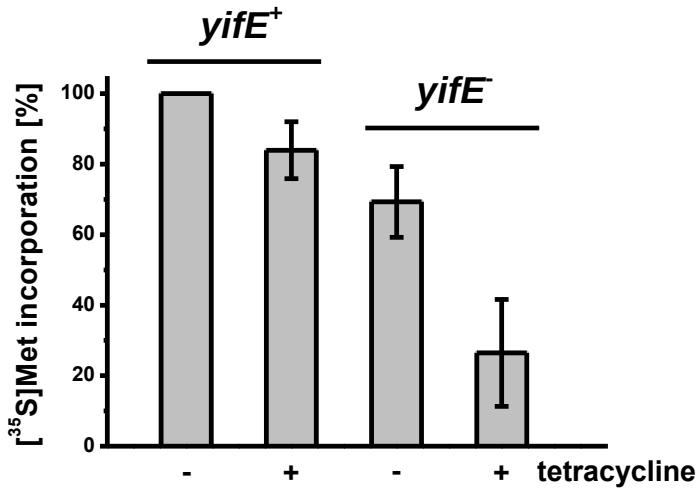


Figure 4-28: Incorporation of [$^{35}$S]Met into newly synthesized proteins. MC4100 cells and

MC4100 *yifE*⁻ cells were cultivated in M9 minimal medium supplemented with all amino acids except methionine. 2 µl [$^{35}$S]Met (10 mCi/ml, 1000 Ci/mmol) were added to 1 ml cultures ($OD_{600}$=0.25) and the cultures were incubated with tetracycline (2 µg/ml, 37°C, 800 rpm, 10 min) or kept unstressed. The unstressed and stressed samples were analyzed by SDS-PAGE and the radiography was analyzed by phosphor screen. The band intensity was quantified using Image J and corresponds to the incorporated [$^{35}$S]Met. The level of incorporated [$^{35}$S]Met in unstressed MC4100 cells was set to 100 % and the average values of incorporated [$^{35}$S]Met were calculated from 3 protein bands for unstressed/stressed samples.

4.2.5.5.2 *In-vitro* Translation

The effect of YifE on translation was analyzed by an *in-vitro* translation assay, a powerful assay to directly follow the translation process. Using the fluorescent labeled fMet, the newly synthesized peptides could be detected and quantified. Without tetracycline, more peptides synthesized in the presence of YifE (with the final arbitrary units of 1600) than in the absence of YifE (with the final arbitrary units of 1200) [Fig. 4-29-A]. This indicated that YifE could slightly improve the translation efficiency under non-stress conditions. Exposed to low concentration of tetracycline (5 µM), translation was generally inhibited, resulting in the final arbitrary units of 900 or 700 in the presence or absence of YifE [Fig. 4-29-B]. Exposed to high concentrations of tetracycline (30 µM), translation was further inhibited and the final arbitrary units declined to 245 or 315 in the presence or absence of YifE [Fig. 4-29-B]. However, the difference in the arbitrary units corresponding to the amount of synthesized peptides between YifE present and absent samples was increased at high concentration of tetracycline [Fig. 4-29-C]. This suggested that YifE is able to promote tetracycline-impaired translation.

These two independent assays, [$^{35}$S]Met incorporation and *in-vitro* translation, delivered the same message: YifE played an important role in translation. In the absence of tetracycline, lack of YifE can already disadvantage translation. But exposure to tetracycline impaired translation to a large extent and under such conditions, YifE can greatly improve the inhibited translation.

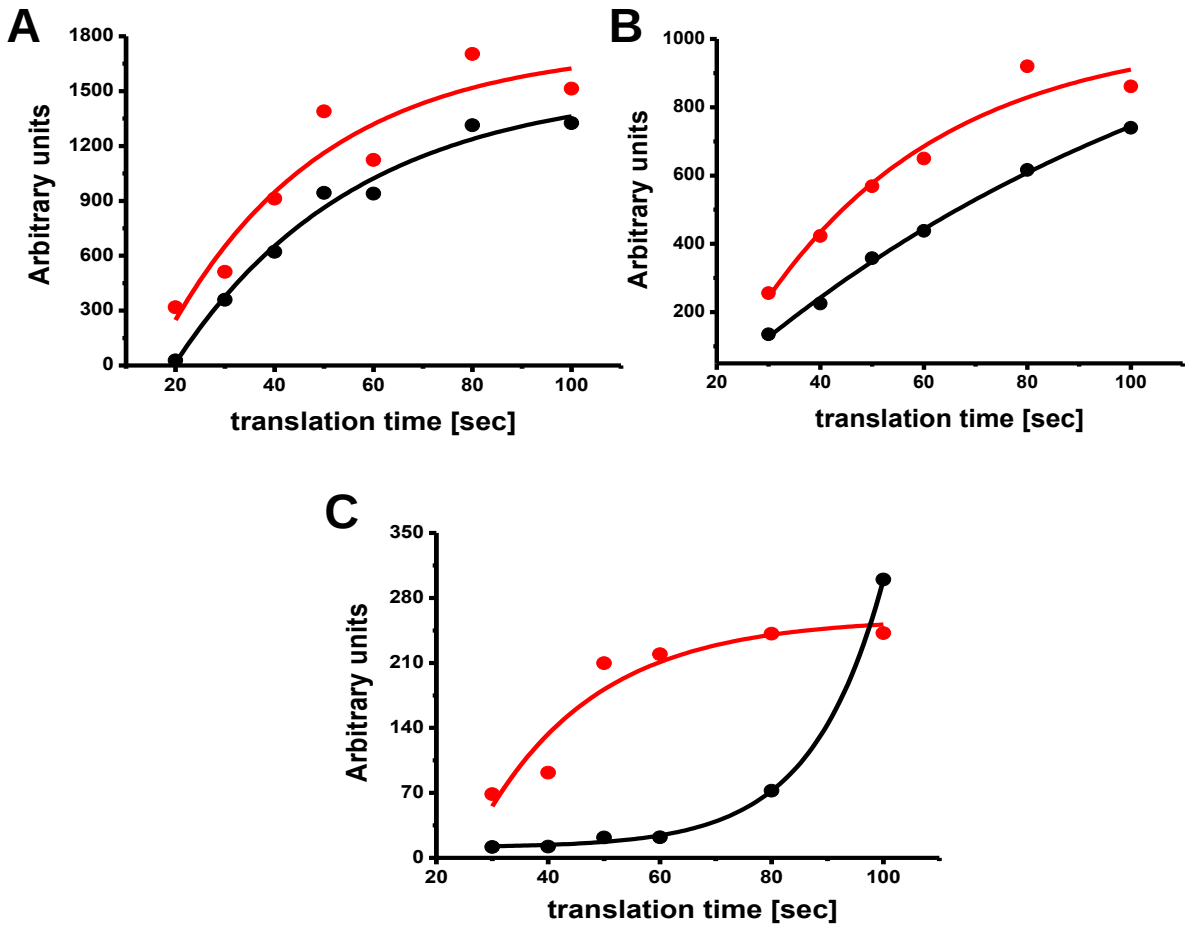


Figure 4-29: *In-vitro* translation assay. The translation was performed *in vitro* in the presence of 3 µM YifE (red) or in the absence of YifE (black). A) no tetracycline; B) 5 µM tetracycline; C) 30 µM tetracycline. The peptides containing fluorescent fMet were analyzed by SDS-PAGE. The fluorescence intensity was quantified using Image TL.

### 4.2.5.6 Analysis of Dipeptide Formation

Since YifE has an effect on translation, it could participate in peptide bond formation, translocation, termination or ribosome recycling. Regarding that tetracycline can interfere with the tRNA binding to the A-site, and consequently disrupt the formation of peptide bond, YifE could be potentially involved in peptide bond formation. To examine this possibility, the dipeptide assay was performed, in which the formation of dipeptide f[$^{3}$H]Met-[$^{14}$C]Phe in the presence/absence of YifE and/or tetracycline was analyzed. Since f[$^{3}$H]Met, as initiator methionine, could bind to the ribosome either as single amino acid or as peptide, the

dipeptide formation was determined by analyzing the amount of [$^{14}$C]Phe in the ribosome-bound dipeptides. With increasing concentrations of tetracycline, the amount of dipeptides, formed in presence or absence of YifE, decreased on average from 15 pmol to 8 pmol, indicating a general inhibited dipeptide formation induced by tetracycline [Fig. 4-30]. Moreover, the dipeptide amount in the YifE absent sample was quite comparable to the YifE present sample [Fig. 4-30], and the increase in the amount of [$^{14}$C]Phe bound to ribosomes seems to be purely a tetracycline-effect. This indicated that YifE failed to restore the inhibited peptide formation. Thus, YifE is not involved in the peptide bond formation step. Further steps in translation will be analyzed in Prof. Dr. Marina Rodnina's lab in Göttingen in summer 2013.

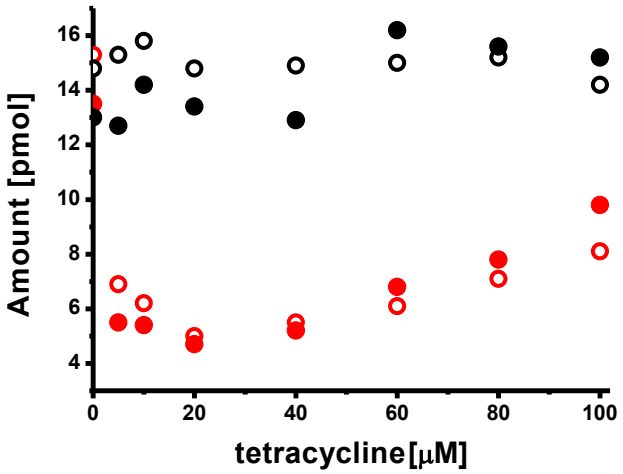


Figure 4-30: Dipeptide formation assay. Dipeptide was formed in the presence of 3 μM YifE (filled circle) or in the absence of YifE (open circle) with the increasing concentration of tetracycline at 37°C. The 70S ribosomes were filtered by nitrocellulose filtration and the ribosome-bound f[$^{3}$H]Met (black circle) and [$^{14}$C]Phe (red circle) were analyzed.

### 4.2.6 Analysis of Acetylated Lysine K15 in YifE Activity

Lysine at the position 15 in YifE was found to be acetylated *in vivo*. About 1 % of the purified YifE was also detected as acetylated using monoclonal antibodies against acetylated lysine (data not shown). Since acetylation is a highly conserved modification in bacterial kingdom (*76*), and a large amount of prokaryotic and eukaryotic proteins have been discovered to be acetylated such as ribosomal proteins (*77*), elongation factors (*77*) and

chaperones (*77*), this acetylated lysine 15 was of potential importance in YifE function. To study the potential role of YifE, lysine 15 was substituted with arginine/glutamine, which mimics the nonacetylated/acetylated lysine (*78*) and the activity of these mutants (K15R, K15Q) was determined by analyzing the growth of *yifE*$^-$ cells expressing wild type *yifE* and *yifE* mutants in the presence of tetracycline, HOCl and $H_2O_2$. Although the overexpressing of *yifE* and *yifE* mutants did not completely complement the stress-originated inhibited growth, the cells producing wild type YifE and YifE mutants grew without any difference under both tetracycline an HOCl stress [Fig. 4-31-A-B]. However, exposed to $H_2O_2$ stress, producing of YifE mutants, compared to wild type YifE, only partially complemented the inhibited growth [Fig. 4-31-C]. Since results from tetracycline stress and HOCl stress are in accordance, it is likely that all mutants were as active as wild type YifE. This suggested that the acetylated lysine 15 was not essential for the activity of YifE.

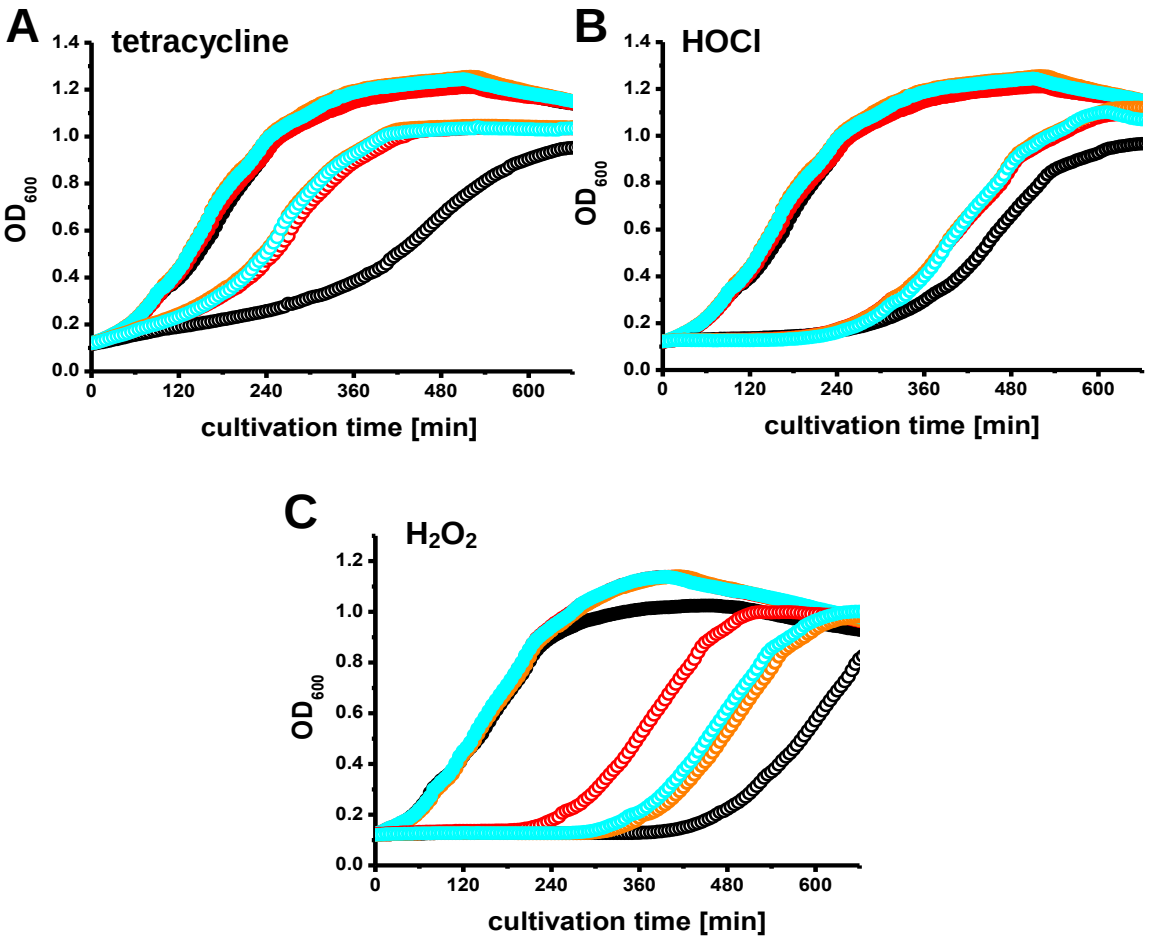


Figure 4-31: Growth of MC4100 *yifE*$^-$ expressing wild type *yifE* and *yifE* mutants from a

pBAD22 plasmid upon tetracycline and HOCl stress. A) Growth under tetracycline stress (1 µg/ml); B) Growth under HOCl stress (2.75 mM); C) Growth under $H_2O_2$ stress (2.5 mM). Filled circle: unstressed cells; open circle: stressed cells. Cells containing an empty pBAD22 plasmid (black curve) or producing wild type YifE (red curve), K15R (orange curve) and K15Q (cyan curve) were cultivated to the exponential growth phase and diluted with LB medium into 96 well plate ($OD_{600}$=0.05 per well). HOCl or tetracycline was added and the growth was followed by measuring $OD_{600}$ every 5 minute using a microtiter plate reader.

# 5 Discussion

## 5.1 Activation Mechanism of the HOCl-Responsive Transcription Factor YjiE

YjiE has been identified as HOCl-responsive LTTR in *E.coli* (*7*, *44*). As LTTR, YjiE contains a highly conserved helix-turn-helix DNA binding motif in its N-terminal DNA binding domain, a co-inducer domain and a C-terminal oligomerization domain (*41*). Generally, LTTRs are activated either by binding of a co-inducer (*46*, *47*), or by direct modifications of amino acids (*34*). According to this knowledge, the activation mechanism of YjiE was investigated in this work by testing these two possibilities.

First of all, conserved amino acids, especially the two hotspot clusters of conserved amino acids in the co-inducer domain, were identified using multiple sequence alignment (see Fig. 4-3). These conserved amino acids could be essential for a potential co-inducer binding that activates YjiE. Therefore, several single point mutants or multiple point mutants of YjiE were accordingly generated and screened for inactive ones. However, the *in-vivo* activity of YjiE mutants remained uncertain because the positive control, cells expressing wild type *yjiE*, did not show a strong and reproducible phenotype. HOCl, being an extremely reactive ROS, can react with most of components in LB medium, molecules in cells and even the pipette tips or tubes (*6*, *57*). Thus, all materials could influence the result, giving birth to the instable phenotype in *in-vivo* assay. The YjiE active species isolated from HOCl stressed cells exhibited an enhanced DNA binding ability (*7*), but no co-inducer bound to the active species was identified, indicating that YjiE is unlikely to be activated by this means.

Methionine and cysteines are primary targets of HOCl (*6*). Identification of the modified amino acids in the active species by mass spectroscopy resulted in two highly conserved methionines (Met206, Met230) of particular interest. To examine whether the oxidation of these methionines plays a key role in the activation of YjiE, glutamine mutants mimicking the oxidized state and isoleucine mutants mimicking the reduced state (*79*) were generated and

the activity of these mutants was analyzed regarding the DNA binding ability and the transcript level of YjiE target genes. Using the most two strongly YjiE up-regulated/down-regulated genes upon HOCl (*metN*, *metB*: up-regulated; *fecD*, *cydA*: down-regulated) (*44*), qRT-PCR, however, did not provide significant and reproducible results regarding the change in the transcript level of these genes. Since RNA is quite unstable und degraded by RNases (*80*), this might result in irreproducible results. Furthermore, analyzing the DNA binding using fluorescence anisotropy showed that both Met206 mutants (M206I, M206Q) and M230I were as active as wild type YjiE, while M230Q was inactive. This implies that oxidation of M206 is not crucial for YjiE activation, while oxidation of Met230 renders YjiE inactive. Although so far oxidation of single methionines, (M206, M230) seems not to be the key to activation of YjiE, this result should be confirmed by other assays using the double methionine mutants (M206, 230I; M206, 230Q) in addition to the single methionine mutants. On the other hand, other methionines or cysteines, which are not conserved, could also be taken into consideration to analyze their effects on activation of YjiE.

In parallel, other assays were established in this work to distinguish between active and inactive YjiE mutants. Using DNase I footprints assay, the potential YjiE-DNA interaction could be detected and the DNA binding site of YjiE on its target gene could be identified (*53*). Nevertheless, no YjiE-specific binding site on its target gene (*metN* promoter DNA) was revealed. Additionally, carbonyl groups, which are commonly introduced into protein side chains upon oxidative stress (*17*), were detected in the wild type strain and *yjiE* deletion strain using Oxyblot assay. Unexpectedly, upon HOCl stress, the *yjiE* deletion strain contained a lower carbonyl level than the wild type strain. Concerning that the cells expressing *yjiE* did not show HOCl-resistance phenotype, this suggests that the strains used in this work might be mutated and lose their original wild type characters, or YjiE might be responsive to another condition besides HOCl stress.

In conclusion, to explore the activation mechanism of YjiE, identification of the inactive mutants becomes the critical step. Both the *in-vivo* assay analyzing the activity of mutants (viability assay) and the *in-vitro* assays determining DNA binding (fluorescence anisotropy, pull-down assay and DNase I footprints), transcript level of YjiE target genes (qRT-PCR), and

the carbonyl content in proteome (carbonylation assay) failed to provide clear, reproducible and accordant results. Therefore, other assays need to be established or developed to assess the activity of YjiE mutants, for example, assays based on the oligomerization state and iron uptake.

## 5.2 Identification and Characterization of A Novel Protein Involved in Bacterial Response to Oxidative stress: YifE

Using a genomic library screen, YifE, a novel bacterial conserved protein, was discovered to be involved in the bacterial defense against $H_2O_2$ (in this work) and HOCl (*64*). Particularly, this protein also mediated resistance to several antibiotics targeting ribosome function, the tetracycline. With unknown structure and unknown function, YifE showed limited sequence similarity to ribosomal protein S6 or ribosome related proteins (Rrf, Hsp15, YbeY). In addition, although the structure prediction suggested that YifE could be a sigma factor, the identified interaction partners (several ribosomal proteins) and target RNA of YifE (ribosomal RNA) demonstrate that YifE is more likely to be a ribosome related protein rather than a sigma factor.

Concerning ribosome biogenesis, various methyltransferases such as RsmD and RlmE introduce methylation in ribosomal RNAs, which are essential for a mature ribosome subunit (*81*). Deletion of these methyltransferases leads to premature ribosomal subunits. However, in *yifE* deleted cells, both ribosomal subunits as well as 70S ribosome were intact. This indicates that YifE is not a methytransferase and it is not involved in ribosome biogenesis or assembly. On the other hand, YifE can bind to ribosomes, ribosomal subunits in addition to ribosomal RNAs. Tetracycline treatment leads to a significant increase in YifE bound to ribosomes. Similarly, Hsp15, a ribosome associated heat shock protein, can bind to RNA and associate predominantly with the 50S ribosomal subunit (*82*, *83*). Upon chloramphenicol treatment or heat shock, more Hsp15 molecules are recruited to 50S ribosomal subunits than under non-stress conditions and this promotes the recycling of free 50S ribosomal subunits

(*83*). Besides, Rrf can also interact with 70S ribosomes and ribosomal subunits and mutation in Rrf renders cells sensitive to antibiotics (*84*). Since YifE bears partial sequence similarity to Hsp15 as well as Rrf, YifE could be such a ribosome associated protein, which improves ribosome recycling under stress. Further functional assays such as [$^{35}$S]Met incorporation and *in-vitro* translation clearly demonstrated that depletion of *yifE* already disadvantages the translation during non-stress conditions. Being a weak sequence homolog of YifE, YbeY, is a conserved protein involved in translation. Although its precise function has not been determined yet, deletion of this protein reduces the activity of the translation machinery in cells (*85*). This similarity may suggest that YifE plays a role in translation. Moreover, recruitment of YifE greatly improves impaired translation under tetracycline stress. This suggests that YifE supports translation especially under stress.

Since translation, being transcription-coupled in bacteria, is a sophisticated process involving various participants such as mRNA, tRNA, ribosomes, elongation factors and GTP, the function of YifE in each step of translation should be analyzed. It was shown that YifE does not affect the peptide bond formation, but its function in initiation, translocation, termination or recycling still need to be investigated. Due to time constraints, this was not possible yet.

Which kind of function could YifE exert during translation? Derived from the above observations, YifE could be a quality control protein of translation. Under non-stress conditions, ribosomes pause at non-stop RNA or mRNA with secondary structure (*86*, *87*). Antibiotics such as tetracycline and chloramphenicol, which interrupt tRNA decoding and peptidyl transferase activity respectively, could also cause ***ribosome stalling*** (*88*). In addition, ROS, which modifies tRNA and sulfer-containing amino acids, could disturb tRNA decoding and charging and consequently trigger ribosome stalling as well (*89*, *90*). In the absence of stress, lack of YifE reduces cell growth to a small extent, but increased production of YifE confers resistance to $H_2O_2$, HOCl, tetracycline and chloramphenicol. Deletion of *yifE* is not lethal just like single knockouts of *ssrA*, *smpB*, *arfA* and *arfB*, which encode proteins in three so-far identified pathways (tmRNA system, ArfA, ArfB) to rescue stalled ribosomes (*91*). Like YifE, ArfB and SmpB, one component in tmRNA system, could also associate with the

70S ribosome, ribosomal subunits and ribosomal RNAs (*92*, *51*) and deletion of SmpB causes only a slight decrease in cell growth (*51*). Thus, YifE is very likely to be involved in rescuing paused ribosomes. So far, none of SmpB, ArfA or ArfB was detected as interaction partner of YifE and YifE could be involved in ribosome recycling just like Hsp15 and Rrf. Hence, YifE could mediate a noval pathway, in which it acts as a potential ribosomal recycling protein to release stalled ribosomes.

Moreover, YifE mediates significant resistance to tetracycline, compared with chloramphenicol and spectinomycin. Tetracycline can cause perturbation of tRNA binding to A-site and, as a result, non-cognate tRNAs would dock into the A-site (*69*). Universally, conserved bases of the 16S ribosomal RNA sense the codon-anticodon complex and can induce a conformational transition. Only the conformation of ribosome with a cognate tRNA bound would be stabilized (*93*). Since YifE could bind to the 16S ribosomal RNA and ribosomes and a largely increased amount of this protein was detected under tetracycline treatment, YifE could also be involved in ***proof-reading*** of protein biosynthesis. However, it is less likely to be the case, since the *yifE* deletion strain was not susceptible to kanamycin, which largely introduces misreading in protein synthesis (*70*).

# 6 Reference


1. Schrader, M., and Fahimi, H. D. (2006) Peroxisomes and oxidative stress. *Biochim. Biophys. Acta. 1763 (12)*, 1755-1766.
2. Kettle, A. J., and Winterbourn, C. C. (1988) Superoxide modulates the activity of myeloperoxidase and optimizes the production of hypochlorous acid. *Biochem. J. 252*, 529-536.
3. Davies, M. J. (2004) The oxidative environment and protein damage. BBA 1703.
4. Imlay, J. A. (2003) Pathways of oxidative damage. *Annu. Rev. Microbiol. 57*, 395-418.
5. Pomposiello, P. J., and Demple, B. (2001) Redox-operated genetic switches: the SoxR and OxyR transcription factors. *Trends in Biotechnology 19*, 109-113.
6. Hawkins, C. L., Pattison, D. I., and Davies, M. J. (2003) Hypochlorite-induced oxidation of amino acids, peptides and proteins. *Amino Acids 25*, 259-274.
7. K. Gebendorfer's Dissertation (2011).
8. Arsène, F., Tomoyasu, T., and Bukau, B. (2000) The heat shock response of *Escherichia coli*. *Int. J. Food Microbiol. 55 (1-3)*, 3-9.
9. Castanie-Cornet, M., Penfound, T. A., Smith, D., Elliott, J. F., and Foster, J. W. (1999) Control of acid resistance in *Escherichia coli*. *J. Bacteriol. 181 (11)*, 3525-3535.
10. Record, M.T., Courtenay, E. S., Cayley, D. S., Guttman, H. J. (1998) Responses of E.coli to osmotic stress: large change in amounts of cytoplasmic solutes and water. *Trends Biochem. Sci. 23 (4)*, 143-148.
11. Forst, S., Delgaod, J., Inouye, M. (1989) Phosphorylation of OmpR by the osmosensor EnvZ modulates espression of the *ompF* and *ompC* genes in *Escherichia coli*. *Proc. Natl. Acad. Sci. U.S.A. 86 (16)*, 6052-6056.
12. Tsao, S. M., Yin, M. C., and Liu, W. H. (2007) Oxidant stress and B vitamins status in patients with non-small cell lung cancer. *Nutr. Cancer 59*, 8-13.
13. Aliev, G., Smith, M. A., Seyidov, D., Neal, M. L., Lamb, B. T., Nunomura, A., Gasimov, E. K., Vinters, H. V., Perry, G., LaManna, J. C., and Friedland, R. P. (2002) The role of oxidative stress in the pathophysiology of cerebrovascular lesions in Alzheimer's disease.

*Brain Pathol. 12*, 21-35.

14. Ha, E. M., Oh, C. T., Bae, Y. S., and Lee, W.J. (2005) A direct role for dual oxidase in Drosophila gut immunity. *Science 310*, 847-850.
15. Kiley, P. J., and Storz G. (2004) Exploiting thiol modifications. *PLoS Bio. 2 (11)*, 1714-1717.
16. Storz, G., and Imlay, J. A. (1999) Oxidative stress. *Curr. Opin. Microbiol. 2*, 188-194.
17. Nyström, T. (2005) Role of oxidative carbonylation in protein quality control and senescence. *EMBO. J. 24 (7)*, 1311-1317.
18. Dizdaroglu, M., Rao, G., Halliwell, B., and Gajewski, E. (1991) Damage to the DNA bases in mammalian chromatin by hydrogen peroxide in the presence of ferric and cupric ions. *Arch. Biochem. Biophys. 285*, 317-324.
19. de Mello Filho, A. C., and Meneghini, R. (1985) Protection of mammalian cells by o-phenanthroline from lethal and DNA-damaging effects produced by active oxygen species. *Biochim. Biophys. Acta. 847*, 82-89.
20. Khor, H. K., Fisher, M. T., and Schoneich, C. (2004) Potential role of methionine sulfoxide in the inactivation of the chaperone GroEL by hypochlorous acid (HOCl) and peroxynitrite (ONOO-). *J. Biol. Chem. 279*, 19486-19493.
21. Barrette, W. C., Hannum, D. M., Wheeler, W. D., and Hurst, J.K. (1989) General mechanism for the bacterial toxicity of hypochlorous acid: abolition of ATP production. *Biochemistry 28*, 9172-9178.
22. Winter, J., Linke, K., Jatzek, A., and Jakob, U. (2005) Severe oxidative stress causes inactivation of DnaK and activation of the redox-regulated chaperone Hsp33. *Mol. Cell 17*, 381-392.
23. Winter, J., Ilbert, M., Graf, P. C., Ozcelik, D., and Jakob, U. (2008) Bleach activates a redox-regulated chaperone by oxidative protein unfolding. *Cell 135*, 691-701.
24. Hawkins, C. L., and Davies, M. J. (2001) Hyprochlorite-induced damage to nucleosides: formation of chloramines and nitrogen-centered radicals. *Chem. Res. Toxicol. 14*, 1071-1081.
25. Winterbourn, C. C., van den Berg, J. M., Roitman, E., and Kuypers, F. A. (1992)

Chlorohydrin formation from unsaturated fatty acids reacted with HOCl. *Arch. Biochem. Biophys. 296*, 547-555.

26. Holmgren, A. (1989) Thioredoxin and glutaredoxin system. *J. Biol. Chem. 264*, 13963-13966.
27. Michiels, C., Raes, M., Toussaint, O., and Remacle, J. (1994) Importance of Se-glutathione peroxidase, catalase and Cu/Zn-SOD for cell survival against oxidative stress. *Free Radical Biol. Med. 17*, 235-248.
28. Imlay, J.A. (2008) Cellular Defenses against superoxide and hydrogen peroxide. *Annu. Rev. Biochem. 77*, 755-776.
29. Brown, N. L., Stoyanov, J. V., Kidd, S. P., and Hobman J. L. (2003) The MerR family of transcriptional regulators. *FEMS 27*, 145-163.
30. Demple, B., Ding, H., and Jorgensen, M. (2002) *Escherichia coli* SoxR protein: sensor/transducer of oxidative stress and nitric oxide. *Methods Enzymol. 348*, 355-364.
31. Watanabe, S., Kita, A., Kobayashi, K., and Miki, K. (2008) Crystal structure of the [2Fe-2S] oxidative stress sensor SoxR bound to DNA. *Proc. Natl. Acad. Sci. U.S.A. 105 (11)*, 4121-4126.
32. Aslund, F., Zheng, M., Beckwith, J., and Storz, G. (1999) Regulation of the OxyR transcription factor by hydrogen peroxide and the cellular thiol-disulfide status. *Proc. Natl. Acad. Sci. U.S.A. 96*, 6161-6165.
33. Schell, M. A. (1993) Molecular biology of the LysR family of transcriptional regulators. *Annu. Rev. 47*, 597-626.
34. Choi, H. J., Kin, S. J., Mukhopadhyay, P., Cho, S., Woo, J. R., Storz, G., and Ryu, S. E. (2001) Structural basis of the redox switch in the OxyR transcription factor. *Cell 105*, 103-113.
35. Zhang, M., Wang, X., Templeton, L. J., Smulski, D. R., LaRossa, R. A., and Storz, G. (2001) DNA microarray-mediated transcriptional profiling of the *Escherichia coli* response to hydrogen peroxide. *J. Bacteriol. 183 (15)*, 4562-4570.
36. Izawa, S., Inoue, Y., and Kimura, A. (1996) Importance of catalase in the adaptive response to hydrogen peroxide: analysis of acatalasaemic *Saccharomyces cerevisiae*.

*Biochem. J. 320 (Pt1)*, 61-67.

37. Prinz, W. A., Aslund, F., Holmgren, A. And Beckwith, J. (1997) The role of the thioredoxin and glutaredoxin pathways in reducing protein disulfide bonds in the *Escherichia coli* cytoplasm. J*. Biol. Chem. 272*, 15661-15667.
38. Zheng, M., and Storz, G. (2000) Redox sensing by prokaryotic transcription factors. *Biochem. Pharmacol. 59*, 1-6.
39. Dukan, S., Dadon, S., Smulski, D. R., and Belkin, S. (1996) Hypochlorous acid activates the heat shock and soxRS system of *Escherichia coli*. *Appl. Environ. Microbiol. 62*, 4003-4008.
40. Habdas, B. J., Smart, J., Kaper, J. B., and Sperandio, V. (2010) The LysR-type transcriptional regulator QseD alters type three secretion in enterohemorrhagic *Escherichia coli* and motility in K12 *Escherichia coli*. *J. Bacteriol. 192*, 3699-3712.
41. Maddocks, S. E., and Oyston, P. C. (2008) Sturcture and function of the LysR-type transcriptional regulator (LTTR) family proteins. *Microbiology 154*, 3609-3623.
42. Lochowska, A., Iwanicka-Nowicka, r., Plochocka, D., and Hryniewicz, M. M. (2001) Functional dissection of the LysR-type CysB transcriptional regulator. Regions important for DNA binding inducer response, oligomerization, and positive control. *J. Biol. Chem. 276*, 2098-2107.
43. Bender, R. A. (2010) A NAC for regulating metabolism: the nitrogen assimilation control protein (NAC) from Klebsiella pneumoniae. *J. Bacteriol. 193*, 4801-4811.
44. Gebendorfer, K. M., Drazic, A., Le, Y., Gundlach, J., Bepperling, A., Kastenmüller, A., Ganzinger, K. A., Braun, N., Franzmann, T. M., and Winter, J. (2012) Identification of a hypochlorite-specific transcription factor from *Escherichia coli*. *J. Biol. Chem. 287 (9)*, 6892-6903.
45. Dukan, S., Touati, D. (1996) Hypochlorous acid stress in *Escherichia coli*: resistance. DNA damage, and comparison with hydrogen peroxide stress. *J. Bacteriol. 178 (21)*, 6145-6150.
46. Lynch, A. S., Tyrrell, R., Smerdon, S. J., Briggs, G. S., and Wilkinson, A. J. (1994) Characterization of the CysB protein of *Klebsiella aerogenes*: direct evidence that

N-acetylserine rather than O-acetylserine serves as the inducer of the cysteine regulon. *Biochem. J. 299 (Pt1)*, 120-136.

47. Ezezika, O. C., Haddad, S., Clark, T. J., Neidle, E. L., and Momany, C. (2007) Distinct effector-binding sites enable synergistic transcriptional activation by BenM, a LysR-type regulator. *J. Mol. Biol. 367 (3)*, 616-629.
48. Hayakawa, H., Kuwano, M., and Sekiguchi, M. (2001) Specific binding of 8-oxoguanine-containing RNA to polynucleotide phosphorylase protein. *Biochemistry 40*, 9977-9982.
49. Li, Z., and Deutscher, M. P. (2004) Exoribonucleases and endoribonucleases. In Curtiss, R., III (Ed.). *EcoSal-Escherichia coli and Salmonella: Cellular and Molecular Biology*, Chapter 4.6.3, ASM Press, Washington, DC.
50. Morales, E. H., Calderon, I. L., Collao, B., Gil, F., Porwollik, S., McClelland, M., and Saavedra, C. (2012) Hypochlorous acid and hydrogen peroxide-induced negative regulation of *Salmonella enterica* serovar Typhimurium *ompW* by the response regulator ArcA. *Bio. Med. Central Microbiol. 12*, 63.
51. Moore, S. D., and Sauer, R. T. (2007) The tmRNA system for translational surveillance and ribosome rescue. *Annu. Rev. Biochem. 76*, 101-124.
52. Datsenko, K. A., and Wanner, B. L. (2000) One-step inactivation of chromosomal genes in *Escherichia coli* K-12 using PCR products.
53. Brenowitz, M., Senear, D. F., and Kingston, R. E. (2001) DNase I footprint analysis of protein-DNA binding. *Curr. Protoc. Mol. Biol. Capter 12*.
54. Luo, S., and Wehr, N. B. (2009) Protein carbonylation: avoiding pitfalls in the 2,4-dinitrophenylhydrazine assay. *Redox Rep. 14 (4)*, 159-166.
55. Hwang, S., Kim, M., Ryu, S., and Jeon B. (2011) Regulation of oxidative stress response by CosR, an essential response regulator in *Campylobacter jejuni*. *PLoS One 6 (7)*, e22300.
56. National Center for Biotechnology Information: http://www.ncbi.nlm.nih.gov/
57. Dr. J. Winter's preliminary results.
58. M. Hillreiner's Bachelor Thesis, 2010

59. H. Miura's Bachelor Thesis, 2011
60. Dr. J. Graumann's preliminary results.
61. Balog, E. M., Norton, L. E., Bloomquist, R. A., Cornea, R. L., Black, D. J., Louis, C. F., Thomas, D. D., and Fruen, B. R. (2003) Calmodulin oxidation and methionine to glutamine substitutions reveal methionine residues critical for functional interaction with Ryanodine receptor-1. *J. Biol. Chem. 278 (18)*, 15615-15621.
62. Shroff, N. P., Bera, S., Cherian-Shaw, M., and Abraham, E. C. (2001) Substituted hydrophobic and hydrophilic residues at methionine-68 influence the chaperone-like function of alphaB-crystallin. *Mol. Cell Biochem. 220 (1-2)*, 127-133.
63. Provided by Dr. J. Winter.
64. J. Gundlach's preliminary results.
65. EcoCyc: http://ecocyc.org/
66. ExPaSy: http://web.expasy.org/blast/
67. Phyre: http://www.sbg.bio.ic.ac.uk/~phyre/
68. PredictProtein: http://www.predictprotein.org/
69. Brodersen, D. E., Clemons, W. M., Carter, J., Morgen-Warren, R. J., Wimberly, B. T., and Ramarkrishnan, V. (2000) The structural basis for the action of the antibiotics tetracycline, pactamycin, and hygromycin B on the 30S ribosomal subunit. *Cell 103*, 1143-1154.
70. Misumi, M., and Tanaka, N. (1980) Mechanism of inhibition of translocation by kanamycin and viomycin: A comparative study with fusidic acid. *Biochem. Biophys. Res. Commun. 92*, 647-654.
71. Drainas, D., Kalpaxis, D. L., and Coutsogeorgapoulos, C. (1987) Inhibition of ribosomal peptidyltransferase by chloramphenicol. Kinetic studies. *Eur. J. Biochem. 164 (1)*, 53-58.
72. PortEco: http://www.porteco.org/
73. Alekshun, M. N., and Levy, S. B. (1999) The mar regulon: multiple resistance to antibiotics and other toxic chemicals. *Trends Microbiol. 7 (10)*, 410-413.
74. M. Schäffner's Research Project Report (2009).
75. Hager, J., Staker, B. L., and Jakob, U. (2004) Substrate binding analysis of the 23S rRNA methyltransferase RrmJ. *J. Bacteriol. 186 (19)*, 6634-6642.

76. Hu, L. I., Lima, B. P., and Wolfe, A. J. (2010) Bacterial protein acetylation: the dawning of a new age. *Mol. Microbiol. 77*, 15-21.
77. Zhang, J., Sprung, R., Pei, J., Tan, X., Kim, S., Zhu, H., Liu, C. F., Grishin, N. V., and Zhao, Y. (2009) Lysine acetylation is a highly abundant and evolutionarily conserved modification in Escherichia coli. *A. S. B. M. B. Molecular & Cellular Proteomics*, 215-225.
78. Liang, W., Malhotra, A., and Deutscher, M. P. (2011) Acetylation regulates the stability of a bacterial protein: growth stage-dependent modification of Rnase R. *Mol. Cell 44*, 160-166.
79. Vogt, W. (1995) Oxidation of methionyl residues in proteins: tools, targets, and reversal. *Free Radic. Biol. Med. 18*, 93-105.
80. Carpousis, A. J. (2007) The RNA degradosome of *Escherichia coli*: An mRNA-degrading machine assembled on RNase E.
81. Kaczanowska, M., and Ryden-Aulin, M. (2007) Ribosome biogenesis and the translation process in *Escherichia coli*. Microbiol. *Mol. Biol. Rev. 71 (3)*, 477-494.
82. Korber, P., Zander, T., Herschlag, D., and Bardwell, J. (1999) A new heat shock protein that binds nucleic acids. *J. Biol. Chem. 274 (1)*, 249-256.
83. Korber, P., Stahl, J. M., Nierhaus, K. H., and Bardwell, J. (2000) Hsp15: a ribosome-associated heat shock protein. *EMBO 19 (4)*, 741-748.
84. Ishino, T., Atarashi, K., Uchiyama, S., Yamami, T., Saihara, Y., Yoshida, T., Hara, H., Yokose, K., Kobayashi, Y., and Nakamura, Y. (2000) Interaction of ribosome recycling factor and elongation factor EF-G with E.coli ribosomes studied by the surface plasmon resonance technique. *Genes Cells 5 (12)*, 953-963.
85. Rasouly, A., Davidovich, C., and Ron, E. Z. (2010) The heat shock protein YbeY is required for optimal activity of the 30S ribosomal subunit. J. Bacteriol. 192 (18), 4592-4596.
86. Sunohara, T., Jojima, K., Yamamoto, Y., Inada, T., and Aiba H. (2004) Nascent-peptide-mediated ribosome stalling at a stop codon induces mRNA cleavage resulting in nonstop mRNA that is recognized by tmRNA. *RNA 10 (3)*, 378-386.
87. Shoemaker, C. J., and Green R. (2012) Translation drives mRNA quality control. *Nat.*

*Struct. Mol. Biol. 19 (6)*, 594-601.

88. Lopez, P. J., Yarchuk, M. O., and Dreyfus, M. (1997) Translation inhibitors stabilize *Escherichia coli* mRNAs independently of ribosome protection. *Proc. Matl. Aca. Sci. U.S.A. 95 (11)*, 6067-6072.
89. Li, Z., Wu, J., and DeLeo, C. J. (2006) RNA damage and surveillance under oxidative stress. *IUBMB Life 58 (10)*, 581-588
90. Nawrot, B., Sochacka, E., and Düchler, M. (2011) tRNA structural and functional changes induced by oxidative stress. *Cell. Mol. Life Sci. 68*, 4023-4032.
91. Pech, M., and Nierhaus, K. H. (2012) Three mechanisms in *Escherichia coli* rescue ribosomes stalled on non-stop mRNAs: one of them requires release factor 2. *Molecular Microbiology 86 (1)*, 6-9.
92. Gagnon, M. G., Seetharaman, S. V., Bulkley, D., and Steitz T. A. (2012) Structural basis for the rescue of stalled ribosomes: structure of YaeJ bound to the ribosome. *Science 335*, 370-372.
93. Demeshkina N., Jenner, L.m Westhof, E., Yusupov, M., and Yusupova, G. (2012) A new understanding of the decoding principle on the ribosome. *Nature 484 (7393)*, 256-259.

# 7 Acknowledgement

*The four years of PhD were full of joys and tears. I give thanks to my faithful God for he has been walking with me all the time and all the way.*

*I greatly thank my P.I. Dr. Jeannette Winter. She offered me the opportunities to work in the amazing field of bacterial oxidative stress response and deeply inspired me in this research area. At all times, she was available for discussion and to give advise. For her excellent supervision during the time and for the critical reading of the dissertation, I am very grateful. Furthermore, I want to thank Prof. Dr. Johannes Buchner for giving me the opportunity to study my favorite major, biochemistry, at my favorite university, Technische Universität München, and for his suggestions on this work.*

*I thank all colleagues, especially Jasmin Gundlach, Bettina Richter, Adrian Dazic, and Katharina Gebendorfer for their kind help and the pleasant teamwork. Particularly, I thank Bettina Richter for the private "Deutschstunde", in which I learned a lot of colloquial speech and phrases, such as "Ich verstehe nur Bahnhof." Moreover, I want to thank all technician assistants for their great support.*

*Additionally, I want to express my gratitude to all collaborators: Dr. N. Braun from Department Electron Microscopy for TEM analysis; Prof. Dr. Groll from Department Biochemistry for crystallization screen; Dr. Ingo Wohlgemuth and Prof. Dr. Marina Rodnina from the Department Physical Biochemistry, Max Plank Institute Göttingen, for the ribosome/translation related assays.*

*Last but not least, I thank Boehringer Ingelheim Fonds for the sponsorship of this work and the impressive personal assistance. I thank my husband Xinxing and my parents for their continuous and indispensable support.*

***O Lord, how manifold are your works!***

***In wisdom have you made them all; the earth is full of your creatures.***

*Psalm 104:2*

# 8 Supplement


Figure S1: Multiple sequence alignment of YjiE from 7 representative organisms using T-coffee. The conserved amino acids are highlighted in blue and the degree of conservation is proportional to the darkness of the colour. The highly conserved amino acids in the hotspot clusters are labelled with red stars.

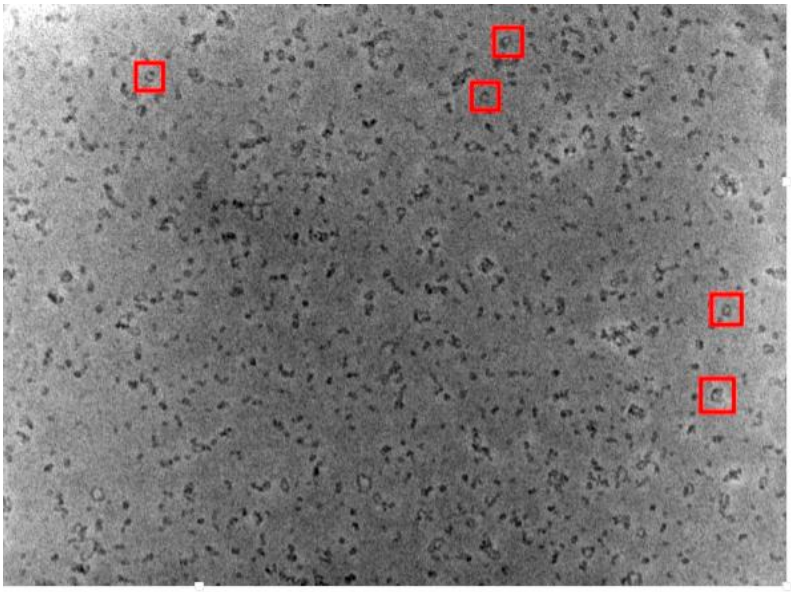

Figure S2: Negative staining transmission electron microscopy of YjiE_A204-208. YjiE_A204-208 (0.02 mg/ml) was negatively stained with 2 % (w/v) uranylacetate. The ring structure is marked with red square. Scale bar: 346 nm.

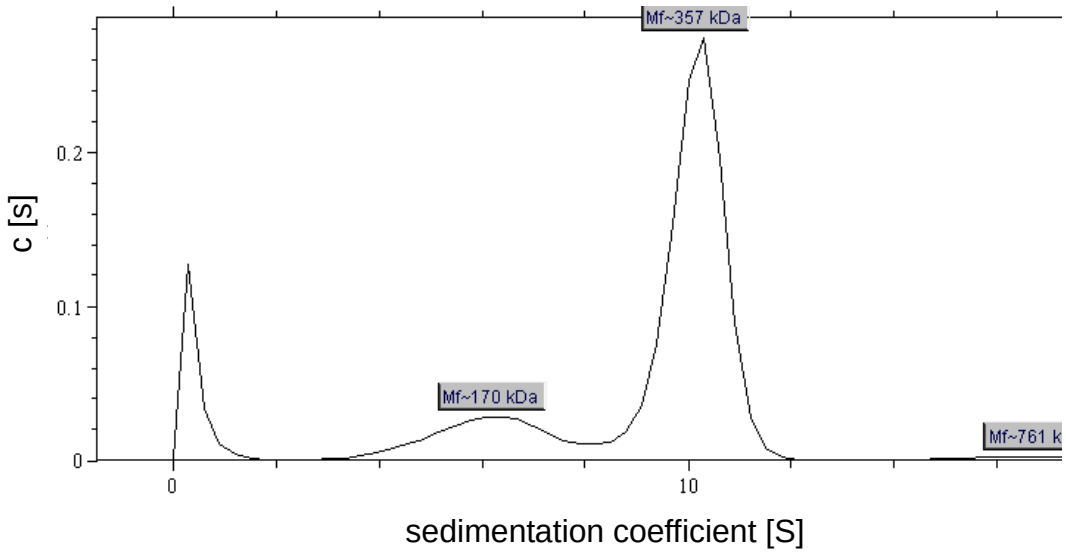


Figure S3: Analytical ultracentrifugation of YjiE_A204-208. The centrifugation was run at 42000 rpm, 20°C.

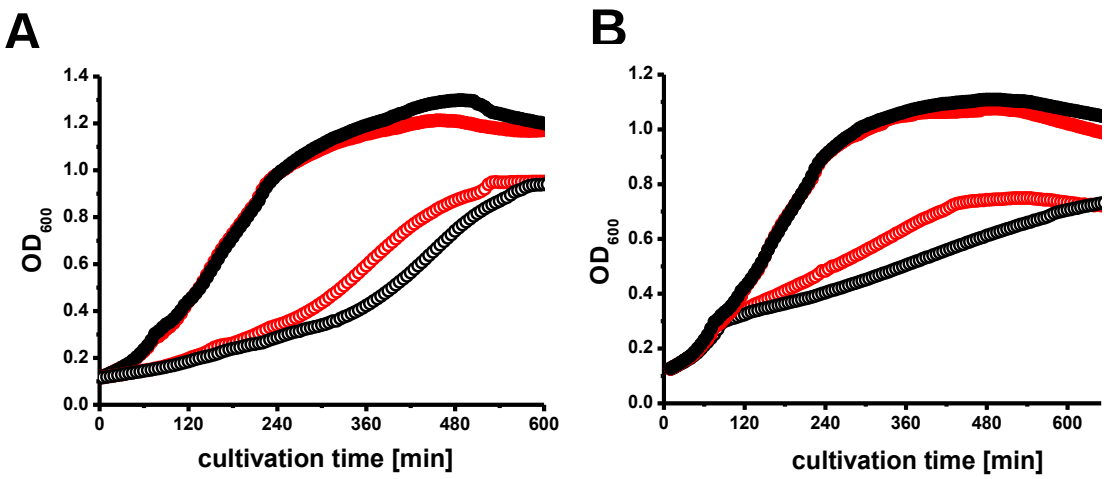


Figure S4: Growth of MC4100 and MC4100 *yifE*⁻ cells upon chloramphenicol and spectinomycin. A) 2.5 µg/ml chloramphenicol; B) 6 µg/ml spectinomycin. Cells were cultivated to the exponential growth phase and diluted with LB medium into 96 well plate ($OD_{600}$=0.05 per well). Oxidants were added and the growth was followed by measuring $OD_{600}$ every 5 minute by a microtiter plate reader.

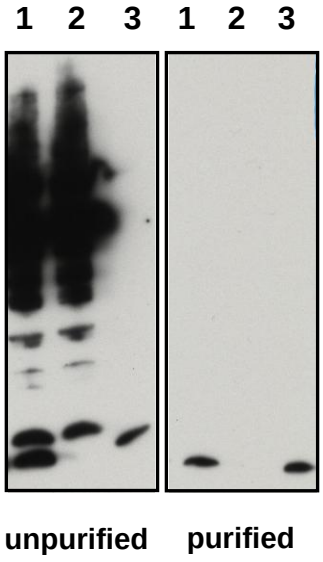


Figure S5: Purification of YifE polyclonal antibody. Left: unpurified YifE antibody; right: purified YifE antibody. Lane 1: lysate of MC4100 cells; lane 2: lysate of MC4100 *yifE*⁻ cells; lane 3: purified YifE (5 ng).

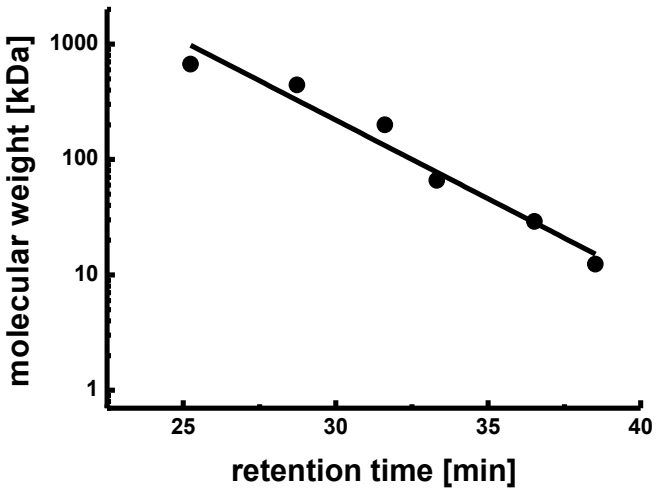


Figure S6: Standard curve for analysis of oligomerization state of YifE *in vivo* by analytical HPLC. Cytochrome C (12.5 kDa), carbonic anhydrase (29 kDa), BSA (66 kDa), alcohol dehydrogenase (150 kDa), ß-amylase (200 kDa), Apoferritin (443 kDa) were used as standard protein. (Figure from *74*).